GEOLOGY OF GREENLAND SURVEY BULLETIN 184 · 1999

Collected research papers: palaeontology, geochronology, geochemistry

GEOLOGICAL SURVEY OF DENMARK AND GREENLAND
MINISTRY OF ENVIRONMENT AND ENERGY

Geology of Greenland Survey Bulletin 184

Keywords
Ammonite fauna, analytical methods, Caledonides, dykes, geochemistry, geochronology, Greenland, K–T boundary, Labrador Sea, ostracode, palaeontology, Palaeoproterozoic, SHRIMP, Silurian, Tertiary.

Cover illustration (related to the paper by Kennedy *et al.*)
Exposure of the Cretaceous–Palaeogene sedimentary and volcanic succession at Annertuneq on the north coast of Nuussuaq. Below the conglomerate are unnamed upper Campanian turbidite slope mudstones. They are unconformably succeeded by Maastrichtian–Paleocene submarine canyon conglomerates and turbidite slope mudstones of the Kangilia Formation. The Cretaceous–Paleocene boundary is placed at 452 m a.s.l. The succession is topped by hyaloclastites of the Vaigat Formation. The mountain is about 1.3 km high. See also the stratigraphical log of the succession in Kennedy *et al.*, p. 15. Photo: F.G. Christiansen.

Chief editor of this series: Peter R. Dawes
Scientific editor of this volume: W. Stuart Watt
Copy editor: Peter R. Dawes
Editorial secretary: Esben W. Glendal
Referees: Tom Andersen (Norway), John H. Callomon (UK), Walter K. Christensen (Denmark), Godfrey Fitton (UK), Tõnu Meidla (Estonia), R. Schallreuter (Germany), Jakob Skogseid (Norway), Svend Stouge (Denmark), John Tarney (UK), Martin J. Whitehouse (Sweden), Marie-Claude Williamson (Canada).
Graphic production and reproduction: Knud Gr@phic Consult, Odense, Denmark
Manuscripts submitted: 24th July, 1996 – 4th August, 1999
Final versions approved: 29th September, 1999
Printed: 15th December, 1999

ISBN 87-7871-071-5
ISSN 1397-1905

Geology of Greenland Survey Bulletin
The series *Geology of Greenland Survey Bulletin* is a continuation of *Bulletin Grønlands Geologiske Undersøgelse* and incorporates *Rapport Grønlands Geologiske Undersøgelse.*

Citation of the name of this series
It is recommended that the name of this series is cited in full, viz. *Geology of Greenland Survey Bulletin*
If abbreviation of this volume is necessary the following form is suggested: *Geology Greenland Surv. Bull.* 184, 62 pp.

Available from
Geological Survey of Denmark and Greenland
Thoravej 8, DK-2400 Copenhagen NV, Denmark
Phone: +45 38 14 20 00, fax: +45 38 14 20 50, e-mail: geus@geus.dk
or
Geografforlaget ApS
Fruerhøjvej 43, DK-5464 Brenderup, Denmark
Phone: +45 63 44 16 83, fax: +45 63 44 16 97, e-mail: go@geografforlaget.dk

Contents

Bold numbers refer to the location map on next page

Editorial note

This is the first volume of *Collected research papers* issued by the Geological Survey of Denmark and Greenland in the *Geology of Greenland Survey Bulletin* series. As shown in the contents above, the six papers form a multidisciplinary collection: four relate to different areas of Greenland (see map on the next page), the final two deal with geochemical analytical standards and procedures at the Survey.

It is the intention to issue volumes of multidisciplinary articles regularly. The volumes are open to contributions on all aspects of Greenland geoscience; all papers will be subjected to peer review. Papers should be submitted to the Editorial office at the Survey's address given on the colophon page and on the back cover of this volume. *Instructions to authors* will be sent on request.

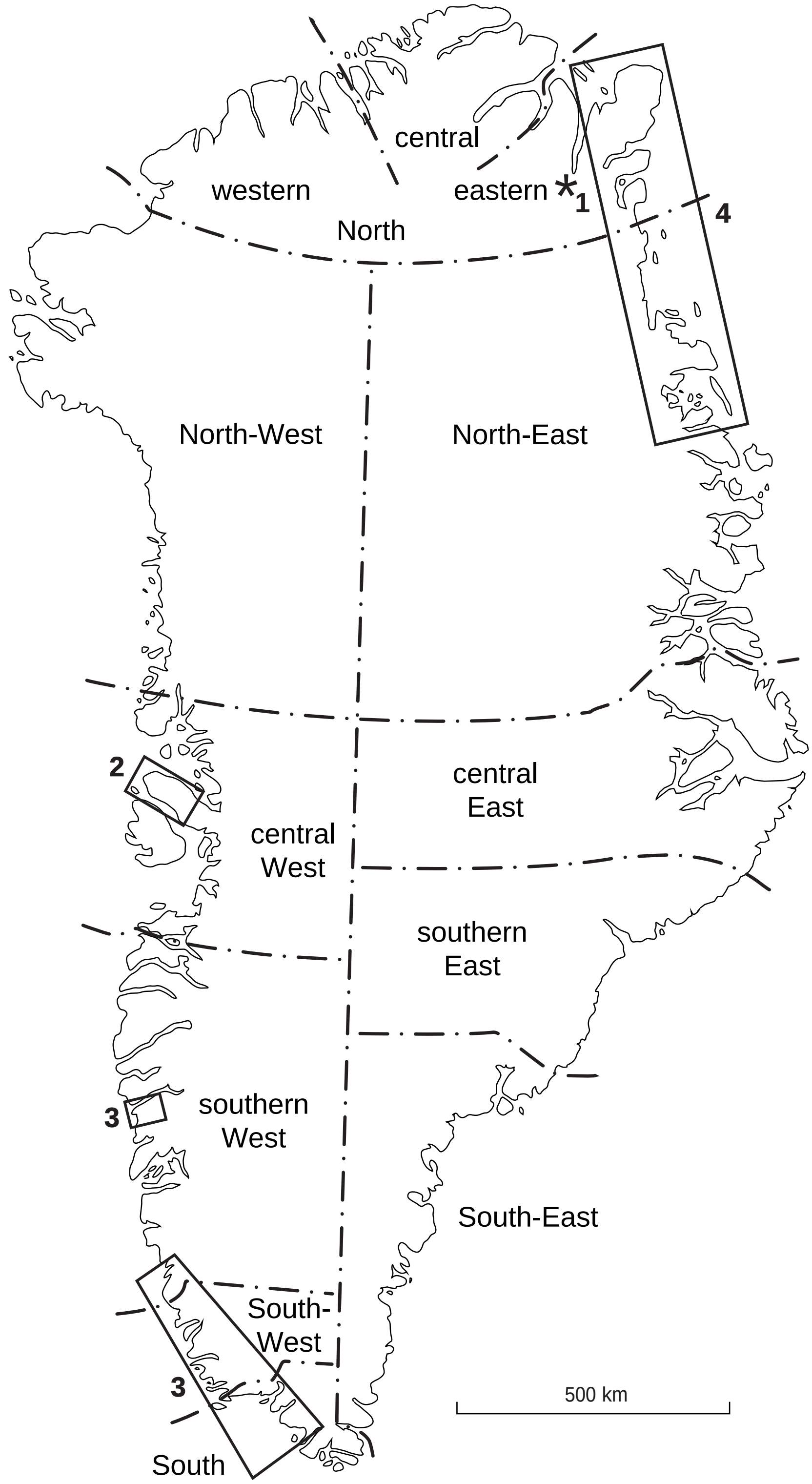

Locality map for contributions in this collection of articles. Numbers 1 (with a star) and 2–4 (frames) locate the individual papers in the table of contents on the preceeding page; the two papers dealing with the Rock Geochemical Laboratory are not located.

The myodocope ostracode *Entomozoe* from an early Silurian (Telychian, Llandovery) carbonate mound of the Samuelsen Høj Formation, North Greenland

David J. Siveter and *Philip D. Lane*

Entomozoe aff. *Entomozoe tuberosa* (Jones 1861), from carbonate mounds of the Samuelsen Høj Formation, represents one of the few ostracodes documented from the Silurian of Greenland and a rare occurrence of *Entomozoe* from outside Scotland. Like its coeval, congeneric Scottish counterparts, the Greenland *Entomozoe* lived on a shallow-water shelf dominated by epibenthonic fauna and probably had a benthonic, swimming(?) lifestyle. Its environmental, ecological and geographical setting is consistent with the idea that these earliest, Lower Silurian myodocopes were benthonic and, therefore, that Upper Silurian pelagic representatives must have resulted from an ecological shift in the group.

D.J.S., *Department of Geology, University of Leicester, University Road, Leicester LE1 7RH, UK.*
P.D.L., *School of Earth Sciences and Geography, University of Keele, Staffordshire ST5 5BG, UK.*
E-mail: *p.d.lane@esci.keele.ac.uk*

Keywords: North Greenland, ostracode, Silurian

A Silurian Llandovery Series fauna collected from eastern North Greenland contains scarce specimens of a myodocope ostracode, *Entomozoe* aff. *Entomozoe tuberosa* (Jones 1861). The find represents a rare Llandovery age myodocope and only the second occurrence of *Entomozoe* known outside the Llandovery of Scotland. The environmental, ecological and geographical setting of the Greenland material, in shallow-water carbonates on the palaeo-continent of Laurentia, is consistent with the notion (Siveter & Vannier 1990; Siveter *et al.* 1991) that the earliest, Lower Silurian (Llandovery–Wenlock) myodocopes were benthic, living on well-oxygenated shelves. Myodocope ostracodes appear to have undergone a benthic to pelagic ecological shift by the Upper Silurian, an event which provides the best evidence for the earliest occurrence of pelagic ostracodes in the fossil record (Siveter 1984; Siveter *et al.* 1987, 1991; Siveter & Vannier 1990; Vannier & Abe 1992).

Material and methods

The myodocope-bearing fauna was obtained by J.W. Cowie (University of Bristol, UK) and P.J. Adams on a Danish state-aided expedition to North Greenland in 1956. The most detailed maps then available were 1:1 000 000 scale aeronautical charts. The fossils are from collections made at "2 km from the north shore of Centrum Sø, at a height of about 300 metres, at approximately 22°20′W, 80°13′N, in Kronprins Christian Land, west of Dijmphna Sund" (Fig. 1; J.W. Cowie, personal communication, as reported in Lane 1972, p. 336). Contrary to Lane 1972 (p. 337, text-fig. 1a) both these collections were made in the Samuelsen Høj Formation (Fig. 2), a unit erected to encompass the isolated carbonate mounds found in several areas of North Greenland, such as Peary Land, Valdemar Glückstadt Land and Kronprins Christian Land (Hurst 1984, p. 52; see Fig. 1 for locations). The locality yields a Llandovery, Telychian Stage, *Pterospathodus celloni* Biozone conodont assemblage (Armstrong & Aldridge 1982; Armstrong 1983, 1990; Hurst 1984, p. 59).

The material consists of two myodocope specimens, housed in the Geological Museum, University of Copenhagen (MGUH), Denmark. Photographs were made using an Aristophot mounted with a Leica camera (methods outlined in Siveter 1990). Morphological terminology of the myodocope shell follows Siveter *et al.* (1987).

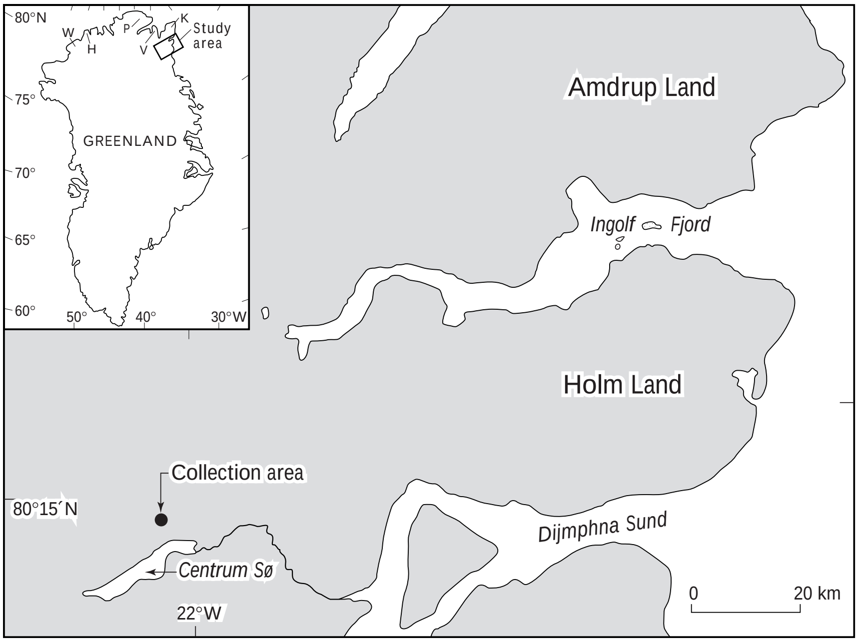

Fig. 1. Locality yielding *Entomozoe* aff. *E. tuberosa:* north side of Centrum Sø, Kronprins Christian Land, eastern North Greenland. **H**: Hall Land, **K**: Kronprins Christian Land, **P**: Peary Land, **V**: Valdemar Glückstadt Land, **W**: Washington Land.

Ostracodes from the Silurian of Greenland

Entomozoe aff. *E. tuberosa* is one of the few ostracode taxa documented from the Silurian of Greenland, though some forms are often common locally. Predominantly smooth-shelled ('non-palaeocope') species are often encountered in the platform carbonates of the Samuelsen Høj Formation from Kronprins Christian Land, Valdemar Glückstadt Land and Peary Land and from correlative formations in Washington Land and Hall Land in western North Greenland (see Fig. 1 for locations). 'Smooth ostracods' (possibly leperditiids) were reported from the probable Rhuddanian of the Turesø Formation (= the 'un-named Silurian(?) dolomite formation') and from the Aeronian of the Ymers Gletscher Formation (= the 'un-named Silurian limestone formation') of Børglum Elv, central Peary Land (Armstrong & Lane 1981, pp. 31–32). Hurst (1984, p. 37) documented abundant ostracodes from probable Aeronian strata in the lower half of the Odins Fjord Formation of Peary Land. From later collections made in the same area (GGU 184145), a beyrichiacean and abundant smooth ostracodes were recorded from the *P. celloni* Biozone near the top of the Odins Fjord Formation (Lane 1988, p. 93). The latter, largely unstudied ostracode fauna, includes smooth *Conbathella*-like thlipsuraceans and the beyrichiacean ?*Apatobolbina* ('*Platybolbina*' of Lane); both genera occur in the late Llandovery – early Wenlock of Anticosti Island, Canada (Copeland 1974).

Poulsen (1934, p. 37) described the unrevised *Ceratocypris symmetrica* gen. et sp. nov. and *Euprimitia*? sp. from the Aeronian – early Telychian Cape Schuchert Formation of Washington Land, western North Greenland. *Monoceratella mazos* Lane 1980, was established from a Telychian – ?earliest Wenlock boulder within a Silurian conglomerate of Kap Schuchert, Washington Land.

Lifestyle of *Entomozoe* aff. *E. tuberosa*

Interpretation of mode of life of fossils depends on evidence from their functional morphology and design, and from independent geological data such as the nature of their faunal associates and their patterns of facies and palaeogeographical distribution (e.g. see Fortey 1985 for trilobites; Siveter 1984 and Siveter *et al*. 1991 for Silurian ostracodes). Interpretation of the mode of life of Silurian ostracodes is not helped by the fact that none range to the Recent. There are also the potential pitfalls inherent in reconstructing the palaeoecology of vagile organisms, such as adopting circular reasoning in allowing notions on probable lifestyle to unduly influence ideas on where the animal was supposedly living.

Morphological evidence

In Recent myodocopes the rostral incisure facilitates protrusion of the first and second antennae for use in locomotion, particularly swimming. The faintly developed rostral incisure in *E.* aff. *E. tuberosa* may imply that its frontal appendages were not especially well developed and that, like *E. tuberosa* from the late Llandovery of the Pentland Hills, Scotland (see Siveter & Vannier 1990), it may not have been an accomplished swimmer. Moreover, intuitively the reasonably thick, relatively heavy(?) shell of *E.* aff. *E. tuberosa* is not a character readily associated with a pelagic lifestyle.

Depositional environment: facies and faunal associates

The carbonate mounds of the Samuelsen Høj Formation have elongate to circular outcrops, of 50 m to 5 km widths or circumferences of 200 m to 10 km, though none of their many lithologies have great lateral extent (Mayr 1976; Hurst 1980, 1984). The mounds accumulated in a relatively shallow, mid- to outer-shelf setting; as such, they are typical of many others in the Palaeozoic and Mesozoic, which often occur as products of rapid subsidence of a mature shelf. Though difficult to estimate accurately the distance from shoreline and the water depth in which the mounds formed, a fairly high-energy environment, well within the euphotic zone, is indicated; moreover, frequent subaerial exposure due to local changes in shelf-subsidence rate can be imagined.

The ostracodes occur in a coquina which is dominated by trilobites constituting the relatively high diversity 'styginid-cheirurid-harpetid trilobite Assemblage' (Lane 1972; Thomas & Lane 1999), all of which probably had a benthonic mode of life; e.g. *Meroperix ataphrus*, *Chiozoon cowei*, *Hyrokybe pharanx*, *Scotoharpes loma*, *Stenopareia* and *Calymene*. Equivalent trilobite faunas occur in similar carbonate mound facies of early Ordovician Arenig (cheirurid-illaenid community of Fortey 1975) to early Devonian Pragian (Chlupáč 1983) age and taxonomically different but homoeomorphic similar trilobite assemblages occur up to the latest Palaeozoic (for example, see Lane & Owens 1982; Owens 1983); however, no myodocopes have been recorded from these other trilobite associations. Rare, undetermined bryozoans and small numbers of brachiopods (e.g. *Lissocoelina*, *Streptis* and a delthyrid; Boucot *in* Thomas & Lane 1999) and rugose and tabulate corals (*Microplasma lovenianum*, *Favosites gothlandicus*, *Dinophyllum*, *Tryplasma* and ?*Tabularia*; Scrutton 1975) represent the sessile epibenthonic components of the myodocope-bearing fauna. Vagile epibenthonic associates are rare gastropods (e.g. *Subulites*, *Gyronema*, *Liospira*, *Megalomphala* and platycerids) and undetermined bivalves and rostroconchs. Rare, undetermined cephalopods are the only possible pelagic associates. Thus, the animals co-occurring with *E.* aff. *E. tuberosa* are almost all epibenthonic forms (Fig. 3). An assignment to Benthic Association 3 of Boucot (1975) is likely (Hurst & Surlyk 1984).

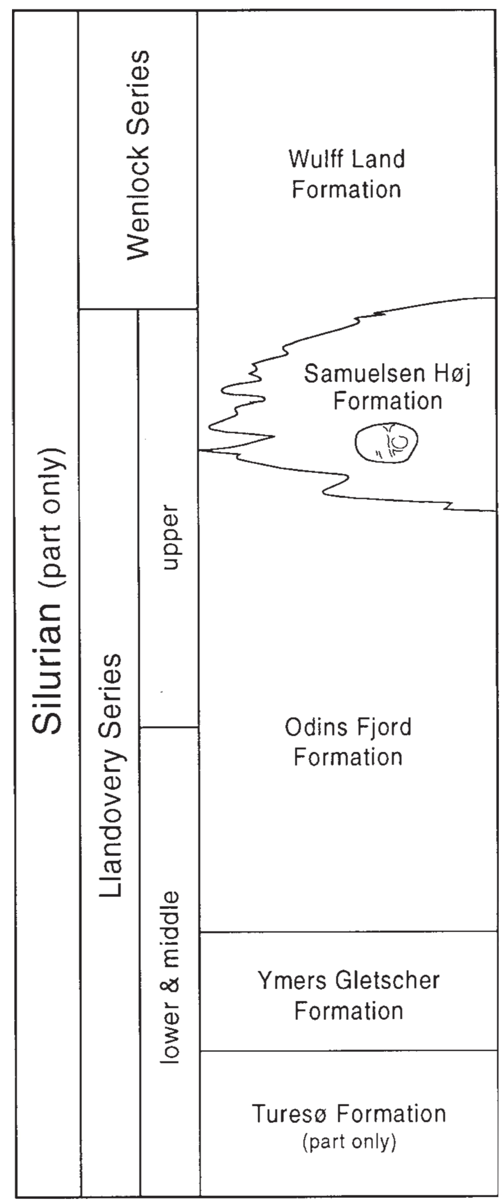

Fig. 2. Stratigraphic position of *Entomozoe* aff. *E. tuberosa*, in the late Llandovery Series, Samuelsen Høj Formation, eastern North Greenland.

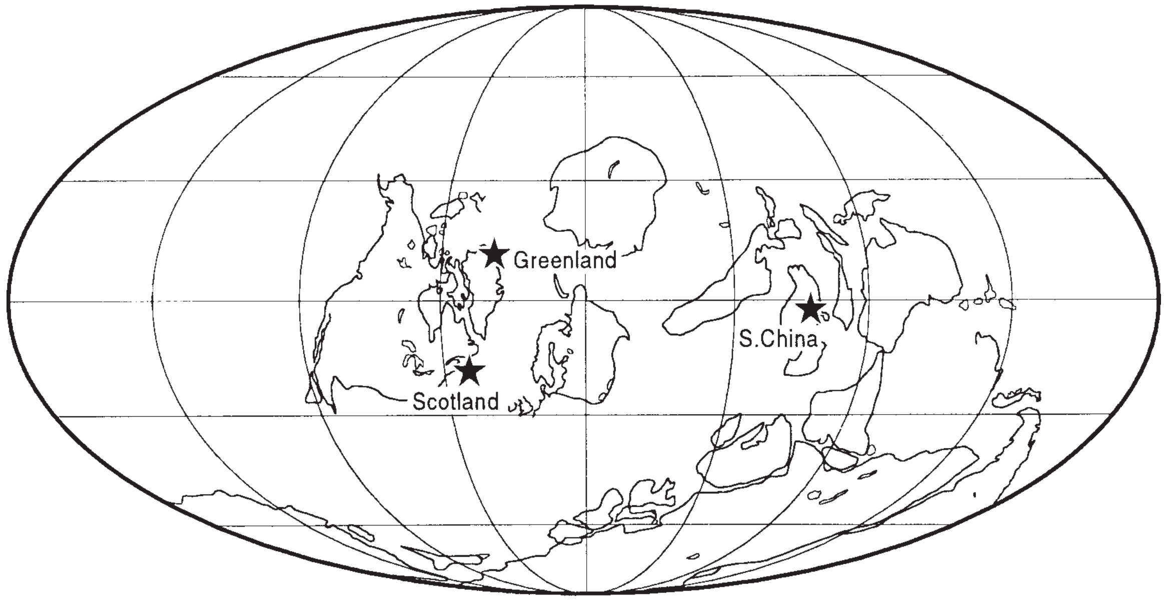

Fig. 3. Known occurrences of *Entomozoe*: the late Llandovery of Scotland (*E. tuberosa*; Siveter & Vannier 1990), eastern North Greenland (*E.* aff. *E. tuberosa*; herein) and south China (*E.* cf. *E. tuberosa*; Siveter *et al.* 1991). Base map for the Llandovery is after Scotese & McKerrow (1990).

Palaeogeographical distribution

Entomozoe is known only from Scotland (*E. tuberosa*; Siveter & Vannier 1990), Greenland (*E.* aff. *E. tuberosa*; herein) and South China (*E.* cf. *E. tuberosa*, Siveter *et al.* 1991, pp. 152, 161, fig. 4), all in late Llandovery strata deposited in tropical latitudes (Fig. 3). Greenland and Scotland were relatively close then, forming part of the eastern margin of the continent of Laurentia (equivalent to mostly present-day North America), but the south China plate was at about 100° palaeolongitude distant across an ocean. This distributional pattern is not easily explained by the dispersal factors known for supposed benthonic ostracodes (pelagic larvae are unknown in extant members of the group) but 'island hopping' is a possible migratory mechanism (e.g. see Cocks & Fortey 1982).

The evidence suggests that *E.* aff. *E. tuberosa* from Greenland lived on a relatively shallow-water, carbonate shelf with a concomitant fauna of almost exclusively epibenthonic taxa and including photosynthesising organisms (Hurst 1984, p. 53). The palaeogeographical distribution of *Entomozoe* does not necessarily imply a pelagic dispersal capacity. The ostracode was probably benthonic and perhaps had some swimming capabilities.

Palaeoecological significance of *E.* aff. *E. tuberosa*

Certain Silurian myodocopes are good candidates for pioneer pelagic ostracodes (Siveter 1984; Siveter *et al.* 1987, 1991; Siveter & Vannier 1990). Characteristically Upper Silurian Ludlow and Pridoli myodocopes lived with low diversity pelagic faunas, in outer shelf topographic lows or off-shelf basin slopes, and are often associated with deposits which imply anoxic or lowered oxygen conditions. In contrast, Lower Silurian Llandovery and Wenlock myodocopes lived with dominantly benthic associates on well-oxygenated shelves. Evidence from Britain, France, the Czech Republic, Sardinia, Australia and China underpins the idea that myodocope ostracodes may have undergone a benthic to pelagic ecological shift in mid-Silurian times (Siveter & Vannier 1990; Siveter *et al.* 1991).

E. tuberosa from Scotland appears preferentially to have inhabited shallow, nearshore, shelf environments and, like most of its associates, is considered to be part of the habitually vagile (swimming?) benthos (Siveter & Vannier 1990). That the coeval *Entomozoe* from Greenland had a similar general habitat and possible lifestyle is consistent with the notion and timing of an ecological shift affecting myodocopes during the Silurian.

Systematic palaeontology

Subclass Ostracoda Latreille 1802 (*nom. correct.* Latreille 1806)
Superorder Myodocopa Sars 1866
Order Myodocopida Sars 1866 (*nom. correct.* Pokorny 1953)
Suborder Myodocopina Sars 1866
Superfamily Bolbozoacea Bouček 1936
1936 Bolbozoacea, Bouček, p. 62
1950 Entomozoacea nov. nom. Přibyl, p. 3
Family Bolbozoidae Bouček 1936
1936 Bolbozoidae n. f., Bouček, p. 62
1950 Entomozoidae nov. nom. Přibyl, p. 4 (= Entomidae Jones 1873)

Type genus. *Bolbozoe* Barrande 1872, from the Silurian of Bohemia, Czech Republic.

Other genera. *Entomozoe* Přibyl 1950 (*pro Entomis* Jones 1861; *non* Herrich-Schaeffer 1856); *Sulcuna* Jones & Kirkby 1884.

Diagnosis. Myodocopids with a generally well-developed adductorial sulcus extended forward and ventrally around a node or bulb to reach or almost reach the anteroventral to anterior valve margin. Posterior sulcus sometimes present. Incisure (= gape) and notch (= indentation) present at anterior margin, usually below a rostrum or above an anteroventral projection. Adductor muscle scar consists of a series of subparallel, radiating, alternating ridges and furrows, typically forming a feather-like pattern overall. Valves reticulate, corrugate, tuberculate, punctate or smooth. (Modified from Siveter & Vannier 1990.)

Remarks. Based on the type genera *Entomozoe* and *Bolbozoe*, Siveter & Vannier (1990) concluded that the families Entomozoidae and Bolbozoidae are synonymous and they tentatively assigned the Bolbozoacea to the myodocope Order Myodocopida. In contrast, Vannier & Abe (1992, p. 498) considered that the type-species of *Entomozoe* “probably belongs to the Entomoconchacea”, an extinct middle Palaeozoic superfamily which they included within the other myodocope order, the Halocyprida.

Genus *Entomozoe* Přibyl 1950

1990 *Entomozoe* Přibyl 1950; Siveter & Vannier, p. 51 (q.v. for full synonomy)

Type species. Subsequently designated by Miller 1892, p. 707; *Entomis tuberosa* Jones 1861, p. 137. Lectotype designated by Siveter & Vannier 1990, p. 53.

Other species. Currently *Entomozoe* is regarded as monotypic. Other published ‘*Entomis*’ or entomozoacean species may be congeneric with *E. tuberosa* but such judgements must await examination of the material (Siveter & Vannier 1990).

Diagnosis. Large bolbozoid having a vertical adductorial sulcus, curved forward below a moderately sized anteroventral node. Anterior indentation in shell outline and rostral incisure present. Adductor muscle scar consists of series of alternating ridges and furrows forming biserial-radial, feather-like pattern. Surface smooth to weakly punctate-reticulate. (Modified from Siveter & Vannier 1990.)

Entomozoe aff. *Entomozoe tuberosa* (Jones 1861)

Fig. 4a–e, g

Material. Two specimens, both with shell preserved: a left valve on a small rock piece (MGUH 24384) and an isolated carapace (MGUH 24385).

Description. Valves approximately almond shaped, weakly inflated overall; maximum height at anterior part of adductorial sulcus, maximum length just above mid-height. Lateral valve outline gently curved ventrally, more strongly curved dorsally about a point just in front of the adductorial sulcus, evenly rounded posteriorly, and is sharply rounded anteriorly at point above mid-height. Anteroventral valve outline inclined forwards is very gently indented along site of presumed weakly developed rostral incisure (this area is damaged and lacks shell in both specimens). Valve bends – at site along lateral outline of valve – to form wide, flattish, ventral admarginal surface which narrows anteroventrally and posteroventrally. Left valve overlaps across to fine ridge at site of valve bend along right valve.

Adductorial sulcus long, narrow, occurs just in front of mid-length, widens to form V-shape area adjacent to hinge line. Faint posterior sulcus, developed just behind adductorial sulcus, in ventral one-third of valve. Both sulci curve gently forward ventrally to become obsolete close to ventral part of valve in lateral view. Dome-like node sited immediately in front of adductorial sulcus and mostly below mid-height, projects

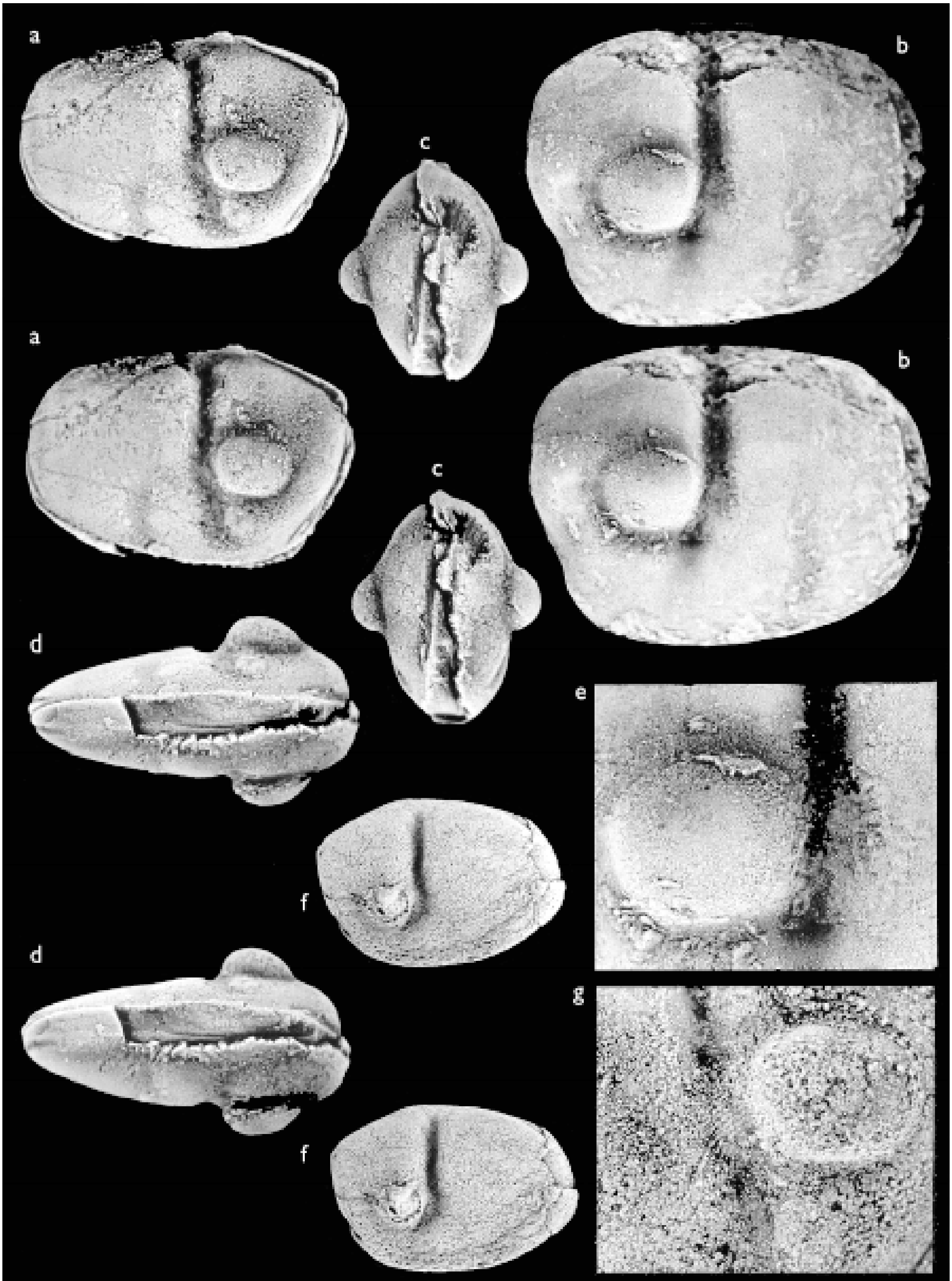
a
b
c
a
b
c
d
e
f
d
g
f

laterally well beyond rest of valve. Adductor muscle scar occurs at height of node, mani-fest externally by at least nine, faint, alternating ridges and furrows arranged into forwardly curved biserial-radial pattern. No external ornament recognised.

Measurements. Maximum valve length–height: 17.1–12 mm (MGUH 24384), 13.5–9.1 mm (MGUH 24385).

Discussion. These two Greenland specimens differ from the smaller, coeval *Entomozoe tuberosa*, from the Wether Law Linn Formation in Scotland (Siveter & Vannier 1990), by having a slightly longer adductorial sulcus, a less obviously developed rostral incisure, a lack of punctae and especially by having a posterior sulcus (compare Fig. 4a–e, g and 4f). Such differences probably represent a separate species but, because of the small amount of available material, a new taxon is not proposed.

Occurrence. Samuelsen Høj Formation, *Pterospathodus celloni* conodont Biozone, Telychian, Llandovery Series; at a height of about 300 m, two kilometres from the northern shore of Centrum Sø (approximately 22°20′W, 80°13′N), Kronprins Christian Land, eastern North Greenland.

Conclusions

1. *Entomozoe* aff. *E. tuberosa* represents only the fourth formally documented ostracode from the Silurian of Greenland and only the second record of *Entomozoe* from outside its Scottish type area.
2. Like its coeval, congeneric Scottish counterparts, the Greenland *Entomozoe* lived on a shallow-water shelf dominated by epibenthonic fauna and probably had a benthonic, swimming(?) lifestyle.
3. The Greenland *Entomozoe* endorses the opinion that the earliest, Lower Silurian myodocopes were benthonic and as such is consistent with the model that myodocopes experienced an ecological shift during the Silurian.

Fig. 4. **a**–**e**, **g**: *Entomozoe* aff. *E. tuberosa* from Cowie's collection localities 1510 (MGUH 24384) and 1511 (MGUH 24385), near Centrum Sø, Kronprins Christian Land, eastern North Greenland, Telychian, Llandovery Series, Silurian.
a, c, d, g, carapace, MGUH 24385; a, c, d: Right lateral, anterior and ventral stereo-pairs, × 4. g: Detail of muscle scar, near base of adductorial sulcus, × 8. b, e: Left valve, MGUH 24384; b: Lateral stereo-pair, × 4. e: Detail of muscle scar, near base of adductorial sulcus, × 9.
f: *Entomozoe tuberosa* (Jones 1861), stereo-pair of cast of external mould of left valve, Geological Survey (Edinburgh, United Kingdom) GSE 10812, × 4. From the right bank of River North Esk, upstream from junction with Wether Law Linn, North Esk Inlier, Pentland Hills, near Edinburgh, Scotland; Wether Law Linn Formation, late Llandovery Series, Silurian.

Acknowledgements

We thank the former Geological Survey of Greenland (amalgamated with its Danish counterpart in 1995 into the Geological Survey of Denmark and Greenland) and the Geological Museum, University of Copenhagen, for placing the material at our disposal and Dr Derek Siveter (University of Oxford) for photographing the specimens.

References

Armstrong, H.A. 1983: The early Silurian conodont micropalaeontology of the North Greenland carbonate platform, 387 pp. Unpublished Ph.D. thesis, University of Nottingham, UK.
Armstrong, H.A. 1990: Conodonts from the Upper Ordovician – Lower Silurian carbonate platform of North Greenland. Bulletin Grønlands Geologiske Undersøgelse **159**, 151 pp.
Armstrong, H.A. & Aldridge, R.J. 1982: Conodont biostratigraphy of Silurian carbonate sequences in North Greenland, 68 pp. Unpublished report, Geological Survey of Greenland, Copenhagen.
Armstrong, H.A. & Lane, P.D. 1981: The un-named Silurian(?) dolomite formation, Børglum Elv, central Peary Land. Rapport Grønlands Geologiske Undersøgelse **106**, 29–34.
Barrande, J. 1872: Systême Silurien du centre de la Bohême **1**, supp., xxx + 647 pp., 35 pls. Prague & Paris.
Bouček, B. 1936: Die Ostracoden des böhemischen Ludlows (Stufe eb). Neues Jahrbuch für Mineralogie, Geologie und Paläontologie. Beilage-Bände **76B**, 31–98.
Boucot, A.J. 1975: Evolution and extinction rate controls. Developments in palaeontology and stratigraphy **1**, 427 pp. Amsterdam, Oxford, New York: Elsevier Publishing Company.
Chlupáč, I. 1983: Trilobite assemblages in the Devonian of the Barrandian area and their relations to palaeoenvironments. Géologie et Paléontologie **17**, 45–73.
Cocks, L.R.M. & Fortey, R.A. 1982: Faunal evidence for oceanic separations in the Palaeozoic of Britain. Journal of the Geological Society (London) **139**, 465–478.

Copeland, M.J. 1974: Silurian Ostracoda from Anticosti Island, Quebec. Geological Survey of Canada Bulletin **241**, 133 pp.

Fortey, R.A. 1975: Early Ordovician trilobite communities. Fossils and Strata **4**, 331–352.

Fortey, R.A. 1985: Pelagic trilobites as an example of deducing the life habits of extinct arthropods. Transactions of the Royal Society of Edinburgh, Earth Sciences **76**, 219–230.

Herrich-Schaeffer, G.A.W. 1856: Sammlung neurer, oder wenig bekanter Aussereuropäischer Schmetterlinge **1**, 52 pp.

Hurst, J.M. 1980: Paleogeographic and stratigraphic differentiation of the Silurian carbonate buildups and biostromes of North Greenland. American Association of Petroleum Geologists Bulletin **64**, 527–548.

Hurst, J.M. 1984: Upper Ordovician and Silurian carbonate shelf stratigraphy, facies and evolution, eastern North Greenland. Bulletin Grønlands Geologiske Undersøgelse **148**, 73 pp.

Hurst, J.M. & Surlyk, F. 1984: Tectonic control of Silurian carbonate-shelf margin morphology and facies, North Greenland. American Association of Petroleum Geologists Bulletin **68**, 1–17.

Jones, T.R. 1861: [*Entomis*] In: Howell, H.H. & Geikie, A. (eds): The geology of the neighbourhood of Edinburgh; appendix list of fossils by J.W. Salter. Memoir of the Geological Survey, United Kingdom, London, 137 pp.

Jones, T.R. 1873: Notes on the Palaeozoic bivalved Entomostraca, no. X. *Entomis* and *Entomidella*. Annals and Magazine of Natural History (4) **11**, 413–417.

Jones, T.R. & Kirkby, J.W. 1884: The Cypridinidae and their allies. In: Jones, T.R., Kirkby, J.W. & Brady, G.S. (eds): A monograph of the British fossil bivalved Entomostraca from the Carboniferous formations. Palaeontographical Society Monographs **38**, Part 1, i–iii + 57–92.

Lane, P.D. 1972: New trilobites from the Silurian of north-east Greenland, with a note on trilobite faunas in pure limestones. Palaeontology **15**, 336–364.

Lane, P.D. 1980: *Monoceratella* (Ostracoda) from the Silurian of Washington Land, North Greenland. In: Peel, J.S. (compiler): Palaeontology and stratigraphy of Greenland: short contributions. Rapport Grønlands Geologiske Undersøgelse **101**, 37–43.

Lane, P.D. 1988: Silurian trilobites from Peary Land, central North Greenland. In: Peel, J.S. (ed.): Cambrian–Jurassic fossils, trace fossils and stratigraphy from Greenland. Rapport Grønlands Geologiske Undersøgelse **137**, 93–117.

Lane, P.D. & Owens, R.M. 1982: Silurian trilobites from Kap Schuchert, Washington Land, western North Greenland. In: Peel, J.S. (ed.): Palaeontology of Greenland: short contributions. Rapport Grønlands Geologiske Undersøgelse **108**, 41–69.

Latreille, P.A. 1802: Histoire naturelle des Crustacés et des Insects. **3**. Familles naturelles des genres. Paris: F. Dufart.

Latrielle, P.A. 1806: Genera crustaceorum et insectorum **1**, 1–303. Paris & Strasbourg: A. Koenig.

Mayr, U. 1976: Middle Silurian reefs in southern Peary Land, North Greenland. Bulletin of Canadian Petroleum Geology **24**, 440–449.

Miller, S.A. 1892: North American geology and palaeontology for the use of amateurs, students and scientists. Class Crustacea. First Appendix. 703–712. Cincinnati, Ohio: Western Methodist Book Concern.

Owens, R.M. 1983: A review of Permian trilobite genera. In: Briggs, D.E.G. & Lane, P.D. (eds): Trilobites and other early arthropods: papers in honour of Professor H.B. Whittington, F.R.S. Special Papers in Palaeontology **30**, 15–41.

Pokorny, V. 1953: A contribution to the taxonomy of the Palaeozoic ostracods. Sborník Ústredního Ustavu Geologického. Oddil geologicky **20**, 213–232.

Poulsen, C. 1934: The Silurian faunas of North Greenland. I. The fauna of the Cape Schuchert Formation. Meddelelser om Grønland **72,** 2(1), 46 pp.

Přibyl, A. 1950: Příspěvik k poznáví českých ostrakodů z čeledí Entomozoidae a Entomconchidae. Rozpravy II. Třídy české Akademie **59**(9), 1–27.

Přibyl, A. 1951: On the Bohemian Ostracoda of the families Entomozoidae and Entomoconchidae. Bulletin international de l'Academie des tchéque Sciences for **1949**, 1–18 (= 101–128 in the English version of Přibyl 1950).

Sars, G.O. 1866: Oversigt af Norges marine Ostracoder. Norske Videnskaps-Akademien Forhandlingar for **1865**, 1–130.

Scotese, C.R. & McKerrow, W.S. 1990: Revised world base maps and introduction. In: Scotese, C.R. & McKerrow, W.S. (eds): Palaeozoic palaeogeography and biogeography. Memoir of the Geological Society (London) **12**, 1–21.

Scrutton, C. 1975: Corals and stromatoporoids from the Ordovician and Silurian of Kronprins Christian Land, northeast Greenland. Meddelelser om Grønland **171**(4), 43 pp.

Siveter, David J. 1984: Habitats and modes of life of Silurian ostracodes. In: Bassett, M.G. & Lawson, J.D. (eds): The autecology of Silurian organisms. Special Papers in Palaeontology **32**, 71–85.

Siveter, David J. & Vannier, J.M.C. 1990: The Silurian myodocope ostracode *Entomozoe* from the Pentland Hills, Scotland; its taxonomic, ecological and phylogenetic significance and the affinity of the bolbozoid myodocopes. Transactions of the Royal Society of Edinburgh, Earth Sciences **81**, 45–67.

Siveter, David J., Vannier, J.M.C. & Palmer, D. 1987: Silurian myodocopid ostracodes: their depositional environments and the origin of their shell microstructures. Palaeontology **30**, 783–813.

Siveter, David J., Vannier, J.M.C. & Palmer, D. 1991: Silurian myodocopes: pioneer pelagic ostracodes and the chronology of an ecological shift. Journal of Micropalaeontology **10**, 151–173.

Siveter, Derek J. 1990: Photography. In: Briggs, D.E.G. & Crowther, P.R. (eds): Palaeobiology: a synthesis, 505–508. Oxford: Blackwell.

Thomas, A.T. & Lane, P.D. 1999: Trilobite assemblages of the North Atlantic region. In: Boucot, A.J. & Lawson, J.D. (eds): Palaeocommunities: a case study from the Silurian and Devonian, 444–457. Cambridge: Cambridge University Press.

Vannier, J.M.C. & Abe, K. 1992: Recent and early Palaeozoic myodocope ostracodes: functional morphology, phylogeny, distribution and lifestyles. Palaeontology **35**, 485–517.

The youngest Maastrichtian ammonite faunas from Nuussuaq, West Greenland

W. James Kennedy, Henrik Nøhr-Hansen and *Gregers Dam*

The Maastrichtian of Nuussuaq, central West Greenland, has yielded two successive ammonite faunas, here placed in sequence on the basis of new stratigraphical and dinoflagellate data. An older assemblage, with *Hoploscaphites angmartussutensis* (Birkelund 1965*), Phylloceras (Hypophylloceras) groenlandicum* Birkelund 1965, *Saghalinites wrighti* Birkelund 1965, *Baculites* cf. *B. meeki* Elias 1933, and *Baculites* sp. belongs to the *Cerodinium diebelii* palynofloral interval (9) of Nøhr-Hansen (1996), and occurs in reworked concretions in the so-called Danian Oyster-ammonite Conglomerate. A younger monospecific assemblage with *H*. aff. *H. angmartussutensis* (Birkelund 1965) occurs to within 10 m of the Cretaceous–Tertiary boundary, and belongs to the *Wodehouseia spinata* palynofloral interval (10) of Nøhr-Hansen (1996).

None of the ammonites collected to date occurs with *Palynodinium grallator* or *Disphaerogena carposphaeropsis*, dinoflagellate markers for the highest Maastrichtian in the area.

W.J.K., *Geological Collections, Oxford University Museum of Natural History, Oxford OX1 3PW, UK.*
H.N.-H. & G.D., *Geological Survey of Denmark and Greenland, Thoravej 8, DK-2400 Copenhagen NV, Denmark*. E-mail: *hnh@geus.dk; gd@geus.dk*

Keywords: ammonite fauna, K–T boundary, Maastrichtian, West Greenland

It is to the monograph by Birkelund (1965) that we owe our knowledge of the Maastrichtian ammonite faunas of West Greenland, specifically those from the Nuussuaq (Nûgssuaq in Birkelund 1965) area (Fig. 1). Following the stratigraphical and sedimentological investigations of Dam & Sønderholm (1994), the establishment of an Upper Cretaceous dinoflagellate stratigraphy by Nøhr-Hansen (1996), and description of the most northerly known Cretaceous–Tertiary boundary section at Annertuneq, on Nuussuaq, by Nøhr-Hansen & Dam (1997), it is possible to place the ammonite faunas in their correct stratigraphic sequence.

Biostratigraphy of the Nuussuaq Maastrichtian

Nøhr-Hansen (1996) established the following palynostratigraphy of the Maastrichtian on Nuussuaq:

Late Maastrichtian: *Wodehouseia spinata* interval (10)
Early Maastrichtian: *Cerodinium diebelii* interval (9)

At the Annertuneq section on the north coast of Nuussuaq (Figs 1, 2), the base of the succeeding Paleocene is marked by the appearance of *Senoniasphaera inornata*, in what appears to be an uninterrupted sequence in sedimentological terms (Nøhr-Hansen & Dam 1997, p. 853).

Birkelund (1965) recognized two Maastrichtian faunas from Nuussuaq, but was unable to reconstruct a composite sequence. The most extensive fauna came from the so-called Oyster-ammonite Conglomerate in Agatdalen (Fig. 1), interpreted by Birkelund as a Danian basal conglomerate containing a huge number of derived concretions, mainly of Maastrichtian age, in a shaly matrix containing Danian oysters and other pelecypods. On the basis of the oysters and other bivalves present in the muddy matrix of the conglomerate it has been possible to correlate the conglomerate

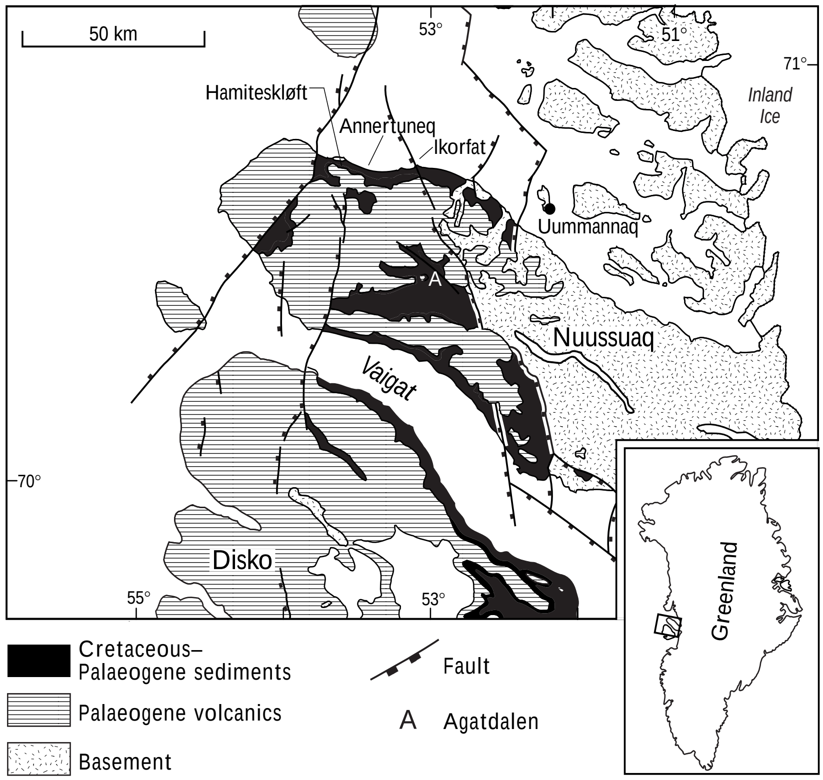

Fig. 1. Geological map showing the position of Nuussuaq and the Annertuneq Cretaceous–Palaeogene section in central West Greenland. Ice is shown white. Based on Survey maps.

with the Thyasira Member (Fig. 2; Rosenkrantz 1970) on the north coast of Nuussuaq. The derived Maastrichtian calcareous concretions in the Oyster-ammonite Conglomerate enclose a rich fauna including *Hypophylloceras (Neophylloceras) groenlandicum* Birkelund 1965, *Saghalinites wrighti* Birkelund 1965, *Baculites* cf. *B. meeki* Elias 1933, *Scaphites (Discoscaphites) waagei* Birkelund 1965, and *S. (D.) angmartussutensis* Birkelund 1965. In addition *Scaphites (Hoploscaphites)* cf. *S. (H.) ravni* Birkelund 1965, *S. (H.)* cf. *S. (H.) greenlandicus* Donovan 1953, *S. cobbani* Birkelund 1965 and *S. rosenkrantzi* Birkelund 1965 occur very occasionally and indicate that some concretions have been derived from the Campanian. The second fauna, from the Ikorfat pass (Fig. 1), 930 m above sea level and in Hamiteskløft some 15 km to the west, comprised what Birkelund called *Scaphites (Discoscaphites)* sp. aff. *S. (D.) angmartussutensis* Birkelund 1965 in sediments overlain by Tertiary pillow lava. *S. (D.) angmartussutensis* and *S. (D.)* aff. *S. (D.) angmartussutensis* were differentiated in that the latter has finer ribbing on the phragmocone, and, more immediately distinctive, broad folds in addition to fine ribs on the body chamber (e.g. compare Birkelund 1965, plate 40; plate 42, fig. 2; plate 43, fig. 1). Also linked to this occurrence were *Pseudophyllites* and *Diplomoceras* from nearby localities. In her conclusions (1965, p. 161) Birkelund states that "The difference between the *S. (Discoscaphites)* assemblage at Ikorfat and that in the Danian Oyster-ammonite Conglomerate may be explained by a small difference in age. Because the Maastrichtian at Ikorfat directly overlies the Upper Campanian these Maastrichtian deposits are probably older than most of the Maastrichtian fauna preserved in the Oyster-ammonite Conglomerate".

These views must now be revised. Figure 2 shows the log for the Annertuneq succession (modified after Nøhr-Hansen & Dam 1997, fig. 2). The top of the Conglomerate Member on the north side of Nuussuaq lies 122 m below the Cretaceous–Tertiary boundary as defined by the palynoflora. However, the conglomerate on the north coast of Nuussuaq yields no ammonites, but there are scattered ammonites from above the conglomerate (Fig. 2). All determinable specimens can be referred to what Birkelund called *S. (D.)* aff. *S. (D.) angmartussutensis*, here referred to *Hoploscaphites* Nowak 1911. They occur in a loose concretion collected 50 m above the top of the conglomerate (MMH 24530 from GGU 369906: Fig. 3A) and *in situ* at 112 m above the conglomerate (MMH 24531, 24532 from GGU 408892, 408893: Fig. 3B), only 10 m below the Cretaceous–Tertiary boundary.

Fig. 2. Stratigraphical log of the Annertuneq section, showing the position of the ammonites mentioned in the text. Modified from Nøhr-Hansen & Dam (1997).

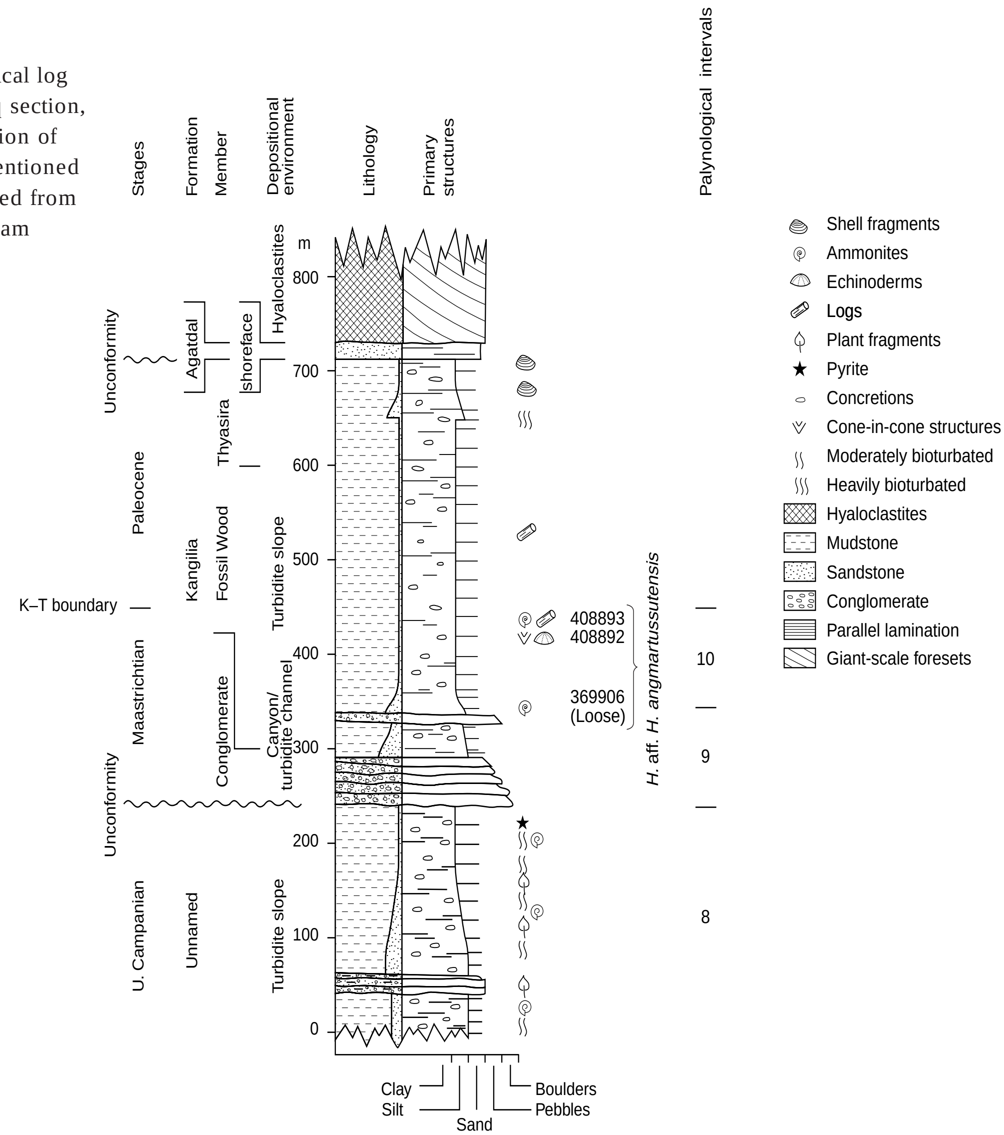

It will be seen that this new evidence shows *Hoploscaphites angmartussutensis* (Birkelund 1965) to be older than *H.* aff. *H. angmartussutensis* (Birkelund 1965), the reverse of the sequence inferred by Birkelund. To check our conclusions, dinoflagellates were extracted from the matrix of a number of Birkelund's original specimens. Matrix from the holotype of *H. angmartussutensis*, MMH 9846 (Birkelund 1965, plate 40, fig. 1) yielded *Isabelidinium* aff. *I. bujaki*, with the pollen species *Wodehouseia* absent, indicating the Early Maastrichtian *Cerodinium diebelii* interval (9). Matrix from MMH 9856, referred to *H.* aff. *H. angmartussutensis* by Birkelund (1965, plate 45, fig. 1), yielded *Wodehouseia spinata* and *W. quadrispina*, indicating a correlation with the Late Maastrichtian *Wodehouseia spinata* interval (10), supporting the sequence proposed above.

The relationship of the *H.* aff. *H. angmartussutensis* sequence to the dinoflagellate succession was further refined by the examination of dinoflagellates from the matrix of additional identifiable ammonites. The specimen of *H.* aff. *H. angmartussutensis* collected loose from 50 m above the conglomerate at Annertuneq (MMH 24530 from GGU 369906) and those from 10 m below the boundary (MMH 24531, 24532 from GGU 408892, 408893), all yielded assemblages of the *Wodehouseia spinata* interval (10).

None of the material from the ammonites examined contain the dinoflagellates *Palynodinum grallator* or *Disphaerogena carposphaeropsis*, which, according to Nøhr-Hansen & Dam (1997) represent the uppermost Maastrichtian in West Greenland.

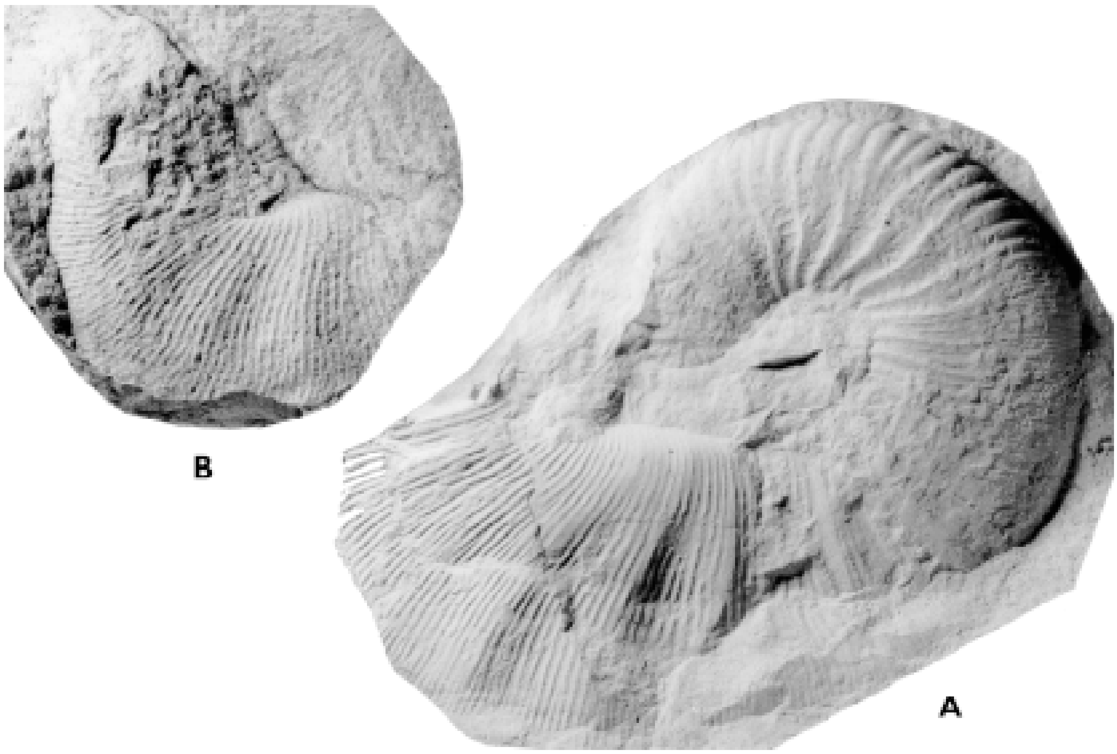

Fig. 3. *Hoploscaphites* aff. *H. angmartussutensis* (Birkelund 1965) from the Maastrichtian of Annertuneq. **A**: MMH 24530 (from GGU 366906), silicone cast from an external mould collected loose from 50 m above the top of the Conglomerate Member, 72 m below the Cretaceous–Tertiary boundary. **B**: MMH 24531 (from GGU 408892), collected *in situ* 112 m above the conglomerate, 10 m below the Cretaceous–Tertiary boundary. Figures × 1. MMH refers to numbers of the Geological Museum, Copenhagen; GGU refers to numbers of the former Geological Survey of Greenland, now in the files of the Geological Survey of Denmark and Greenland.

Conclusions

The Maastrichtian ammonite faunas from Nuussuaq, West Greenland, described by Birkelund (1965) are reappraised on the basis of newly published stratigraphic, sedimentological and dinoflagellate data. A lower assemblage, characterised by *Hoploscaphites angmartussutensis* (Birkelund 1965) is known only from reworked clasts in the Danian Oyster-ammonite Conglomerate in Agatdalen. The matrix of the holotype of *H. angmartussutensis* yields a flora indicating the Early Maastrichtian *Cerodinium diebelii* interval (9) of Nøhr-Hansen (1996). The succeeding sediments yield only *H.* aff. *H. angmartussutensis* (Birkelund 1965), collected loose at 50 m above the top of the Conglomerate Member on the north coast of Nuussuaq, and *in situ* 112 m above, 10 m below the Cretaceous–Tertiary boundary (Fig. 2). The matrix of concretions yielding this form, including Birkelund's original material, all yield dinoflagellates and pollen indicating the *Wodehouseia spinata* interval (10) of Nøhr-Hansen (1996). None of the ammonites collected to date are associated with *Palynodinium grallator* or *Disphaerogena carposphaeropsis,* floral indicators for the uppermost Maastrichtian.

Acknowledgements

We thank the Carlsberg Foundation for financial support, and W.K. Christensen (Geological Museum, University of Copenhagen) for technical advice. W.J. Kennedy acknowledges the technical support of the staff of the Department of Earth Sciences, Oxford, and Geological Collections, Oxford University Museum of Natural History. H. Midtgaard and C.J. Bjerrum are thanked for their finds of ammonites. J.H. Callomon, W.K. Christensen, T.C.R. Pulvertaft and W.S. Watt are thanked for critical reviews and suggestions to the manuscript.

References

Birkelund, T. 1965: Ammonites from the Upper Cretaceous of West Greenland. Bulletin Grønlands Geologiske Undersøgelse **56**, 192 pp. (also Meddelelser om Grønland **179**(7)).

Dam, G. & Sønderholm, M. 1994: Lowstand slope channels of the Itilli succession (Maastrichtian – Lower Paleocene), Nuussuaq, West Greenland. Sedimentary Geology **94**, 49–71.

Donovan, D.T. 1953: The Jurassic and Cretaceous stratigraphy and palaeontology of Traill Ø, East Greenland. Meddelelser om Grønland **111**(4), 148 pp.

Elias, M.K. 1933: Cephalopods of the Pierre Formation of Wallace County, Kansas, and adjacent area. Kansas University Science Bulletin **21**, 289–363.

Nøhr-Hansen, H. 1996: Upper Cretaceous dinoflagellate cyst stratigraphy, onshore West Greenland. Bulletin Grønlands Geologiske Undersøgelse **170**, 104 pp.

Nøhr-Hansen, H. & Dam, G. 1997: Palynology and sedimentology across a new Cretaceous–Tertiary boundary section on Nuussuaq, West Greenland. Geology **25**, 851–854.

Nowak, J. 1911: Untersuchungen über die Cephalopoden der oberen Kreide in Polen. II. Teil. Die Skaphiten. Bulletin de l'Academie des Sciences de Cracovie. Classe des Sciences Mathematiques et Naturelles. Série B. Sciences Naturelles for **1911**, 547–589.

Rosenkrantz, A. 1970: Marine Upper Cretaceous and lowermost Tertiary deposits in West Greenland. Meddelelser fra Dansk Geologisk Forening **19**, 406–453.

$^{40}Ar–^{39}Ar$ dating of alkali basaltic dykes along the south-west coast of Greenland: Cretaceous and Tertiary igneous activity along the eastern margin of the Labrador Sea

Lotte Melchior Larsen, David C. Rex, W. Stuart Watt and *Philip G. Guise*

A 380 km long coast-parallel alkali basalt dyke swarm cutting the Precambrian basement in south-western Greenland has generally been regarded as one of the earliest manifestations of rifting during continental stretching prior to break-up in the Labrador Sea. Therefore, the age of this swarm has been used in models for the evolution of the Labrador Sea, although it has been uncertain due to earlier discrepant K–Ar dates. Two dykes from this swarm situated 200 km apart have now been dated by the $^{40}Ar–^{39}Ar$ step-heating method. Separated biotites yield plateau ages of 133.3 ± 0.7 Ma and 138.6 ± 0.7 Ma, respectively. One of the dykes has excess argon. Plagioclase separates confirm the biotite ages but yield less precise results. The age 133–138 Ma is earliest Cretaceous, Berriasian to Valanginian, and the dyke swarm is near-coeval with the oldest igneous rocks (the Alexis Formation) on the Labrador shelf.

A small swarm of alkali basalt dykes in the Sukkertoppen (Maniitsoq) region of southern West Greenland was also dated. Two separated kaersutites from one sample yield an average plateau age of 55.2 ± 1.2 Ma. This is the Paleocene–Eocene boundary. The swarm represents the only known rocks of that age within several hundred kilometres and may be related to changes in the stress regime during reorganisation of plate movements at 55 Ma when break-up between Greenland and Europe took place.

L.M.L. & W.S.W., *Geological Survey of Denmark and Greenland, Thoravej 8, DK-2400 Copenhagen NV, Denmark.* Also *Danish Lithosphere Centre, Øster Voldgade 10, DK-1350 Copenhagen K, Denmark.* E-mail: *lml@geus.dk*
D.C.R. & P.G.G., *Department of Earth Sciences, The University, Leeds LS2 9JT, UK.*

Keywords: basaltic dykes, geochronology, Labrador Sea, south-western Greenland, Tertiary

The Labrador Sea between Labrador (Canada) and south-western Greenland (Fig. 1) has a long history of slow extension and basin formation leading up to continental rupture and the start of ocean-floor spreading (e.g. Balkwill *et al.* 1990). The time of the start of extension and the time of continental rupture are important parameters for models of the extension process and the extension rate (e.g. Chian *et al.* 1995a, b; Chalmers *et al.* 1997), and for the interpretation of the geology and hydrocarbon potential in the offshore areas (Chalmers *et al.* 1993; 1995a). However, neither of these times are well constrained. The start of ocean-floor spreading is placed between magnetic anomalies 33 and 27 and cannot at present be more precisely defined owing to the anomalous character of the crust in question (Roest & Srivastava 1989; Chian & Louden 1994; Chalmers & Laursen 1995; Chian *et al.* 1995a, b; Srivastava & Roest 1995; Chalmers 1997).

Ages varying from 160 Ma to 130 Ma have been used to define the onset of rifting between Labrador and Greenland (160 Ma: Chian & Louden 1994; Chian *et al.* 1995b; 130–135 Ma: Keen *et al.* 1994; Chian *et al.* 1995a; Chalmers 1997). Well stratigraphy in the Labrador Sea basins indicates that rifting started there in the early Cretaceous at around 130 Ma. Other evidence comes from the dating of dykes in West Greenland. Watt (1969) described an extensive, coast-parallel swarm of dykes along the south-west coast of Greenland. Their extent, dip directions, and coast-parallel behaviour suggest that they were emplaced during a

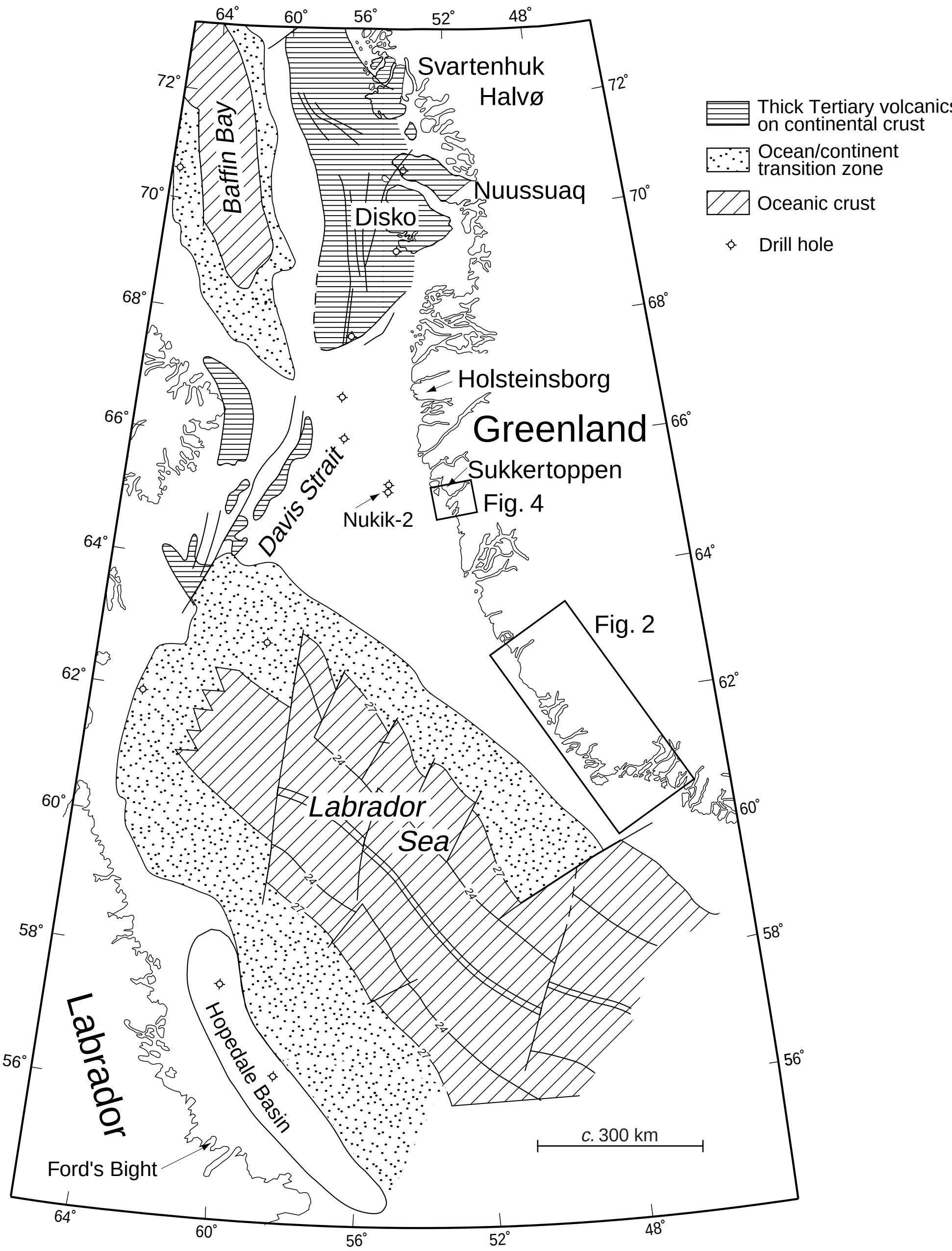

Fig. 1. Map of the Labrador Sea and surrounding areas, after Whittaker (1995). Details of the two dated dyke swarms are given in Figs 2 and 4.

major regional rifting event. This is the earliest known indication of a regional rifting event on the Greenland side of the Labrador Sea. Watt (1969) reported a whole-rock K–Ar age of 138 Ma for one basalt dyke but also noted that a lamprophyre dyke cutting a basalt dyke gave a K–Ar biotite age of 162 Ma – hence the two different ages for the start of extension used by different authors as noted above. The age discrepancy may be caused either by excess argon in the 'old' sample or by loss of argon from the 'young' sample; the K–Ar dating method does not allow distinction between these two possibilities.

Other Mesozoic igneous rocks in western Greenland are mafic alkaline and undersaturated rocks such as kimberlites and lamprophyres which form small dyke swarms occurring intermittently from Ivittuut in the south to Sukkertoppen (Maniitsoq) in the north (Figs 1, 2; Larsen & Rex 1992). These rocks have ages up to 200 Ma and do not appear to be related to any regional tectonic events. In contrast, later Tertiary igneous activity related to continental break-up gave rise to the voluminous tholeiitic flood lavas farther north in the Disko – Svartenhuk Halvø region (e.g. Clarke & Pedersen 1976). A small swarm of alkali basaltic dykes of hitherto unknown age occurs in the Sukkertoppen area some 300 km north of the major coast-parallel dyke swarm and 500 km south of the onshore Tertiary igneous rocks (Fig. 1).

The objective of this work is to constrain better the onset of continental extension in the Labrador Sea by new dating of the coast-parallel dyke swarm with the ^{40}Ar–^{39}Ar step-heating method. The results show that the older K–Ar age of 162 Ma is in error. The Sukkertoppen dyke swarm was included in the present dating project, and a Tertiary age is reported.

Analytical procedures

The ^{40}Ar–^{39}Ar analyses were carried out at the University of Leeds, UK, and the analytical procedures followed those outlined in Rex *et al.* (1993). Standard hornblendes Fy12a, MMHb1 and Hb3gr and biotite LP-6 were used for J calibrations. In addition, Tinto biotite (409 Ma), a Leeds laboratory standard, was also used. All irradiations were carried out at the Ford reactor, Ann Arbor, Michigan, USA. Two irradiations (Runs 1426, 1428 and 1534, 1536, Table 2) were of duration 50 hours in position L67. Runs 1896 and 1897 (Table 3) were of duration 48 hours in position H75. Correction factors used for runs 1426 and 1428 were (40/39)K = 0.031, (37/39)Ca = 1280 and (36/39)Ca = 0.26. The remaining runs used correction factors (40/39)K = 0.031, (37/39)Ca = 1000 and (36/39)Ca = 0.24. Errors are quoted at the one sigma level. Correlation plot data were processed using the program 'Isoplot' (Ludwig 1990).

South-West Greenland coast-parallel dyke swarm

The dykes in this swarm occur in a broad, up to 30 km wide strip that stretches along the coast for about 380 km from Sydprøven in the south to Frederikshåb Isblink in the north (Fig. 2; Watt 1969; Nielsen 1987). The dykes strike parallel to the coast and follow the direction of the coast also in the south where it abruptly changes direction. Because of the parallel alignment of the dykes, cross-cutting relations are very rarely observed. The dykes are on average 10 m thick, with dips usually near vertical except in the south-westernmost part of the swarm, on the Nunarsuit peninsula, where the dips become shallower towards the coast, to *c.* 30° seawards. The rocks are doleritic with subophitic to intergranular textures. They consist of plagioclase, brown augite, Fe-Ti-oxides, olivine, minor amounts of brown primary biotite, accessory apatite, and sometimes some green secondary biotite. Many rocks are relatively unaltered, with preserved fresh olivine, but all have somewhat clouded plagioclase. Chemical analyses of the two dated rocks are given in Table 1. According to the IUGS chemical classification system (Le Maitre 1989) one sample is an alkali basalt and the other is a basalt.

Two samples were chosen for Ar–Ar dating: GGU 45293 from the southern part of the swarm and GGU

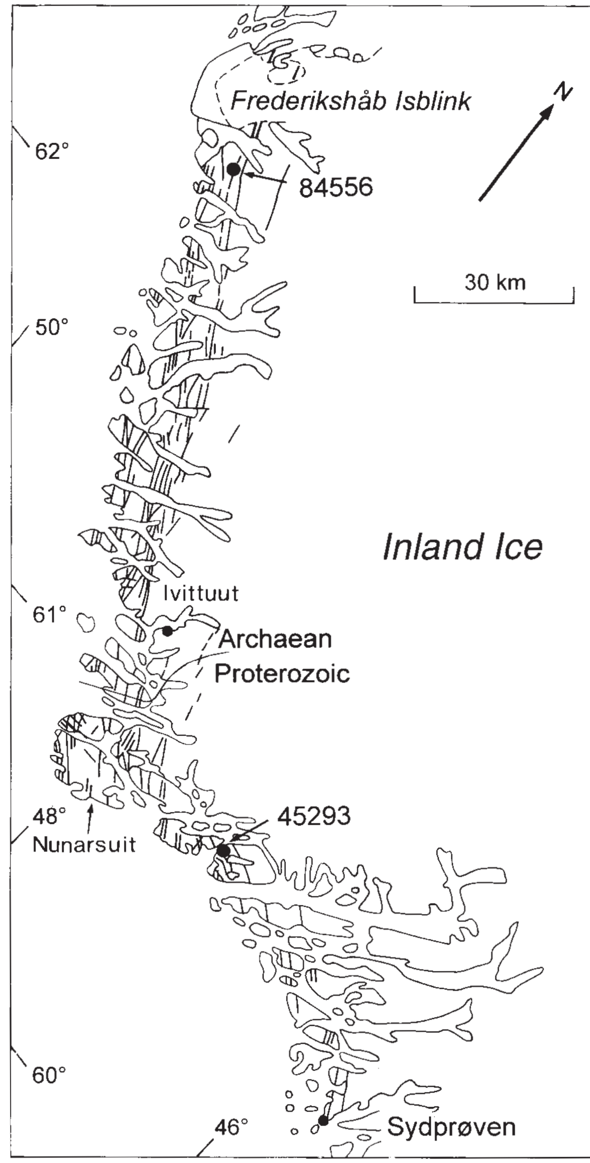

Fig. 2. The South-West Greenland coast-parallel dyke swarm. The locations of the two dated samples GGU 45293 and GGU 84556 are indicated.

Table 1. Chemical analyses of alkali basaltic dykes from south-western Greenland

GGU no.	45293	84556	265424	265880
SiO_2	44.79	45.71	45.67	44.78
TiO_2	3.99	2.75	1.95	1.31
Al_2O_3	14.30	15.04	16.24	14.00
Fe_2O_3	4.02	5.14	1.71	2.42
FeO	10.47	7.32	7.18	6.45
MnO	0.23	0.21	0.12	0.16
MgO	4.93	6.29	4.61	9.97
CaO	9.20	10.81	6.83	11.00
Na_2O	3.50	2.65	3.59	1.96
K_2O	1.37	0.87	2.19	2.48
P_2O_5	1.45	0.70	0.53	0.62
Vol	1.46	2.10	8.92	4.30
	99.71	99.59	99.54	99.44
Rb	29	15	57	78
Ba	856	1038	1194	1790
Pb	7	6	8	6
Sr	949	634	1016	1090
La	46	25	91	125
Ce	95	54	156	211
Nd	49	29	53	69
Y	30	23	21	20
Th	4	4	10	14
Zr	137	82	237	146
Nb	45	23	71	141
Zn	141	115	87	76
Cu	41	55	37	74
Co	36	47	31	49
Ni	12	86	34	204
Sc	19	22	16	20
V	240	322	140	177
Cr	6	129	38	636
Ga	31	28	19	16

Major elements (in wt%): GEUS' Rock Geochemical Laboratory, mainly XRF analyses; FeO by titration and Na_2O by AAS.
Vol: Loss on ignition corrected for iron oxidation during ignition.
Trace elements (in ppm): J.C. Bailey, Geological Institute, University of Copenhagen, XRF analyses.
Samples GGU 45293 and 84556 from the South-West Greenland coast-parallel dyke swarm. Locations in Fig. 2.
Samples GGU 265424 and 265880 from the Sukkertoppen dyke swarm. Locations in Fig. 4.

84556 from the northern part (locations in Fig. 2). Plagioclase and biotite were separated from each sample and dated independently. The results are given in Table 2 and shown in Fig. 3. The biotites from both samples give well defined plateau ages of 133.3 ± 0.7 Ma and 138.6 ± 0.7 Ma respectively, and isochron ages on correlation diagrams (intercept ages) of 133.2 ± 0.8 Ma and 136 ± 4 Ma respectively (errors quoted at 1σ level). The isochron ages are within 1σ of each other, and the average age is 135 Ma. The two plagioclase separates show much less well-defined age plateaus. Selected steps representing in all 39.0% and 26.5% released argon give 122.7 ± 0.8 Ma and 140.9 ± 0.8 Ma, respectively, with isochron ages on correlation diagrams of 127 ± 12 Ma and 134 ± 12 Ma. The plagioclase data thus support the biotite ages but have considerably larger uncertainties.

In the correlation diagrams the minerals from the southern sample (45293) show $^{40}Ar/^{36}Ar$ intercepts within errors of the atmospheric value (295.5). In contrast, both biotite and plagioclase from the northern sample (84556) have $^{40}Ar/^{36}Ar$ intercepts considerably higher than the atmospheric value, indicating that excess argon is present in this sample. The two samples are petrographically quite similar although 84556 is more altered than 45293. The most obvious difference between them is that the southern dyke is intruded into Proterozoic basement of age around 1800 Ma whereas the northern dyke is intruded into Archaean basement of age around 2800 Ma (Kalsbeek *et al.* 1990). An apparent dependence of the argon spectra on the nature of the side wall was also found by Reid & Rex (1994) in the Mehlberg dyke in southern Africa. The part of this dyke that cuts high-K granitoids contains excess argon, whereas the part of the dyke that cuts massive K-poor quartzites does not. Regional variations in excess argon in basement rocks have been found across the Grenville Front in Ontario and are ascribed to interaction of mineral blocking trajectories with the ambient pressure of argon (Smith *et al.* 1994). A similar explanation may apply to igneous rocks intruded into basement of different ages and lithology.

Sukkertoppen dyke swarm

The dykes in this swarm were found during prospecting work by Kryolitselskabet Øresund A/S and were described in a company report by Juhava (1974). The dykes occur in a *c.* 20 km by 40 km area east of the town Sukkertoppen (Maniitsoq) (Fig. 4). It is possible

Table 2. Results of stepwise degassing of separated biotite and plagioclase from the South-West Greenland coast-parallel dyke swarm

Step	T °C	$^{39}Ar_K$	$^{37}Ar_{Ca}$	$^{38}Ar_{Cl}$	Ca/K	$^{40}Ar^*/^{39}Ar_K$	% $^{40}Ar_{Atm}$	Age, Ma	Error, Ma	%^{39}Ar
GGU 45293 biotite Run no. 1428, J = 0.01017 ± 0.5%										
1	600	5.3	0.91	0.97	0.34	2.622	48.2	47.5	7.4	1.5
2	680	4.7	0.33	0.36	0.14	7.444	58.2	131.7	1.1	1.3
3	720	17.9	0.27	0.83	0.03	7.521	12.7	133.0	0.6	4.9
4	750	23.4	0.20	0.89	0.02	7.485	6.9	132.4	0.4	6.4
5	785	34.4	0.23	1.21	0.01	7.490	3.4	132.4	0.3	9.4
6	835	49.9	0.30	1.82	0.01	7.523	1.7	133.0	0.5	13.7
7	940	71.1	0.45	2.87	0.01	7.584	1.7	134.1	0.3	19.5
8	1075	151.4	1.22	4.22	0.02	7.554	2.4	133.5	0.3	41.6
9	1250	5.8	2.05	0.15	0.71	30.55	4.3	488.2	1.4	1.6
Plateau age = 133.3 ± 0.7 Ma (steps 2–8); intercept age = 133.2 ± 0.8 Ma.										
$^{40}Ar^*/^{39}Ar_K$ = 7.834 ± 0.2; Wt% K = 8.5; $^{40}Ar^*$ = 477 × 10^{-7} cm^3g^{-1}.										
GGU 84556 biotite Run no. 1534, J = 0.01041 ± 0.5%										
1	630	2.0	0.91	0.42	0.92	59.39	7.6	868.4	1.9	0.8
2	705	2.4	0.20	0.35	0.16	11.65	49.6	206.5	3.1	0.9
3	750	5.8	0.24	0.70	0.08	9.541	14.8	170.8	0.7	2.3
4	790	9.2	0.23	0.83	0.05	8.781	9.2	157.8	1.4	3.6
5	840	15.9	0.29	1.22	0.04	8.254	5.3	148.7	0.4	6.3
6	945	42.5	0.55	2.89	0.03	8.131	2.7	146.6	0.6	16.8
7	1040	63.4	0.55	3.51	0.02	7.708	2.3	139.2	0.3	25.1
8	1110	87.3	1.01	3.20	0.02	7.634	1.3	138.0	0.2	34.5
9	1340	24.4	5.55	0.78	0.45	7.691	3.3	139.0	0.4	9.6
Plateau age = 138.6 ± 0.7 Ma (steps 7–9); intercept age = 136 ± 4 Ma.										
$^{40}Ar^*/^{39}Ar_K$ = 8.309 ± 0.14; Wt% K = 5.6; $^{40}Ar^*$ = 341 × 10^{-7} cm^3g^{-1}.										
GGU 45293 plagioclase Run no. 1426, J = 0.01056 ± 0.5%										
1	600	3.2	8.5	0.19	5.29	7.828	77.9	143.3	19.0	2.6
2	720	8.0	13.5	0.09	3.36	6.792	56.7	125.0	1.1	6.5
3	805	8.7	14.0	0.06	3.19	7.437	17.0	136.4	0.6	7.1
4	905	7.8	6.6	0.06	1.68	6.710	23.6	123.5	1.2	6.4
5	985	13.1	4.9	0.14	0.75	6.547	27.3	120.6	0.6	10.7
6	1070	26.8	9.4	0.44	0.70	6.707	27.1	123.5	0.3	21.9
7	1130	37.7	14.5	0.77	0.76	7.104	25.7	130.5	0.3	30.8
8	1200	12.5	14.8	0.49	2.36	7.847	35.4	143.6	0.5	10.2
9	1325	4.8	12.4	0.24	5.15	8.012	41.6	146.5	1.0	3.9
Total gas age = 129.8 ± 0.6 Ma; intercept age = 127 ± 12 Ma.										
$^{40}Ar^*/^{39}Ar_K$ = 7.066 ± 0.4; Wt% K = 2.4; $^{40}Ar^*$ = 124 × 10^{-7} cm^3g^{-1}.										
GGU 84556 plagioclase Run no. 1536, J = 0.01041 ± 0.5%										
1	600	1.7	5.4	0.07	6.17	16.74	43.7	289.8	3.3	2.3
2	780	9.0	18.7	0.12	4.16	8.186	23.9	147.5	0.5	11.7
3	910	12.5	20.8	0.16	3.30	7.813	4.5	141.1	0.6	16.4
4	1015	9.1	6.0	0.13	1.31	7.789	6.7	140.6	0.9	11.9
5	1070	8.5	4.9	0.14	1.15	8.044	9.1	145.1	1.0	11.1
6	1105	11.2	4.4	0.20	0.78	8.211	10.0	148.0	0.6	14.6
7	1145	17.0	7.6	0.33	0.89	8.923	10.8	160.2	0.4	22.3
8	1330	7.5	17.2	0.31	4.59	15.04	11.4	262.4	1.0	9.8
Total gas age = 163.2 ± 0.3 Ma; intercept age = 134 ± 12 Ma.										
$^{40}Ar^*/^{39}Ar_K$ = 9.094 ± 0.2; Wt% K = 1.8; $^{40}Ar^*$ = 119 × 10^{-7} cm^3g^{-1}.										

Columns 3–5 are volumes (× 10^{-9} cm^3). $^{40}Ar^*$ = radiogenic ^{40}Ar, gas volumes corrected to S.T.P.
Errors are quoted at the 1σ level.

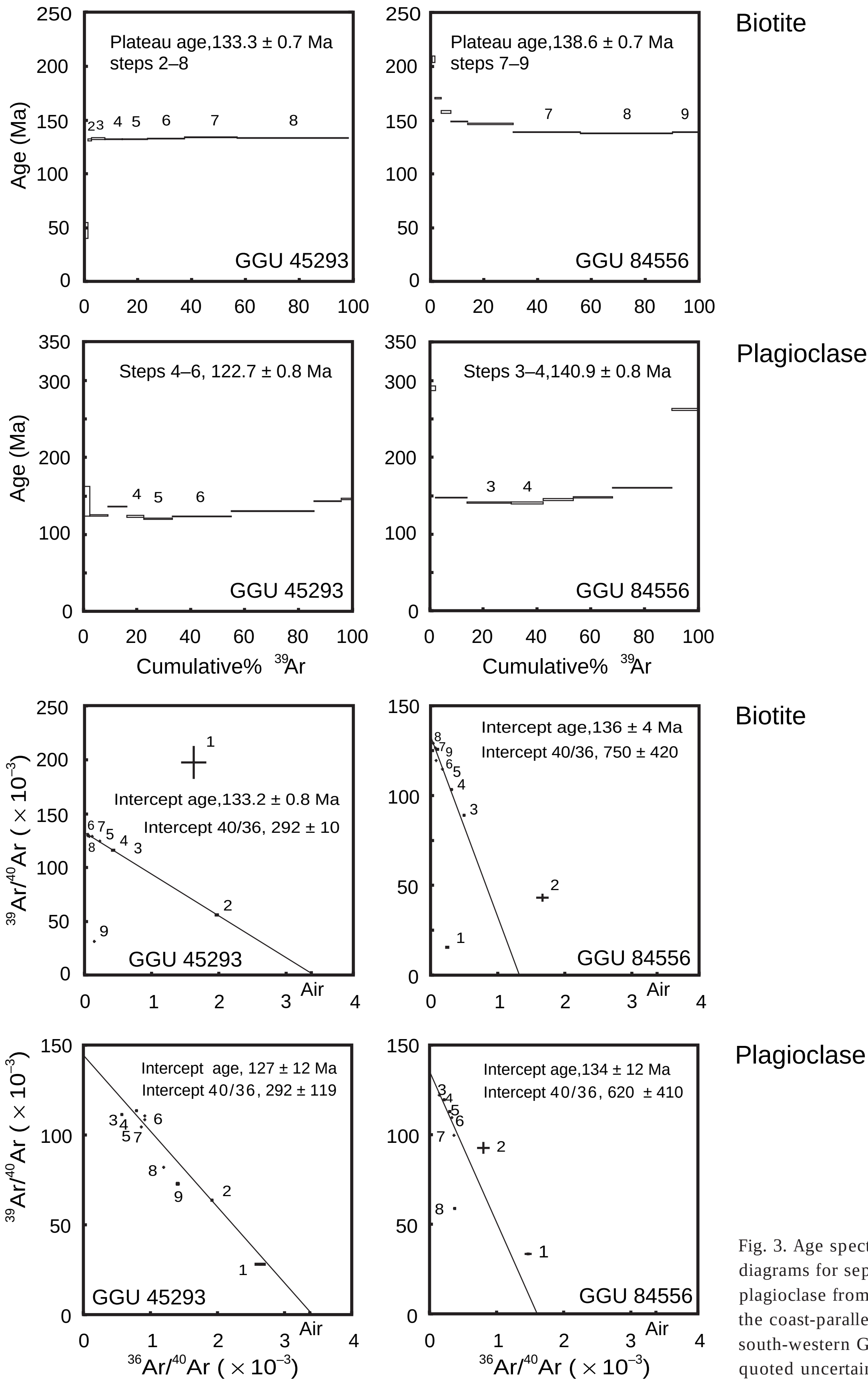

Fig. 3. Age spectra and correlation diagrams for separated biotite and plagioclase from two samples from the coast-parallel dyke swarm in south-western Greenland. The quoted uncertainties are 1σ.

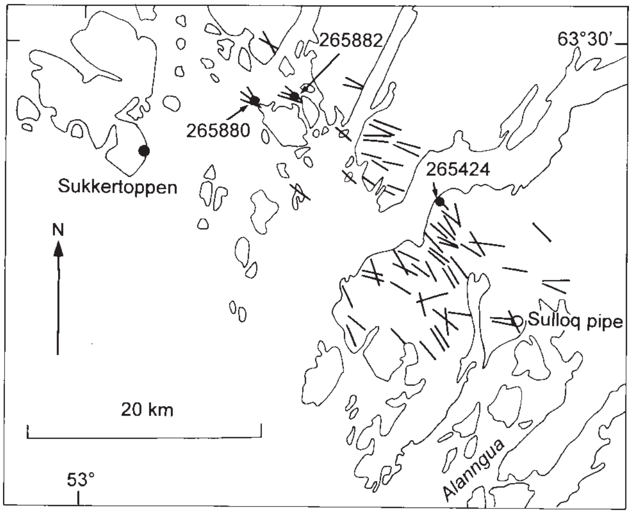

Fig. 4. The Sukkertoppen dyke swarm, after Juhava (1974). The dykes are shown schematically by strike lines with exaggerated lengths. In the field, each dyke can only be followed over a short distance. The locations of the dated (GGU 265882) and analysed (GGU 265424 and 265880) samples are indicated.

that they continue farther to the north; this area was not investigated. The dykes strike mostly NW, approximately parallel to the coast in the area, but the strikes vary between N and W. Dips are steep. The dykes are usually 0.2–2 m thick, with variable thickness along strike and frequent *en echelon* displacements. They have brownish pitted weathering surfaces. Many dykes have a zonal structure with contact-parallel variations in grain size and mineral distribution. At Alanngua fjord one dyke shows a diatreme-like, 45 m by 65 m enlargement named the Sulloq pipe (Fig. 4). This is rich in gneiss inclusions, but no mantle inclusions have been found.

The dykes are porphyritic and are described by Juhava (1974) as lamprophyres because of the ubiquitous mafic phenocrysts. However, many samples also have plagioclase phenocrysts. Chemically, they are potassic trachybasalts and basalts (Le Maitre 1989). The appropriate lamprophyre name would be camptonite (Rock 1991). Two analyses are presented in Table 1.

Table 3. Results of stepwise degassing of separated amphibole from the Sukkertoppen dyke swarm

Step	*T* °C	$^{39}Ar_K$	$^{37}Ar_{Ca}$	$^{38}Ar_{Cl}$	Ca/K	$^{40}Ar^*/^{39}Ar_K$	% $^{40}Ar_{Atm}$	Age, Ma	Error, Ma	%^{39}Ar
GGU 265882 kaersutite		Run no. 1896, J = 0.00257 ± 0.5%								
1	725	0.07	0.17	0.01	4.90	8.08	98.4	37.1	73.3	0.8
2	975	0.12	0.24	0.02	4.10	24.79	54.4	111.4	17.1	1.3
3	1040	2.40	9.18	0.83	7.61	11.70	16.7	53.4	0.8	27.2
4	1065	2.69	10.54	0.90	7.80	12.32	5.6	56.2	1.0	30.4
5	1085	1.42	5.69	0.45	7.98	12.85	3.9	58.6	2.5	16.0
6	1115	0.28	1.20	0.09	8.50	14.80	14.3	67.3	3.9	3.2
7	1210	0.89	4.59	0.29	10.30	13.41	12.2	61.1	1.4	10.0
8	1340	0.98	5.24	0.31	10.65	25.94	18.0	116.4	2.9	11.1
Plateau age = 55.7 ± 0.8 Ma (steps 3–5).										
$^{40}Ar^*/^{39}Ar_K$ = 14.06 ± 1.4; Wt% K = 0.9; $^{40}Ar^*$ = 24.1 × 10^{-7} cm^3g^{-1}.										
GGU 265882 kaersutite		Run no. 1897, J = 0.00258 ± 0.5%								
1	735	0.07	0.16	0.01	4.26	42.74	91.9	188.7	39.5	0.7
2	825	0.04	0.04	0.00	2.09	66.61	22.9	286.1	35.3	0.4
3	945	0.05	0.09	0.01	3.41	16.59	75.6	75.6	18.6	0.5
4	980	0.05	0.12	0.01	5.41	29.80	58.2	133.6	44.5	0.4
5	1025	0.66	2.50	0.24	7.52	11.55	33.1	53.0	4.0	6.4
6	1075	5.24	20.39	1.78	7.74	11.73	10.4	53.8	0.5	50.8
7	1145	2.86	11.63	0.93	8.09	12.39	5.0	56.8	0.6	27.7
8	1330	1.35	7.58	0.43	11.18	23.49	10.6	106.1	1.5	13.1
Plateau age = 54.7 ± 0.5 Ma (steps 5–7).										
$^{40}Ar^*/^{39}Ar_K$ = 13.96 ± 1.0; Wt% K = 1.0; $^{40}Ar^*$ = 24.7 × 10^{-7} cm^3g^{-1}.										

Columns 3–5 are volumes (× 10^{-9} cm^3). $^{40}Ar^*$ = radiogenic ^{40}Ar, gas volumes corrected to S.T.P.
Errors are quoted at the 1σ level.

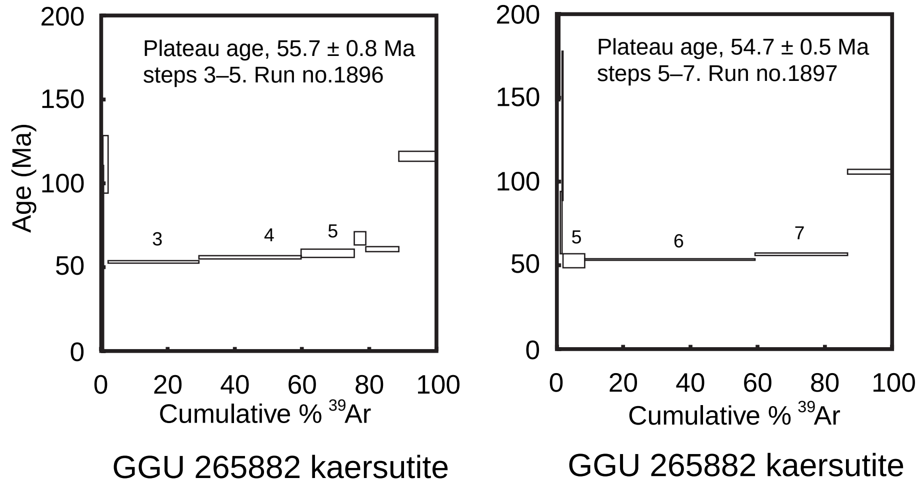

Fig. 5. Age spectra for two kaersutite separates from one sample from the Sukkertoppen dyke swarm.

The mafic phenocrysts are augite, kaersutite and olivine in varying proportions. The groundmass has panidiomorphic-granular to intersertal texture and consists of augite, plagioclase, kaersutite, Fe-Ti-oxides, brown mica, apatite, and a nearly isotropic matrix of zeolite(?). The rock may contain ocelli filled with carbonate or zeolite or both. The dated sample (GGU 265882) contains up to 1 cm kaersutite megacrysts which were separated for dating.

Two samples were originally selected for separation and dating of kaersutite (no samples had sufficient amounts of mica). Kaersutite from sample GGU 265880 was run in duplicate with disappointing results. The very low potassium content resulted in poor spectra and uncertain correlation plot isochron ages (53 ± 15 and 70 ± 12 Ma). The first analysis of sample GGU 265882 was spoilt by operational difficulties resulting in one step with age 54.7 ± 1.8 Ma from 75% of the gas and a correlation plot isochron age of 56 ± 10 Ma. A new separate was subsequently analysed in duplicate, and the results are shown in Table 3 and Fig. 5. The mean of two plateau ages is 55.2 ± 1.2 Ma. The correlation plots produced very poor isochrons (not shown). In both runs the last heating step produced excess argon. How this argon is hosted in apparently homogeneous megacrysts is not clear; the side wall is of Archaean age and there may be a side wall effect as described above for the coast-parallel dyke swarm.

Discussion

The development of the Labrador Sea during the Mesozoic and Tertiary is known from reflection and refraction seismic surveys, magnetic profiling, and exploratory wells drilled on the shelves of both West Greenland and eastern Canada. Data from the Canadian side have been reviewed by Balkwill *et al.* (1990) and Keen *et al.* (1990) and the igneous rocks by Pe-Piper *et al.* (1990). Data from the Greenland side have been summarised by Chalmers *et al.* (1993, 1995a). In the following, the absolute ages given for chronostratigraphic units are from Gradstein *et al.* (1994).

Start of extension in the Labrador Sea area

The oldest rocks known from the Labrador–Greenland basins are the volcanic rocks of the Alexis Formation drilled in wells in the Hopedale Basin on the Labrador shelf (Fig. 1). Rocks from the Alexis Formation have yielded whole-rock K–Ar ages in the interval 139–104 Ma, i.e. Early Cretaceous (Umpleby 1979). They are reported to be alkali basalts (Balkwill *et al.* 1990; Williamson *et al.* 1995), but no analyses are published. Possible coeval onshore igneous rocks are lamprophyre–carbonatite dykes at Ford's Bight on the coast of central Labrador (King & McMillan 1975), K–Ar dated at 145 and 129 Ma (Umpleby 1979). The Alexis Formation is overlain by the sedimentary Bjarni Formation, and the oldest age assigned to this is Barremian (127–121 Ma) based on spores and pollen (Umpleby 1979).

On the Greenland shelf, the oldest sequences have not been drilled. Chalmers *et al.* (1993) tentatively correlated the oldest sequence (Kitsissut sequence) with the lower Bjarni Formation on the Labrador shelf. It is not known whether the Kitsissut sequence includes igneous rocks or whether igneous intrusive rocks of similar age are present in the offshore areas. Chalmers *et al.* (1993) suggested that the main phase of rifting is represented by the overlying Appat sequence which is correlated with the upper Bjarni Formation of Albian age (112–99 Ma).

Onshore West Greenland, Mesozoic igneous rocks form two age groups (Larsen & Rex 1992). One broad group at 220–166 Ma comprises small dyke swarms of kimberlite, carbonatite, and ultramafic and alkaline lamprophyre. These rocks show no obvious tectonic relations to regional rifting events. A younger group at 141–119 Ma includes the coast-parallel dyke swarm considered here and also comprises ultramafic and alkaline lamprophyre dykes north of Frederikshåb Isblink (Hansen & Larsen 1974). These lamprophyre dykes occur at the northernmost extent of the regional coastal dyke swarm and may be related to it; the age interval is right but is too broad to allow any firm conclusions on the relationship.

The South-West Greenland coast-parallel dyke swarm dated in this work is generally regarded as one of the earliest manifestations of rifting in the Labrador Sea region (Watt 1969; Balkwill *et al.* 1990; Pe-Piper *et al.* 1990; Chalmers *et al.* 1993; Chian & Louden 1994, Chian *et al.* 1995b). The dyke swarm is situated adjacent to that part of the Labrador Sea where sea-floor spreading subsequently took place, whereas the swarm is not present farther north adjacent to the broad and tectonically complicated continental shelf areas of the northern Labrador Sea and the Davis Strait (Fig. 1; e.g. Chalmers *et al.* 1995a). The two dated samples are situated 200 km apart (Fig. 2). Although the biotite *plateau* ages of 133.3 ± 0.7 Ma and 138.6 ± 0.7 Ma suggest that the southern sample (45293) may be slightly younger than the northern sample (84556), the biotite *isochron* ages of 133 ± 0.8 Ma and 136 ± 4 Ma are within the analytical uncertainty of each other. This supports the notion that the coast-parallel dyke swarm was emplaced along its entire length within a short time span as a consequence of a regional stretching event. Our data indicate that this event is of earliest Cretaceous age, Berriasian to Valanginian, and that the earlier age determination of 162 Ma (Watt 1969) is in error. The dyke swarm is nearly coeval with the alkali basalts of the Alexis Formation on the Labrador shelf, perhaps slightly older. More precise dating of the Alexis Formation is necessary to determine if these igneous rocks situated on conjugate rift margins were produced in the same event.

Tertiary rocks

Tertiary igneous rocks are widespread and voluminous in the Labrador Sea – Davis Strait region. Biostratigraphic and radiometric (mostly K–Ar) ages of drilled and onshore exposed rocks are dominantly Paleocene, ranging back into the late Cretaceous (Balkwill *et al.* 1990; Pe-Piper *et al.* 1990; Larsen *et al.* 1992; Storey *et al.* 1998). The start of normal velocity ocean floor spreading in the Labrador Sea took place in the Paleocene, around geomagnetic chrons C27–C28 (61–63 Ma, Berggren *et al.* 1995) (Chalmers 1991; Chian & Louden 1994; Chalmers & Laursen 1995) and was accompanied by a burst in volcanic activity, where large amounts of tholeiitic picrites and basalts were erupted onto the continental margins of West Greenland and Labrador (Clarke & Pedersen 1976; Chalmers *et al.* 1995b; Storey *et al.* 1998). This period of volcanic activity ended at about 59 Ma (Storey *et al.* 1998). Eocene volcanic activity in West Greenland at around 52 Ma is also reported by Storey *et al.* (1998), and intrusion of sills and dykes took place between the two volcanic episodes.

The age of 55.2 ± 1.2 Ma obtained in this work for the alkali basalt dyke swarm in the Sukkertoppen area is unusual in West Greenland, the only other known examples being some dykes and sills on Disko and Nuussuaq *c.* 400 km north of Sukkertoppen (Storey *et al.* 1998). South of Disko Bugt (69°N) the Sukkertoppen dyke swarm represents the only known occurrence of onshore Tertiary rocks. Offshore, 100 km due west of Sukkertoppen, the Nukik-2 well (Fig. 1) terminated in tholeiitic dolerites of Paleocene age according to biostratigraphy (Rolle 1985) and K–Ar dating (68–62 Ma; Hald & Larsen 1987) and thus apparently unrelated to the onshore dyke swarm. The Sukkertoppen dykes have no obvious relations to other features either onshore or offshore, although the arcuate trend of the swarm (Fig. 4) is reminiscent of the arcuate fault pattern seen offshore between Sukkertoppen (Maniitsoq) and Holsteinsborg (Sisimiut) (Fig. 1; Chalmers *et al.* 1995a). However, 55 Ma (magnetochron C24r) is the time at which sea-floor formation started along the East Greenland margin (Talwani & Eldholm 1977), accompanied by reorganisation of the plate movements on a regional scale. Even though the Sukkertoppen dyke swarm is far removed from the sites of construction of new ocean floor (min. 500 km), it is possible that stresses related to the plate reorganisation and the opening in the east could have produced tension in the west, leading to reactivation of old faults and small degrees of melting and production of the alkaline dyke swarm.

Conclusions

$^{40}Ar–^{39}Ar$ ages for two samples situated 200 km apart in the 380 km long coast-parallel dyke swarm in South-West Greenland indicate that the swarm was emplaced within a short time interval in the earliest Cretaceous, 133–138 Ma (Berriasian to Valanginian). An age of 162 Ma reported by Watt (1969) is thus in error. The coast-parallel dyke swarm comprises the oldest known rocks (igneous or other) that can be related to regional rifting in the Labrador Sea region. Possibly coeval igneous rocks on the Labrador side are the offshore basalts of the Alexis Formation, known from drill holes.

An $^{40}Ar–^{39}Ar$ age for kaersutite from one sample from a small swarm of alkali basalt dykes in the Sukkertoppen region indicates an Early Tertiary age, around the Paleocene–Eocene boundary at 55 Ma. These rocks are the only known Tertiary igneous rocks onshore in West Greenland south of Disko Bugt, although older (Paleocene) tholeiitic basalts occur offshore adjacent to the Sukkertoppen region. The activity at 55 Ma may be caused by tension due to changes in the stress regime during reorganisation of plate movements and the onset of sea-floor spreading along the East Greenland margin.

Acknowledgements

Jim Chalmers, Chris Pulvertaft and Asger Ken Pedersen are thanked for valuable discussions and comments on the manuscript.

References

Balkwill, H.R., McMillan, N.J., Maclean, B., Williams, G.L. & Srivastava, S.P. 1990: Geology of the Labrador Shelf, Baffin Bay, and Davis Strait. In: Keen, M.J. & Williams, G.L. (eds): Geology of the continental margin of eastern Canada. Geology of Canada **2**, 293–348. Ottawa: Geological Survey of Canada (also The geology of North America **I-1**, Geological Society of America).

Berggren, W.A., Kent, D.V., Swisher, C.C. & Aubry, M.-P. 1995: A revised Cenozoic geochronology and chronostratigraphy. In: Berggren, W.A. *et al.* (eds): Geochronology, time scales and global stratigraphic correlation. Special Publication Society of Economic Palaeontologists and Mineralogists **54**, 129–212.

Chalmers, J.A. 1991: New evidence on the structure of the Labrador Sea/Greenland continental margin. Journal of the Geological Society (London) **148**, 899–908.

Chalmers, J.A. 1997: The continental margin off southern Greenland – along-strike transition from a volcanic margin. Journal of the Geological Society (London) **154**, 571–576.

Chalmers, J.A. & Laursen, K.H. 1995: Labrador Sea: the extent of continental crust and the timing of the start of sea-floor spreading. Marine and Petroleum Geology **12**, 205–217.

Chalmers, J.A., Pulvertaft, T.C.R., Christiansen, F.G., Larsen, H.C., Laursen, K.H. & Ottesen, T.G. 1993: The southern West Greenland continental margin: rifting history, basin development, and petroleum potential. In: Parker, J.R. (ed.): Petroleum geology of Northwest Europe: Proceedings of the 4th Conference, 915–931. London: Geological Society.

Chalmers, J.A., Dahl-Jensen, T., Bate, K.J. & Whittaker, R.C. 1995a: Geology and petroleum prospectivity of the region offshore southern West Greenland – a summary. Rapport Grønlands Geologiske Undersøgelse **165**, 13–21.

Chalmers, J.A., Larsen, L.M. & Pedersen, A.K. 1995b: Widespread Paleocene volcanism around the northern North Atlantic and Labrador Sea – evidence for a large, hot, early plume head. Journal of the Geological Society (London) **152**, 965–969.

Chian, D. & Louden, K.E. 1994: The continent-ocean crustal transition across the southwest Greenland margin. Journal of Geophysical Research **99**, B, 9117–9135.

Chian, D., Keen, C., Reid, I & Louden, K.E. 1995a: Evolution of nonvolcanic rifted margins: new results from the conjugate margins of the Labrador Sea. Geology **23**, 589–592.

Chian, D., Louden, K.E. & Reid, I. 1995b: Crustal structure of the Labrador Sea conjugate margin and implications for the formation of nonvolcanic continental margins. Journal of Geophysical Research **100**, B, 24239–24253.

Clarke, D.B. & Pedersen, A.K. 1976: Tertiary volcanic province of West Greenland. In: Escher, A. & Watt, W.S. (eds): Geology of Greenland, 364–385. Copenhagen: Geological Survey of Greenland.

Gradstein, F.M., Agterberg, F.P., Ogg, J.G., Hardenbol, J., van Veen, P., Thierry, J. & Huang, Z. 1994: A Mesozoic time scale. Journal of Geophysical Research **99**, B, 24051–24074.

Hald, N. & Larsen, J.G. 1987: Early Tertiary, low potassium tholeiites from exploration wells on the West Greenland shelf. Rapport Grønlands Geologiske Undersøgelse **136**, 25 pp.

Hansen, K. & Larsen, O. 1974: K/Ar age determinations on Mesozoic lamprophyre dykes near Ravns Storø, Fiskenæsset region, southern West Greenland. Rapport Grønlands Geologiske Undersøgelse **66**, 9–11.

Juhava, R. 1974: On young generations of kimberlitic and lamprophyric dyke rocks from Søndre Isortoq area, West Greenland, 25 pp. Unpublished report, Kryolitselskabet Øresund A/S, Copenhagen, Denmark (in archives of Geological Survey of Denmark and Greenland, GEUS Report File 21387).

Kalsbeek, F., Larsen, L.M. & Bondam, J. 1990: Geological map of Greenland, 1:500 000, Sydgrønland, sheet 1. Descriptive text, 36 pp. Copenhagen: Geological Survey of Greenland.

Keen, C.E., Loncarevic, B.D., Reid, I., Woodside, J., Haworth, R.T. & Williams, H. 1990: Tectonic and geophysical overview. In: Keen, M.J. & Williams, G.L. (eds): Geology of the continental margin of eastern Canada. Geology of Canada **2**,

31–85. Ottawa: Geological Survey of Canada (also The geology of North America **I-1**, Geological Society of America).
Keen, C.E., Courtney, R.C., Dehler, S.A. & Williamson, M.-C. 1994: Decompression melting at rifted margins: comparison of model predictions with the distribution of igneous rocks on the eastern Canadian margin. Earth and Planetary Science Letters **121**, 403–416.
King, A.F. & McMillan, N.J. 1975: A mid-Mesozoic breccia from the coast of Labrador. Canadian Journal of Earth Sciences **12**, 44–51.
Larsen, L.M. & Rex, D.C. 1992: A review of the 2500 Ma span of alkaline-ultramafic, potassic and carbonatitic magmatism in West Greenland. Lithos **28**, 367–402.
Larsen, L.M., Pedersen, A.K., Pedersen, G.K. & Piasecki, S. 1992: Timing and duration of Early Tertiary volcanism in the North Atlantic: new evidence from West Greenland. In: Storey, B.C., Alabaster, T. & Pankhurst, R.J. (eds): Magmatism and the causes of continental break-up. Geological Society Special Publication (London) **68**, 321–333.
Le Maitre, R.W. (ed.) 1989: A classification of igneous rocks and glossary of terms. Recommendations of the IUGS subcommission on the systematics of igneous rocks, 193 pp. Oxford: Blackwell Scientific Publications.
Ludwig, K.R. 1990: Isoplot. A plotting and regression program for radiogenic-isotope data, for IBM-PC compatible computers. US Geological Survey Open File Report **88-557**, 44 pp.
Nielsen, T.F.D. 1987: Mafic dyke swarms in Greenland: a review. In: Halls, H.C. & Fahrig, W.F. (eds): Mafic dyke swarms. Special Paper Geological Association of Canada **34**, 349–360.
Pe-Piper, G., Piper, D.J.W., Keen, M.J. & McMillan, N.J. 1990: Igneous rocks of the continental margin. In: Keen, M.J. & Williams, G.L. (eds): Geology of the continental margin of eastern Canada. Geology of Canada **2**, 75–85. Ottawa: Geological Survey of Canada (also The geology of North America **I-1**, Geological Society of America).
Reid, D.L. & Rex, D.C. 1994: Cretaceous dykes associated with the opening of the South Atlantic: the Mehlberg dyke, northern Richtersveld. South African Journal of Geology **97**, 135–145.
Rex, D.C., Guise, P.G. & Wartho, J.-A. 1993: Disturbed ^{40}Ar–^{39}Ar spectra from hornblendes: Thermal loss or contamination? Chemical Geology (Isotope Geoscience Section) **103**, 271–281.
Rock, N.M.S. 1991: Lamprophyres, 285 pp. Glasgow and London: Blackie and Son.
Roest, W.R. & Srivastava, S.P. 1989: Sea-floor spreading in the Labrador Sea: a new reconstruction. Geology **17**, 1000–1003.
Rolle, F. 1985: Late Cretaceous – Tertiary sediments offshore central West Greenland: lithostratigraphy, sedimentary evolution, and petroleum potential. Canadian Journal of Earth Sciences **22**, 1001–1019.
Smith, P.E., York, D., Easton, R.M., Özdemir, Ö. & Layer, P.W. 1994: A laser ^{40}Ar–^{39}Ar study of minerals across the Grenville Front: investigation of reproducible excess Ar patterns. Canadian Journal of Earth Sciences **31**, 808–817.
Srivastava, S.P. & Roest, W.R. 1995: Nature of thin crust across the southwest Greenland margin and its bearing on the location of the ocean-continent boundary. In: Banda, E. *et al.* (eds): Rifted ocean-continent boundaries, 95–120. Amsterdam: Kluwer Academic Publishers.
Storey, M., Duncan, R.A., Pedersen, A.K., Larsen, L.M. & Larsen, H.C. 1998: $^{40}Ar/^{39}Ar$ geochronology of the West Greenland Tertiary volcanic province. Earth and Planetary Science Letters **160**, 569–586.
Talwani, M. & Eldholm, O. 1977: Evolution of the Norwegian–Greenland Sea. Geological Society of America Bulletin **88**, 969–999.
Umpleby, D.C. 1979: Geology of the Labrador Shelf. Geological Survey of Canada Paper **79-13**, 34 pp.
Watt, W.S. 1969: The coast-parallel dike swarm of southwest Greenland in relation to the opening of the Labrador Sea. Canadian Journal of Earth Sciences **6**, 1320–1321.
Whittaker, R.C. 1995: A preliminary assessment of the structure, basin development and petroleum potential offshore central West Greenland. Open File Series Grønlands Geologiske Undersøgelse **95/9**, 33 pp.
Williamson, M.-C., Courtney, R.C., Keen, C.E. & Dehler, S.A. 1995: The volume and rare earth concentrations of magmas generated during finite stretching of the lithosphere. Journal of Petrology **36**, 1433–1453.

Geochronology of granitic and supracrustal rocks from the northern part of the East Greenland Caledonides: ion microprobe U–Pb zircon ages

Feiko Kalsbeek, Allen P. Nutman, Jan C. Escher, Johan D. Friderichsen, Joseph M. Hull, Kevin A. Jones and *Stig A. Schack Pedersen*

Granitoid rocks from different settings within the northern part of the East Greenland Caledonian fold belt have yielded U–Pb zircon dates between 2000 and 1730 Ma, confirming the Palaeoproterozoic origin of the crystalline basement. Widespread sandstone sequences occur both in the Caledonian fold belt and in the foreland to the west; all of these have been assigned to the Independence Fjord Group, and attributed a Mesoproterozoic age on geological maps. However, metarhyolitic rocks associated with the sandstones in the Caledonian fold belt have yielded an age of 1740 ± 6 Ma, significantly older than anticipated. Zircon ages for a sandstone sample in the same area suggest deposition after the end of Palaeoproterozoic orogenic events, but in part prior to emplacement of the rhyolitic rocks at 1740 Ma; sandstone from another locality may have been deposited before emplacement of the latest Proterozoic granite sheets.

Field relations suggest that some granitic veins and sheets might be Caledonian in age, but, with one possible exception, all those analysed proved to be Proterozoic. The apparent absence of Caledonian granites in the northern part of the East Greenland Caledonides, despite regional high-grade metamorphism, may be related to the lack of major occurrences of pelitic supracrustal rocks within the crystalline basement complexes.

F.K., J.C.E., J.D.F. & S.A.S.P., *Geological Survey of Denmark and Greenland, Thoravej 8, DK-2400 Copenhagen NV, Denmark*. E-mail: *fk@geus.dk*
A.P.N., *Research School of Earth Sciences, Australian National University, Canberra, ACT 0200, Australia.*
J.M.H., *Division of Science and Mathematics, Seattle Central Community College, Seattle WA 98122, USA.*
K.A.J., *Geology and Cartography Division, School of Construction and Earth Sciences, Oxford Brookes University, Oxford OX3 0BP, UK.*

Keywords: Caledonides, granites, Greenland, Palaeoproterozoic, SHRIMP, supracrustal rocks, zircon

The East Greenland Caledonian fold belt (Haller 1971; Henriksen & Higgins 1976; Henriksen 1985; Higgins 1995a) stretches from 70°N to 81°N, a distance of nearly 1300 km along strike. Between 76°N and 79°N the fold belt is dominated by crystalline basement complexes (Fig. 1), mainly grey gneisses and somewhat later metagranitoid rocks of Palaeoproterozoic age (gneisses *c*. 2000–1850 Ma; some granitic rocks down to about 1750 Ma; Kalsbeek *et al*. 1993; Nutman & Kalsbeek 1994). The gneisses contain local enclaves of supracrustal rocks, and are cut by several generations of mafic dykes, most of which are strongly deformed (Hull *et al*. 1994). Eclogite pods (Gilotti 1993), formed during high-grade Caledonian metamorphism (Brueckner *et al*. 1998), occur at many localities. North of *c*. 79°N the fold belt is built up of Caledonian nappe complexes involving basement gneisses together with Proterozoic and Palaeozoic supracrustal sequences (Higgins 1995b).

In this paper we report ion microprobe U–Pb zircon data on granitoid, metavolcanic and metasedimentary rocks in order to establish a broad geochronological framework for the northernmost parts of the East Greenland Caledonides. One question we wished to assess

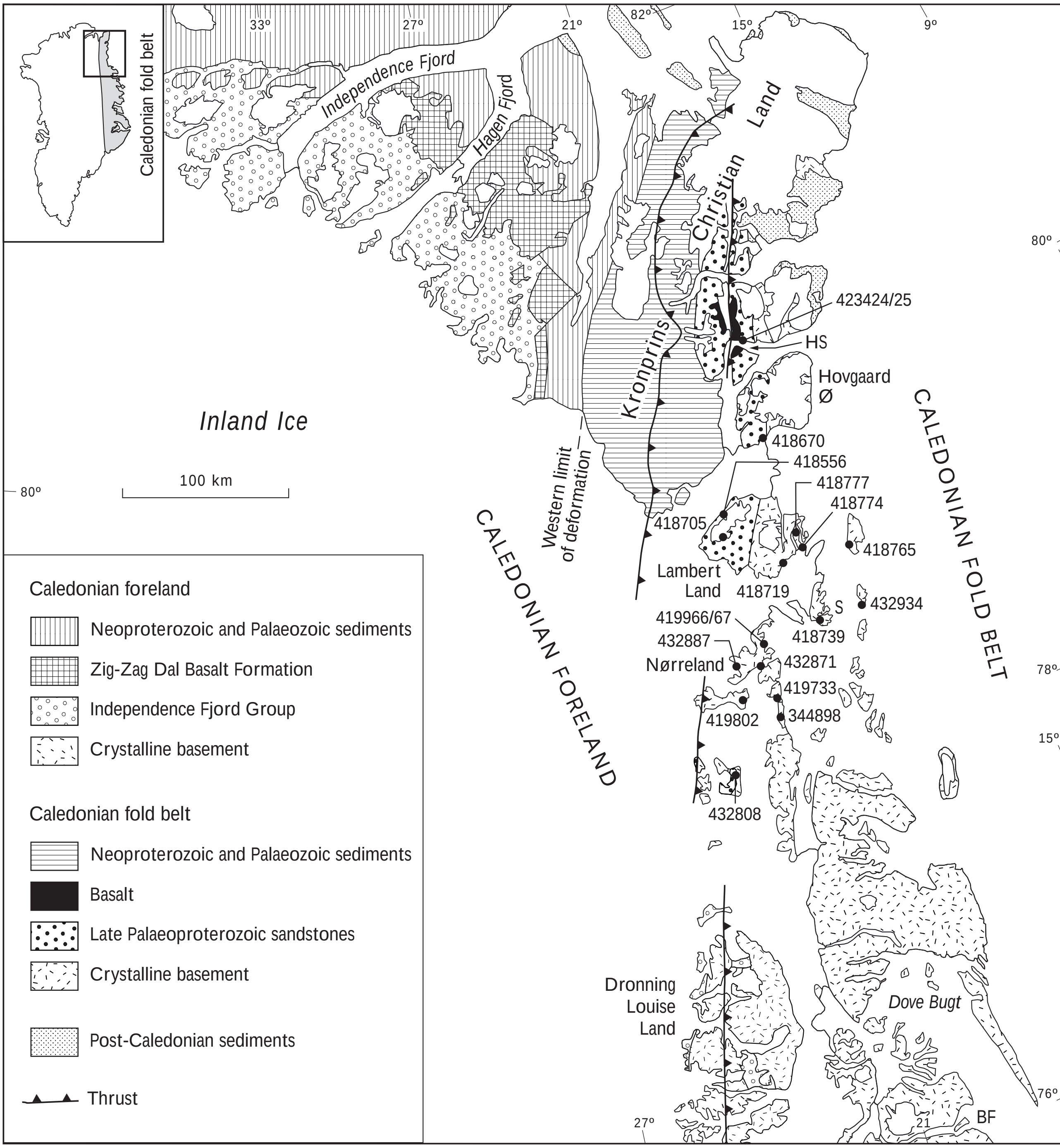

Fig. 1. Geological map of the northern part of the Caledonian fold belt and the adjoining Caledonian foreland (modified after Escher & Pulvertaft 1995). Stratigraphic correlations between the fold belt and the foreland are not entirely certain, but the late Palaeoproterozoic sandstones from the fold belt probably correlate with the Independence Fjord Group of the foreland. Correlation of the 1740 Ma basalts at Hekla Sund with the Zig-Zag Dal Basalt Formation of the foreland is unlikely. **BF**: Bessel Fjord; **HS**: Hekla Sund; **S**: Schnauder Ø. **Dots** with six digit numbers represent sample localities that refer to the files of the former Geological Survey of Greenland (GGU).

Fig. 2. Simplified stratigraphy for the Caledonian foreland and the Caledonian fold belt in North-East and eastern North Greenland.

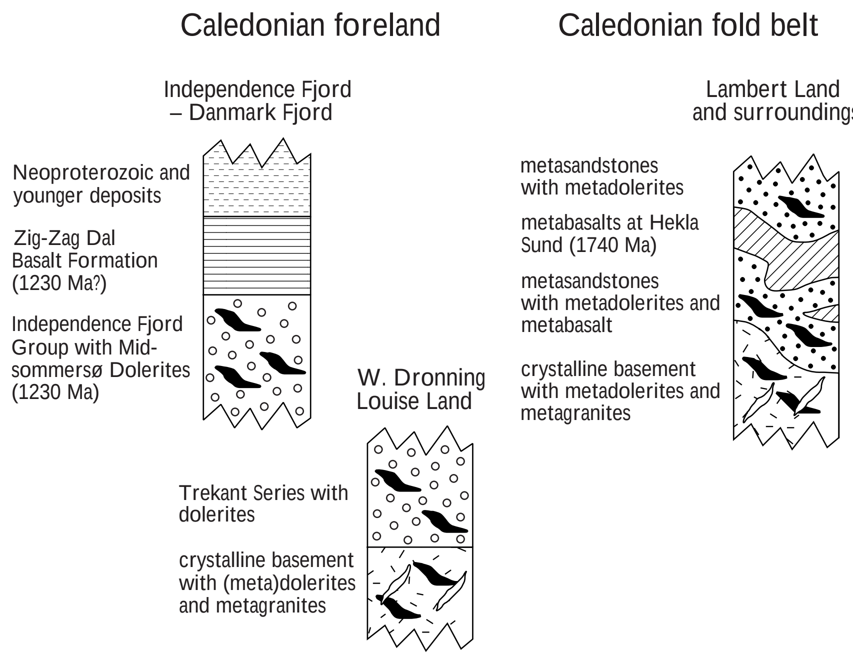

was whether some of the granitoid rocks in the region could represent Caledonian granites; no granites of certain Caledonian age were detected by the present geochronology, however, and a possible explanation is suggested for their apparent absence in this part of the Caledonian fold belt.

Regional geology

Caledonian foreland

The foreland to the East Greenland Caledonian fold belt is widely exposed west of Kronprins Christian Land (80–81°N) and also outcrops at the margin of the Inland Ice in western Dronning Louise Land (77°N, 25°W; Fig. 1). Crystalline basement rocks are not exposed west of Kronprins Christian Land, but in North Greenland the basement consists of Archaean rocks affected by Palaeoproterozoic orogenic events, and in North-East Greenland it is made up of juvenile Palaeoproterozoic rocks (Escher & Pulvertaft 1995). Most Proterozoic orogenic activity took place 2000–1800 Ma ago; some late granites in North-East Greenland have been dated at *c*. 1750 Ma (Kalsbeek *et al*. 1993).

Between Independence Fjord and Danmark Fjord (Fig. 1) in the Caledonian foreland the lowermost unit exposed is the Independence Fjord Group, a sequence of sandstones, the base of which is not exposed (Figs 1, 2; Collinson 1980, 1983; Sønderholm & Jepsen 1991). These sandstones are undeformed and unmetamorphosed, and clearly post-date the Palaeoproterozoic orogenic events recorded in North-East Greenland. The Independence Fjord Group is cut by numerous sheets and dykes of dolerite, the Midsommersø Dolerites, for which Rb–Sr whole-rock isochron ages of *c*. 1230 Ma have been obtained (Kalsbeek & Jepsen 1983). Deposition of the Independence Fjord Group in the Caledonian foreland must thus have taken place between *c*. 1750 and 1230 Ma ago. Rb–Sr data on clay minerals from siltstone samples have suggested diagenesis at about 1380 Ma (Larsen & Graff-Petersen 1980), and on the Geological map of Greenland, 1:2 500 000 (Escher & Pulvertaft 1995) the Independence Fjord Group is consequently shown as Mesoproterozoic.

The Independence Fjord Group is overlain by the Zig-Zag Dal Basalt Formation. The age of this formation is not known, but it is believed to be contemporaneous with emplacement of the Midsommersø Dolerites (Kalsbeek & Jepsen 1984). The Zig-Zag Dal Basalt Formation is overlain by Neoproterozoic and Palaeozoic strata.

In western Dronning Louise Land the crystalline basement of the foreland to the Caledonian fold belt is unconformably overlain by a sequence of sandstones, the Trekant Series (Figs 1, 2; Peacock 1956, 1958; Strachan *et al*. 1994), which are lithologically similar to the Independence Fjord Group sandstones west of Kronprins Christian Land. Both the crystalline basement and the sandstones of the Trekant Series contain numerous dolerite sheets, and are increasingly affected by Caledonian deformation and metamorphism further east in Dronning Louise Land. No radiometric ages are available for the dolerites or the sandstones, but a broad correlation with respectively the Midsommersø Dolerites and the Independence Fjord Group is assumed (see e.g. Escher & Pulvertaft 1995).

Caledonian fold belt

The northernmost part of the East Greenland Caledonian fold belt consists mainly of gneisses and metagranitoid rocks, which are tectonically interleaved with units of quartzitic and feldspathic metasandstones traditionally correlated with the Independence Fjord Group. Sheets and dykes of metadolerite are common in all these rocks. In the area around Hekla Sund in Kronprins Christian Land (HS, Fig. 1) the metasandstones are interlayered with low-grade metamorphic pillow lavas of basaltic composition with subordinate occurrences of metarhyolitic rocks (Pedersen *et al.* 1995a, b). Pedersen *et al.* (1995a) describe syn-sedimentary faults within this sequence, and suggest that the basalts were deposited in an alluvial fan setting during subsidence along rift margin escarpments. On the Geological map of Greenland, 1:2 500 000 (Escher & Pulvertaft 1995) the basalts are correlated with the Zig-Zag Dal Basalt Formation west of Kronprins Christian Land. However, our age determinations show that this correlation is unlikely (p. 44).

A complex sequence of Caledonian thrust sheets in Lambert Land (just north of 79°N, Fig. 1) include sandstones with locally well-preserved sedimentary structures (Jones & Escher 1995). The eastern part of Lambert Land and adjoining areas consist of granitoid rocks, for some of which a Caledonian age was considered possible during field work. For example, a Caledonian age was considered likely for a complex of granites and granodiorites on Schnauder Ø (S, Fig. 1) and eastern Lambert Land; the 'Schnauder Ø complex' can be distinguished from the surrounding regional gneisses on the basis of a significantly lower degree of deformation and the lack of mafic dykes, and is shown on one of John Haller's maps as post-tectonic granite (Haller 1971, p. 267). Rafts of gneiss with remnants of mafic dykes are present within the complex. Presumed Caledonian granite sheets were also locally found within Caledonian shear zones, and interpreted as syntectonic. Granite sheets were also found cutting mafic dykes similar to the Midsommersø Dolerites, in areas mainly composed of sandstone. However, due to limited exposure and strong deformation, it was not possible to establish detailed field relationships, and nowhere were intrusive contacts observed between the granites and the sandstones. As in Kronprins Christian Land the sandstones in Lambert Land are traditionally correlated with the Independence Fjord Group of the Caledonian foreland and the metadolerites that cut the sandstones with the Midsommersø Dolerites.

A small tectonic window in the Nørreland area (latitude 78°40′N, Fig. 1) exposes a sequence of sandstones and dolerite sheets, associated with granitoid rocks, beneath a major Caledonian thrust (Hull & Friderichsen 1995); sheared carbonates in the thrust zone have yielded Ordovician conodonts (M.P. Smith, personal communication 1998), clearly demonstrating the Caledonian age of westward thrust displacement. Field observations within the window suggest that the granitoid rocks are younger than the sandstones, although strong deformation precludes unambiguous assessment of their mutual relationships.

The northernmost part of the Caledonian fold belt was remapped by the Geological Survey of Greenland (GGU, amalgamated with its Danish counterpart in 1995 into the Geological Survey of Denmark and Greenland). The isotopic investigations reported in this paper were carried out in connection with this mapping project. Details of the field setting of the various rocks appear in an unpublished volume 'Express report: eastern North Greenland and North-East Greenland 1995' (Higgins 1995b), copies of which are available from the Survey.

Scope of the present investigation and methods used

Ion microprobe U–Pb zircon dating has been carried out on metagranitoid rocks from different settings within the fold belt: (1) orthogneisses from the crystalline basement, (2) metagranitoid sheets intruded into basement gneisses, (3) metagranitoid rocks from the tectonic window in Nørreland, (4) granitoid rocks from the Schnauder Ø complex, (5) granitoid sheets from Lambert Land and surroundings which occur within Caledonian shear zones or were intruded into mafic dykes that are lithologically similar to the Midsommersø Dolerites. In addition, zircons were studied from (6) two samples of rhyolitic rocks associated with the unit of metabasalts at Hekla Sund, and detrital zircons

Fig. 3. Classification of the investigated samples. **A**: CIPW normative An–Ab–Or diagram for granitoid rocks (O'Connor 1965, modified after Barker 1979). **B**: Q–A–P diagram (Streckeisen 1976; Q: quartz, A: alkali feldspar, P: plagioclase). Modal compositions were estimated from chemical analyses (kation-norms, with orthoclase + hypersthene recalculated into biotite + quartz: 5 or + 6 hy = 8 bi + 3 qz). The quartz dioritic sample GGU 419967 is too mafic to be represented in Fig. 3A.

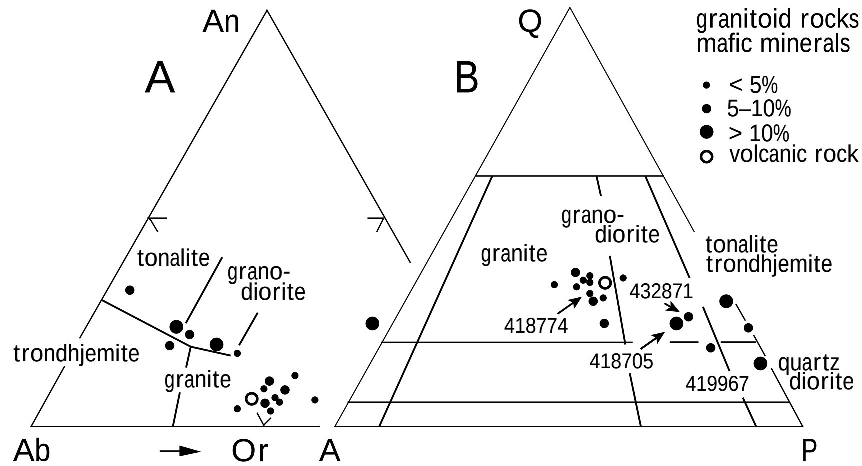

were analysed from (7) two metasandstone samples, one from Lambert Land and one from the Nørreland window, to obtain an impression of the time of deposition and the source areas of the sediments.

The investigated samples vary from quartz dioritic to granitic in composition (Fig. 3). In the CIPW normative Ab–An–Or diagram (Fig. 3A; O'Connor 1965; Barker 1979) as well as in the Q–A–P (quartz–alkali feldspar–plagioclase) diagram (Fig. 3B; Streckeisen 1976; modal compositions estimated from chemical analyses) they plot as quartz diorite, tonalite, granodiorite and (leuco-) granite. The total proportion of (normative) mafic minerals is low in most cases; most granitic rocks have < 5 per cent mafic minerals.

Zircons were separated from 1–2 kg samples and mounted in 1-inch epoxy disks (20–50 grains for most samples, 5–10 samples per disk). U-Th-Pb isotopic ratios and concentrations were determined with SHRIMP 1 (SHRIMP = Sensitive High Resolution Ion MicroProbe) at the Research School of Earth Sciences, Australian National University (ANU), Canberra, using the ANU standard zircon SL13 (572 Ma; $^{206}Pb/^{238}U$ = 0.0928) for reference. Descriptions of analytical procedure and data assessment are given by Compston *et al.* (1984), Claoué-Long *et al.* (1995) and Williams (1998). As a check on the accuracy of $^{207}Pb/^{206}Pb$ ratios obtained by SHRIMP, analyses of zircons from a Palaeoproterozoic norite, QGNG, were run interspersed with unknowns. Isotope dilution thermal ionisation mass spectrometry for different QGNG zircon fractions has yielded $^{207}Pb/^{206}Pb$ ages of 1850 ± 2 Ma (C.M. Fanning, personal communication 1995) and 1850 Ma to as low as 1810 Ma (T. Skjöld, personal communication 1996). Most of the analyses of QGNG run during the present investigation yielded $^{207}Pb/^{206}Pb$ ages of 1820 to 1860 Ma, the same range as found by thermal ionisation isotope dilution analyses, with 1σ errors on individual ages typically of about 15–20 Ma.

In the context of the regional geological understanding of the study area, reconnaissance data yielding a general rather than a precisely defined age were considered sufficient for a number of samples; in these cases only three to five zircons were analysed, each spot was analysed using only four mass scans (instead of the usual five), and to compensate for the reduced counting time a larger than usual spot (50 vs. 30 µm in diameter) was employed where size and homogeneity of the zircons permitted (most granitoid rocks). Even though the precision of such age determinations is low we regard this as a useful approach as part of regional projects, since a large number of samples can be analysed in this way, providing useful results on the scale of the orogen.

Ages were calculated in two ways: (1) as the mean of the most concordant $^{207}Pb/^{206}Pb$ ages, and (2) as the upper intercept of the best-fit discordia line with concordia, using all analytical data together with an additional data point at 400 ± 50 Ma. The use of this additional data point is based on the assumption that the discordance of non-concordant data is the result of Pb loss during Caledonian metamorphism. Because most samples did not yield strongly discordant zircons, the calculations (York 1969; regressions calculated in $^{207}Pb/^{206}Pb$ vs. $^{238}U/^{206}Pb$ space assuming non-correlated errors) without this extra point yield very poorly defined lower intercepts which, however, all encompass 400 Ma as a possible time of Pb loss. A summary of results is given in Table 1 (all ages quoted with 2σ errors), and analytical data in Tables 2 and 3. For sample localities see Fig. 1 and Table 1.

Table 1. SHRIMP U–Pb zircon ages for granitoid and metavolcanic rocks from the Caledonian fold belt

GGU sample no.	Rock type	Latitude, Longitude	N spots	Age (Ma) (1)	Age (Ma) (2)	MSWD
(1) Gneisses from the crystalline basement						
344898	trondhjemitic gneiss	78°15.8′N, 21°21′W	2/3	1994 ± 38	1978 ± 112	2.2
418765	biotite gneiss	79°00.0′N, 18°00′W	2/3	1935 ± 24	1949 ± 27	0.7
418719	granitic bi. gneiss	79°02.0′N, 20°13′W	3	*c.* 1900?		
(2) Granitoid sheets intruded into basement gneisses						
419733	metagranite	78°24.8′N, 21°15′W	2/3	1751 ± 31	1769 ± 36	0.1
432934	metagranite	78°45.0′N, 18°30′W	3	1800 ± 100	1822 ± 118	0.4
419802	metagranite	78°27.8′N, 22°09′W	4			
432808	metagranite	78°01.1′N, 22°46′W	3		2013 ± 103	0.1
(3) Granitoid rocks from the tectonic window at 78°40′N						
419967	meta-quartz diorite	78°41.2′N, 21°14′W	3/5	1858 ± 35	1889 ± 42	0.6
419966	metagranite	78°41.2′N, 21°14′W	5/6	1731 ± 38	1733 ± 43	0.3
432871	metagranodiorite	78°37.4′N, 21°17′W	5	*c.* 1900	1912 ± 46	0.4
(4) Granitoid rocks from the Schnauder Ø complex						
418739	foliated granite	78°41.5′N, 19°25′W	2/3	1974 ± 18		
418777	fol. musc.-bi. granodiorite	79°08.1′N, 19°21′W	4/6	*c.* 2000		
(5) Granitoid sheets from Caledonian shear zones or intruded into metadolerites in Lambert Land						
418670	meta-augen granite	78°59.5′N, 17°58′W	6/7*	1986 ± 23	1959 ± 35	2.7
418774	musc.-bi. metagranite	79°08.8′N, 19°06′W	9#	404 ± 11	2018 ± 39	1.3
418705	meta-augen granodiorite	79°14.8′N, 21°22′W	5	1994 ± 20	1999 ± 25	0.6
(6) Rhyolitic rocks from the basalt sequence at Hekla Sund						
423424	metarhyolite	80°15.0′N, 19°13′W	9/10	1742 ± 10		
423425	metarhyolite	80°15.0′N, 19°13′W	10	1738 ± 11		

Ages were calculated in two ways: (1) as the mean of the most concordant $^{207}Pb/^{206}Pb$ ages, and (2) as the upper intercept of the best-fit discordia using all data points plus an extra point at 400 ± 50 Ma (see text).
'N spots' is the number of spots analysed and used in age calculations, for example, 3/5 indicates that 5 spots were analysed of which 3 were used for the $^{207}Pb/^{206}Pb$ age estimate and 5 for the discordia calculation.
* For 418670 two rims were not included in the discordia calculation.
\# For 418774 two spots were not included in the discordia calculation, and no extra point at 400 ± 50 Ma was employed.
Errors at 2σ.

Results

Basement gneisses

Three samples of basement orthogneisses have been studied (GGU 344898, 418765, 418719; Fig. 1). Precise ages were not considered necessary, as the main aim of the age determinations was to determine whether the rocks belonged to the same age category as samples analysed previously (1850–2000 Ma, Kalsbeek *et al.* 1993; Nutman & Kalsbeek 1994), or whether Archaean rocks were also present. Therefore only three zircons were analysed per sample. Two samples with relatively fresh (transparent) zircons (GGU 344898 and 418765) gave ages of about 2000 and 1950 Ma, respectively (Table 1). For both samples the data show some scatter along reference discordia lines with lower intercepts at 400 Ma (shown for 418765 in Fig. 4A), indicating that the discordance of non-concordant analyses can be interpreted as the result of Pb loss during Caledonian metamorphism. These results are in agreement with ages obtained earlier from the crystalline basement (Kalsbeek *et al.* 1993; Nutman & Kalsbeek 1994).

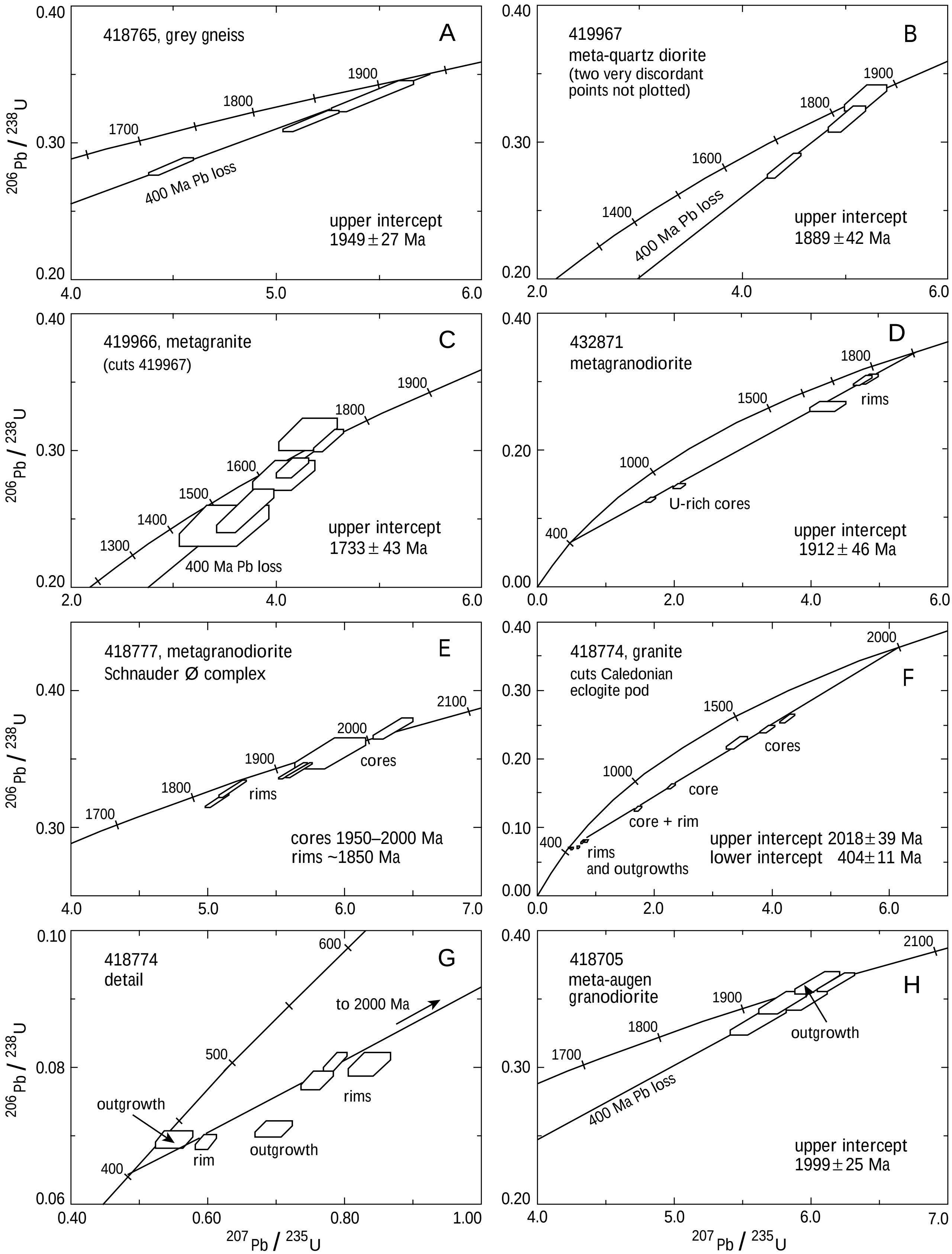

Fig. 4. Selected concordia diagrams for zircons from granitoid rocks, East Greenland Caledonian fold belt; error boxes display 1σ errors. For localities see Fig. 1. Discordia lines down to 400 Ma are for reference only.

Table 2. SHRIMP U–Pb zircon data for metagranitoid rocks from the Caledonian fold belt

Spot	U (ppm)	Th/U	f_{206} (%)	$^{206}Pb/^{238}U$	$^{207}Pb/^{206}Pb$	Age	Disc. (%)
GGU 344898							
1.1	130	0.15	0.33	0.327 ± 8	0.1208 ± 25	1967 ± 38	7
2.1	201	0.17	0.15	0.351 ± 7	0.1232 ± 15	2003 ± 22	–3
3.1	198	0.31	0.43	0.308 ± 7	0.1167 ± 14	1907 ± 22	–9
GGU 418765							
1.1	488	0.40	0.10	0.316 ± 8	0.1186 ± 10	1935 ± 14	–9
2.1	449	0.51	0.27	0.283 ± 6	0.1149 ± 10	1878 ± 16	–14
3.1	535	0.42	0.14	0.334 ± 11	0.1186 ± 13	1935 ± 19	–4
GGU 418719							
1.1	57	0.72	1.96	0.348 ± 11	0.1099 ± 48	1798 ± 81	7
2.1	245	0.78	0.32	0.268 ± 6	0.1154 ± 17	1886 ± 27	–19
3.1	330	0.11	0.69	0.216 ± 5	0.1516 ± 25	2364 ± 29	–47
GGU 419733							
1.1	412	0.40	0.19	0.285 ± 6	0.1064 ± 13	1739 ± 22	–7
2.1	328	0.28	0.24	0.297 ± 6	0.1076 ± 12	1760 ± 21	–5
3.1	452	0.23	0.42	0.196 ± 4	0.0997 ± 15	1618 ± 28	–29
GGU 432934							
1.1	65	0.93	0.48	0.310 ± 9	0.1119 ± 42	1830 ± 70	–5
2.1	44	0.76	1.26	0.265 ± 11	0.1100 ± 64	1799 ± 110	–16
3.1	77	0.90	0.67	0.278 ± 9	0.1045 ± 61	1706 ± 112	–7
GGU 419802							
1.1	175	0.50	0.56	0.342 ± 8	0.1211 ± 17	1972 ± 25	–4
2.1	649	0.57	6.86	0.119 ± 2	0.1044 ± 40	1703 ± 72	–57
3.1	138	0.30	0.89	0.284 ± 11	0.1937 ± 31	2774 ± 26	–42
4.1	1352	0.29	3.60	0.066 ± 2	0.0559 ± 30	447 ± 125	–8
GGU 432808							
1.1	2444	0.05	0.56	0.128 ± 2	0.0920 ± 8	1468 ± 17	–47
2.1	2187	0.07	0.52	0.155 ± 3	0.1007 ± 12	1636 ± 22	–43
3.1	2312	0.05	2.55	0.093 ± 2	0.0738 ± 16	1037 ± 44	–45
GGU 419967							
1.1	395	0.30	0.44	0.283 ± 9	0.1130 ± 15	1847 ± 24	–13
2.1	168	0.39	0.35	0.332 ± 9	0.1135 ± 29	1856 ± 46	0
3.1	250	0.29	0.23	0.317 ± 9	0.1150 ± 21	1880 ± 34	–6
4.1	548	0.49	1.69	0.129 ± 3	0.0980 ± 23	1586 ± 45	–51
5.1	522	0.37	1.19	0.154 ± 3	0.0995 ± 28	1614 ± 54	–43
GGU 419966							
1.1	153	1.29	1.38	0.312 ± 12	0.1004 ± 49	1631 ± 94	7
2.1	25	0.92	2.15	0.245 ± 15	0.1032 ± 106	1683 ± 204	–16
3.1	178	0.80	0.35	0.287 ± 7	0.1049 ± 26	1712 ± 46	–5
4.1	84	1.31	0.19	0.256 ± 16	0.1047 ± 38	1709 ± 68	–14
5.1	106	1.75	0.00	0.307 ± 8	0.1065 ± 13	1740 ± 23	–1
6.1	93	1.27	0.54	0.282 ± 11	0.1049 ± 61	1713 ± 110	–7
GGU 432871							
1.1*	167	0.60	0.47	0.303 ± 7	0.1155 ± 20	1888 ± 32	–10
1.2	546	0.46	1.42	0.128 ± 4	0.0940 ± 26	1508 ± 53	–49
1.3*	180	0.69	0.33	0.302 ± 8	0.1143 ± 16	1869 ± 26	–9
2.1*	235	0.33	0.16	0.264 ± 7	0.1164 ± 60	1902 ± 95	–21
3.1	551	0.42	1.94	0.147 ± 3	0.1022 ± 32	1664 ± 59	–47
GGU 418739							
1.1*	1434	0.02	0.12	0.343 ± 7	0.1175 ± 10	1919 ± 15	–1
2.1	118	0.73	0.53	0.367 ± 10	0.1222 ± 22	1988 ± 33	1
3.1*	1494	0.17	0.23	0.361 ± 6	0.1212 ± 6	1973 ± 9	1

Table 2 *(continued)*

Spot	U (ppm)	Th/U	f_{206} (%)	$^{206}Pb/^{238}U$	$^{207}Pb/^{206}Pb$	Age	Disc. (%)
GGU 418777							
1.1*	1559	0.04	0.09	0.320 ± 5	0.1150 ± 6	1879 ± 10	–5
2.1	5098	0.10	0.02	0.372 ± 7	0.1237 ± 12	2011 ± 17	2
3.1*	1771	0.05	0.30	0.341 ± 6	0.1195 ± 5	1949 ± 7	–3
4.1*	752	0.15	0.28	0.328 ± 6	0.1145 ± 6	1871 ± 10	–2
5.1*	3079	0.16	0.03	0.342 ± 6	0.1204 ± 4	1962 ± 6	–3
6.1	92	0.51	1.11	0.354 ± 11	0.1209 ± 31	1970 ± 47	–1
GGU 418670							
1.1	294	0.55	0.17	0.353 ± 11	0.1219 ± 21	1984 ± 30	–2
2.1	177	0.35	0.34	0.356 ± 9	0.1232 ± 24	2003 ± 35	–2
3.1	232	0.36	0.18	0.342 ± 9	0.1215 ± 11	1978 ± 16	–4
4.1	720	0.30	0.51	0.115 ± 2	0.0955 ± 14	1538 ± 28	–54
5.1	66	0.42	0.18	0.338 ± 8	0.1253 ± 25	2033 ± 36	–8
6.1	80	0.46	0.36	0.347 ± 10	0.1204 ± 36	1962 ± 54	–2
7.1*	2030	0.03	0.25	0.352 ± 8	0.1186 ± 6	1936 ± 10	0
8.1*	1727	0.04	0.68	0.311 ± 6	0.1165 ± 10	1904 ± 15	–8
9.1	38	0.45	2.72	0.366 ± 19	0.1161 ± 67	1897 ± 107	6
GGU 418774							
1.1	180	0.19	1.11	0.224 ± 9	0.1105 ± 28	1807 ± 47	–28
2.1*	3115	0.03	0.46	0.081 ± 1	0.0705 ± 9	944 ± 25	–47
3.1*	1805	0.07	4.88	0.080 ± 2	0.0754 ± 22	1079 ± 59	–54
4.1	909	0.17	2.50	0.127 ± 3	0.0979 ± 20	1584 ± 39	–51
5.1*	1795	0.02	0.99	0.078 ± 1	0.0706 ± 16	945 ± 48	–49
6.1#	994	0.02	2.50	0.070 ± 1	0.0575 ± 25	509 ± 99	–15
7.1#	918	0.02	2.49	0.071 ± 1	0.0712 ± 24	963 ± 69	–54
8.1*	1226	0.01	0.80	0.069 ± 1	0.0626 ± 13	696 ± 43	–38
9.1	489	0.37	0.38	0.259 ± 6	0.1195 ± 16	1949 ± 23	–24
10.1	395	0.31	1.90	0.244 ± 6	0.1168 ± 22	1907 ± 34	–26
11.1	511	0.06	1.11	0.159 ± 4	0.1039 ± 16	1694 ± 29	–44
GGU 418705							
1.1	162	0.43	0.05	0.362 ± 7	0.1238 ± 11	2012 ± 16	–1
2.1#	157	0.39	0.40	0.362 ± 8	0.1211 ± 16	1973 ± 23	1
3.1	125	0.45	1.08	0.349 ± 7	0.1232 ± 24	2003 ± 35	–4
4.1	185	0.52	0.93	0.333 ± 10	0.1221 ± 21	1986 ± 31	–7
5.1	159	0.59	0.93	0.347 ± 8	0.1209 ± 21	1970 ± 31	–2

Spots marked with * represent rims; spots marked # are outgrowths; f_{206} is the proportion of ^{206}Pb that is not radiogenic; Age is the apparent $^{207}Pb/^{206}Pb$ age; Disc. is the degree of discordance between the $^{207}Pb/^{206}Pb$ and $^{206}Pb/^{238}U$ ages. All errors quoted at 1σ level.

The third sample (GGU 418719), a K-rich granitic biotite gneiss, yielded nearly exclusively metamict zircons and did not provide a reliable age. All three zircons analysed were discordant; one had a $^{207}Pb/^{206}Pb$ age of 2360 Ma and probably represents an inherited Archaean zircon which experienced severe Pb loss during one or more metamorphic events.

Granitoid sheets within basement gneisses

Four samples were studied of metaporphyritic granite sheets cutting basement gneisses. Two of these (GGU 419733, 432934; Fig. 1) yielded transparent zircons with ages around 1750–1800 Ma (three analyses each, Table 1).

Two other granite sheets (GGU 419802, 432808; Fig. 1) yielded only metamict zircons. Nearly opaque zircons were recovered from GGU 419802, a metagranite cutting paragneisses in the crystalline basement south of Lambert Land. Four grains were analysed, but no satisfactory age was obtained. Two analyses were nearly concordant: one, on a transparent part of a zircon, at *c*. 1970 Ma, and a metamict high-U grain (1350 ppm U) at *c*. 410 Ma ($^{206}Pb/^{238}U$ age); the remaining two analyses were very discordant, and one grain with a $^{207}Pb/^{206}Pb$ age of 2770 Ma is probably an inherited Archaean zircon.

Three analyses on zircons from GGU 432808 plot on a discordia line between 2000 and 450 Ma, but are too discordant to define a precise age.

Granitoid rocks associated with metaquartzitic sandstones in the Nørreland window

About 25 per cent of the area within the Nørreland window consists of felsic metaporphyritic rocks which appear to have intrusive relationships with the associated metasandstones, although strong deformation has made interpretation of the field observations difficult. Three samples were investigated.

A metaporphyritic quartz diorite (GGU 419967, Fig. 3B) yielded nearly opaque zircons with thin clear rims (too thin to be analysed). Three out of five zircons are close to concordant at *c*. 1860 Ma (Fig. 4B, Table 1); the two remaining grains yielded highly discordant data. All data points plot on a discordia line between 400 and 1890 Ma.

The meta-quartz diorite is cut by a metagranite sheet (GGU 419966) which yielded clear euhedral zircons with an upper intersection age of *c*. 1730 Ma (Fig. 4C); this we interpret as the age of emplacement of the granite.

A metagranodiorite (GGU 432871) from the Nørreland window yielded zircons with brown euhedrally zoned U-rich cores and wide clear rims. Five spot analyses (two cores and three rims) plot on a discordia line between 1900 and 400 Ma (Fig. 4D). The rims fall close to the upper intercept with concordia, while the cores plot nearer the lower intercept. The most plausible interpretation of this feature is that the upper intersection at *c*. 1900 Ma defines the emplacement of the granitoid rock, and that the scatter in isotopic compositions is due to variable Pb loss during Caledonian metamorphism, the metamict (more U-rich) cores (analyses 1.2 and 3.1, Table 2) having lost more Pb than the non-metamict rims.

Granitoid rocks from the Schnauder Ø complex

Two samples (GGU 418739 and 418777) were studied from the Schnauder Ø complex to test the possibility suggested by field observations that it could be of Caledonian age (Haller 1971; Jones & Escher 1995). Zircons from the two investigated samples are relatively clear and euhedral; a number of grains display distinct cores and rims. Three analyses were carried out on zircons from GGU 418739 including two rims, and six on zircons from GGU 418777, including four rims (Fig. 4E). All analyses are near-concordant and plot on or just below concordia between 1850 and 2000 Ma. Discordia calculations for these samples did not give meaningful results.

Granitoid rocks from Lambert Land and Hovgaard Ø

Three samples of granitoid rocks from Lambert Land and Hovgaard Ø were analysed, for which a Caledonian age was considered likely in the field either because they cut metadolerites lithologically similar to Midsommersø Dolerites or because of their occurrence within Caledonian shear zones.

Sample GGU 418670, a strongly deformed augen granite, was collected from a late Caledonian shear zone on southern Hovgaard Ø (Fig. 1), north of Lambert Land, to test whether it could have been emplaced during formation of the shear zone. Zircons vary from clear to metamict; many crystals are euhedral with sharp terminations, while some grains have distinct cores. Nine spots were analysed, two rims and seven cores. The seven analyses on cores plot close to a discordia with upper intersection at *c*. 1960 Ma. The two rims (one concordant) have high U concentrations and a very low Th/U ratio, suggesting formation during high-grade metamorphism (Williams & Claesson 1987); they have yielded $^{207}Pb/^{206}Pb$ ages of 1904 and 1936 Ma (Table 2).

A muscovite-biotite granite (GGU 418774, for composition see Fig. 3) was collected from a granite sheet within a presumed Caledonian thrust zone in the basement complex. This granite cuts across a Caledonian eclogite pod as well as its retrograde amphibolite border, suggesting that it might have been emplaced during Caledonian thrusting (Jones & Escher 1995). Most zircons from GGU 418774 are metamict to varying degrees and possess a complex structure: cores, more or

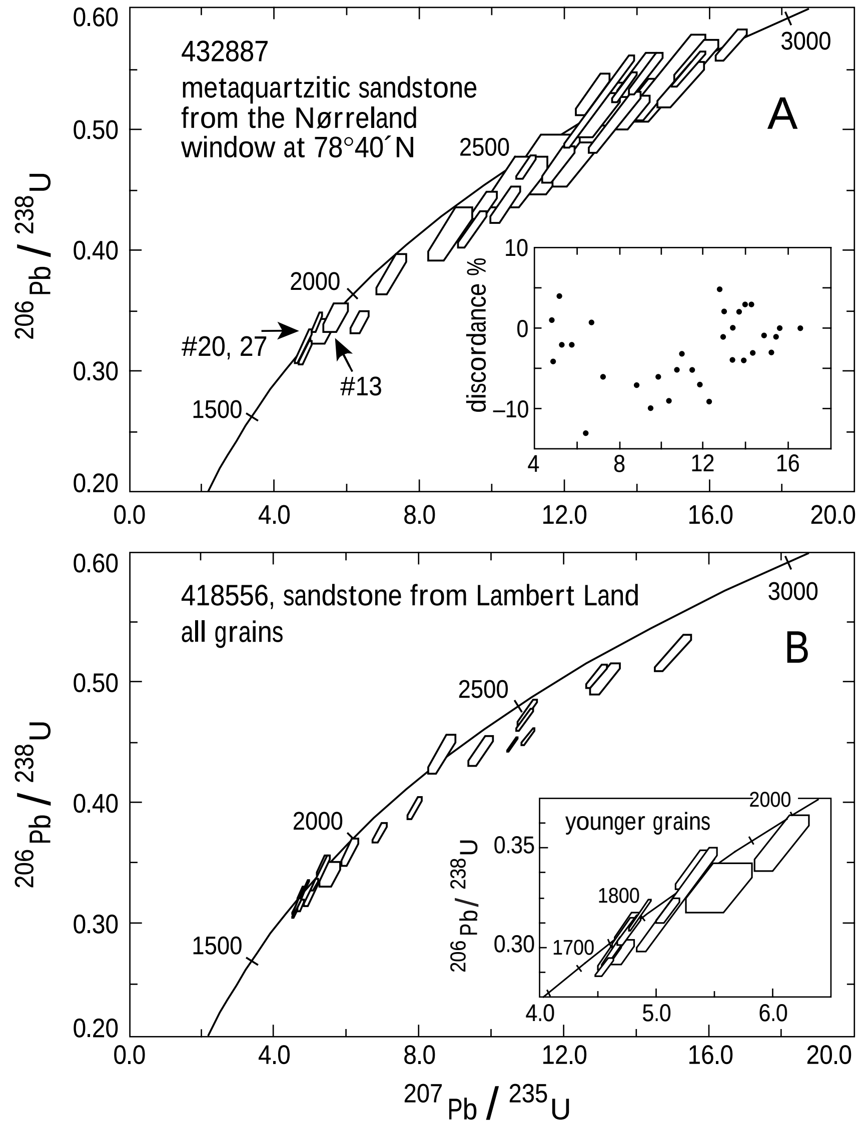

Fig. 5. Concordia diagrams for zircons from metasandstones, East Greenland Caledonian fold belt; error boxes display 1σ errors. For localities see Fig. 1.

less free of inclusions are surrounded by wide inclusion-rich rims which, in turn, have local inclusion-free protuberances ('outgrowths'). Eleven spots were analysed: four cores, four rims, one core overlapping rim, and two outgrowths. Most analyses yielded discordant data (Fig. 4F). They scatter along a discordia line with an upper intercept at *c*. 2000 Ma and lower intercept at *c*. 400 Ma. Rims and outgrowths plot near the lower intercept (Fig. 4G); cores fall more towards the upper intercept (Fig. 4F). There is a clear chemical difference between cores and rims (Table 2): cores having 180–510 ppm U and Th/U 0.06–0.37; rims 1230–3100 ppm U and Th/U 0.01–0.07. The outgrowths have intermediate values (900–1000 ppm U, Th/U 0.02). Two interpretations are consistent with the isotope data: either the upper intercept dates emplacement of the granite, and the scatter down to 400 Ma is due to strong Caledonian disturbance and new zircon growth, or GGU 418774 represents a Caledonian granite with inherited 2000 Ma zircons.

The last sample of this group, a deformed augen granodiorite (GGU 418705) cutting a mafic dyke, was collected on Lambert Land from an isolated outcrop in an area dominated by sandstones. The sample yielded clear to slightly turbid euhedral zircons with sharp terminations. No cores are present, but some grains have metamorphic (?) outgrowths. Five grains were analysed, including one outgrowth. All analyses are concordant or near-concordant and yield an age of *c*. 2000 Ma (Fig. 4H).

Table 3. SHRIMP U–Pb zircon ages for supracrustal rocks from the Caledonian fold belt

Spot	U (ppm)	Th/U	f_{206} (%)	$^{206}Pb/^{238}U$	$^{207}Pb/^{206}Pb$	Age	Disc. (%)
Metasandstones							
GGU 432887, Nørreland							
1.1	38	0.93	0.27	0.438 ± 15	0.1718 ± 31	2575 ± 31	–9
2.1	129	0.72	0.11	0.535 ± 12	0.1852 ± 13	2700 ± 12	2
3.1	79	0.80	0.38	0.529 ± 17	0.1753 ± 28	2608 ± 27	5
4.1	39	0.97	0.27	0.521 ± 18	0.1860 ± 47	2707 ± 42	0
5.1	46	0.70	0.02	0.471 ± 15	0.1821 ± 33	2672 ± 31	–7
6.1	15	1.02	0.02	0.471 ± 18	0.1889 ± 46	2733 ± 41	–9
7.1	101	1.31	0.06	0.570 ± 13	0.2111 ± 24	2914 ± 18	0
8.1	25	0.50	0.09	0.524 ± 18	0.1984 ± 67	2813 ± 56	–3
9.1	78	0.88	0.07	0.437 ± 11	0.1628 ± 33	2485 ± 34	–6
10.1	18	0.76	0.25	0.456 ± 21	0.1706 ± 87	2564 ± 88	–5
11.1	40	0.75	0.38	0.471 ± 25	0.1765 ± 106	2620 ± 104	–5
12.1	57	0.61	0.12	0.556 ± 18	0.2039 ± 37	2858 ± 30	0
13.1	47	0.52	0.47	0.333 ± 10	0.1158 ± 54	1892 ± 86	–2
13.2	28	0.75	0.34	0.344 ± 12	0.1199 ± 51	1955 ± 78	–2
14.1	130	0.68	0.02	0.550 ± 15	0.2036 ± 12	2855 ± 9	–1
15.1	62	0.55	1.45	0.340 ± 9	0.1356 ± 36	2171 ± 47	–13
15.2	59	0.42	0.02	0.380 ± 17	0.1382 ± 38	2205 ± 48	–6
16.1	72	0.93	0.02	0.546 ± 17	0.1891 ± 18	2734 ± 16	3
17.1	154	0.95	0.36	0.514 ± 14	0.1959 ± 33	2793 ± 28	–4
18.1	134	0.43	0.17	0.543 ± 36	0.1984 ± 42	2813 ± 35	–1
19.1	183	0.24	0.19	0.506 ± 25	0.1919 ± 24	2759 ± 21	–4
20.1	442	0.13	0.93	0.193 ± 4	0.1089 ± 20	1781 ± 34	–36
20.2	358	0.15	0.45	0.315 ± 10	0.1123 ± 15	1837 ± 24	–4
21.1	74	0.50	0.29	0.417 ± 15	0.1646 ± 24	2504 ± 25	–10
22.1	237	0.91	0.20	0.523 ± 38	0.1798 ± 16	2651 ± 15	2
23.1	49	0.69	0.35	0.537 ± 19	0.2055 ± 35	2870 ± 28	–3
24.1	104	0.81	0.17	0.675 ± 27	0.2563 ± 19	3224 ± 12	3
25.1	103	0.74	0.57	0.512 ± 18	0.1833 ± 46	2683 ± 42	–1
26.1	32	0.71	1.44	0.413 ± 22	0.1556 ± 55	2409 ± 62	–7
27.1	339	0.50	0.15	0.340 ± 8	0.1108 ± 12	1812 ± 19	4
27.2	325	0.48	0.08	0.320 ± 14	0.1089 ± 14	1780 ± 24	1
28.1	84	1.69	0.13	0.545 ± 18	0.1864 ± 26	2711 ± 23	3
29.1	121	0.30	0.07	0.469 ± 10	0.1695 ± 18	2552 ± 18	–3
GGU 418556, Lambert Land							
1.1	271	0.44	1.47	0.329 ± 21	0.1144 ± 13	1871 ± 20	–2
2.1	190	0.37	0.57	0.462 ± 9	0.1713 ± 10	2571 ± 10	–5
3.1	984	0.09	0.39	0.441 ± 6	0.1738 ± 5	2595 ± 5	–9
4.1	851	0.04	0.22	0.308 ± 5	0.1112 ± 13	1819 ± 22	–5
5.1	834	0.03	0.26	0.302 ± 4	0.1096 ± 7	1793 ± 12	–5
6.1	126	0.70	0.63	0.498 ± 10	0.1876 ± 16	2722 ± 14	–4
7.1	493	1.02	2.57	0.448 ± 7	0.1783 ± 9	2637 ± 9	–9
8.1	194	0.45	0.47	0.325 ± 5	0.1140 ± 10	1864 ± 16	–3
9.1	967	0.06	6.78	0.368 ± 8	0.1363 ± 18	2180 ± 23	–7
10.1	1510	0.04	0.14	0.318 ± 6	0.1083 ± 11	1771 ± 18	1
11.1	213	0.30	0.35	0.389 ± 9	0.1469 ± 15	2310 ± 18	–8
12.1	117	0.41	0.08	0.436 ± 12	0.1613 ± 25	2469 ± 27	–5
13.1	223	0.59	0.11	0.468 ± 11	0.1698 ± 13	2556 ± 13	–3
14.1	1117	0.04	2.01	0.306 ± 5	0.1089 ± 10	1782 ± 17	–3
15.1	175	0.95	0.15	0.517 ± 15	0.2105 ± 23	2910 ± 18	–8

Table 3 *(continued)*

Spot	U (ppm)	Th/U	f_{206} (%)	$^{206}Pb/^{238}U$	$^{207}Pb/^{206}Pb$	Age	Disc. (%)
16.1	107	0.19	0.50	0.341 ± 8	0.1136 ± 18	1858 ± 28	2
17.1	69	0.77	0.34	0.496 ± 13	0.1918 ± 27	2758 ± 23	–6
18.1	125	0.47	0.01	0.352 ± 11	0.1252 ± 24	2032 ± 34	–4
19.1	699	0.03	0.15	0.317 ± 6	0.1093 ± 7	1787 ± 12	–1
20.1	1138	0.05	0.22	0.308 ± 6	0.1091 ± 7	1785 ± 12	–3
21.1	1651	0.03	0.11	0.323 ± 6	0.1091 ± 3	1784 ± 6	1
22.1	46	1.34	0.95	0.334 ± 10	0.1204 ± 46	1963 ± 70	5
23.1	70	0.54	0.68	0.433 ± 16	0.1443 ± 28	2280 ± 34	2
24.1	1743	0.04	0.10	0.316 ± 6	0.1088 ± 10	1779 ± 17	–1
Metarhyolitic rocks							
GGU 423424							
1.1	742	0.61	0.05	0.278 ± 7	0.1052 ± 10	1718 ± 17	–8
2.1	38	0.77	1.22	0.304 ± 11	0.1008 ± 49	1638 ± 93	5
3.1	76	0.51	0.17	0.304 ± 10	0.1047 ± 30	1709 ± 53	0
4.1	793	0.84	0.01	0.284 ± 7	0.1055 ± 10	1723 ± 17	–7
5.1	52	0.99	0.08	0.300 ± 17	0.1094 ± 29	1789 ± 49	–5
6.1	46	0.75	0.35	0.304 ± 11	0.1062 ± 26	1735 ± 46	–1
7.1	199	1.00	0.02	0.307 ± 13	0.1072 ± 15	1753 ± 25	–2
7.2	170	0.97	0.03	0.309 ± 10	0.1077 ± 16	1760 ± 27	–1
8.1	70	1.10	0.00	0.306 ± 9	0.1098 ± 25	1796 ± 42	–4
9.1	511	0.73	0.03	0.298 ± 9	0.1065 ± 7	1741 ± 12	–3
10.1	1077	1.62	0.03	0.306 ± 8	0.1068 ± 4	1746 ± 7	–1
GGU 423425							
1.1	379	1.66	0.24	0.303 ± 8	0.1062 ± 10	1735 ± 17	–2
2.1	228	0.65	0.34	0.310 ± 6	0.1059 ± 18	1731 ± 31	0
3.1	341	0.71	0.21	0.308 ± 6	0.1065 ± 18	1741 ± 31	–1
4.1	311	0.81	0.27	0.313 ± 8	0.1062 ± 11	1734 ± 19	1
5.1	144	0.90	0.77	0.310 ± 6	0.1057 ± 23	1727 ± 41	1
6.1	448	1.13	0.04	0.307 ± 9	0.1065 ± 8	1740 ± 14	–1
7.1	402	0.18	0.11	0.307 ± 8	0.1056 ± 9	1725 ± 16	0
8.1	535	0.65	0.14	0.305 ± 5	0.1064 ± 7	1739 ± 12	–1
9.1	353	0.70	0.11	0.304 ± 6	0.1077 ± 11	1760 ± 20	–3
10.1	183	0.77	0.24	0.312 ± 8	0.1078 ± 25	1762 ± 43	–1

f_{206} is the proportion of ^{206}Pb that is not radiogenic; Disc. is the degree of discordance between the $^{207}Pb/^{206}Pb$ and $^{206}Pb/^{238}U$ ages; Age is the apparent $^{207}Pb/^{206}Pb$ age. All errors quoted at 1σ level.

Sandstones

Detrital zircons were investigated from two samples of metasandstone from the fold belt, traditionally correlated with the Independence Fjord Group: GGU 432887 from the Nørreland window, and GGU 418556 from Lambert Land.

The sample from Nørreland is a strongly strained quartzite. Nearly all zircons appear detrital; they are rounded and have pitted surfaces. Most grains have low U (< 100 ppm) and most analyses yielded Archaean $^{207}Pb/^{206}Pb$ ages with a significant scatter along a discordia line between *c.* 1800 and 2800 Ma (Fig. 5A). Analyses with a $^{207}Pb/^{206}Pb$ age between 1800 and 2700 Ma appear to be more discordant than those around 1800 and 2700–2900 Ma (Fig. 5A, inset), which suggests that most of these ages may have no chronological meaning but, more probably, are the result of Pb loss from Archaean zircons during a Palaeoproterozoic metamorphic event. One zircon (No. 13, Table 3,

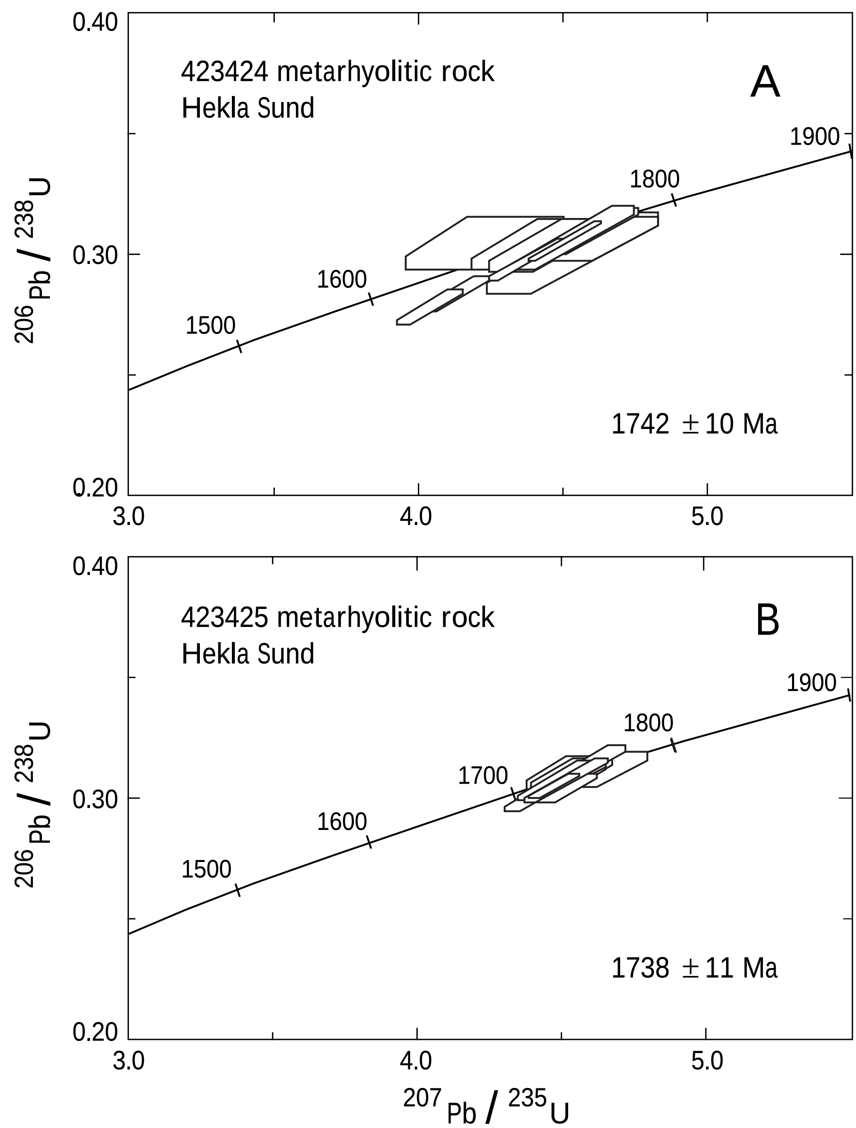

Fig. 6. Concordia diagrams for zircons from metarhyolitic rocks interlayered with metabasaltic pillow lavas at Hekla Sund; error boxes display 1σ errors. For locality see Fig. 1.

Fig. 5A), with a $^{207}Pb/^{206}Pb$ age of *c.* 1900 Ma, is concordant and probably represents a truly Proterozoic detrital zircon. Two grains (Nos 20 and 27, Fig. 5A) yielded concordant $^{207}Pb/^{206}Pb$ ages of about 1800 Ma. These grains have significantly higher U than all other analysed zircons and could be metamorphic in origin.

Most zircons from the Lambert Land sample (GGU 418556) are abraded and variably rounded and are thus clearly of detrital origin. $^{207}Pb/^{206}Pb$ ages for this group range from 1900 to 2900 Ma (Table 3, Fig. 5B). Most of these zircons yielded discordant data, and the ages cannot be taken at face value, but a few grains gave near-concordant ages between 1800 and 2050 Ma (Fig. 5B, inset) which we interpret as close to their true age. Another group of zircons is not obviously abraded; these grains are strongly coloured and show spectacular twinning in some cases. Eight grains were analysed; they have high U and low Th/U ratios (Table 3) and all yielded ages of about 1775 Ma (Fig. 5B, inset). If the strongly coloured zircons were derived from 1775 Ma granitic rocks their well-preserved structures suggest they were not transported far. The isotope data do not exclude the possibility that these grains represent metamorphic zircons formed within the sandstone, but in view of the twinning this would appear less likely to be the case.

Rhyolitic rocks

Two samples were studied of feldspar-phyric metarhyolitic rocks associated with the basalt sequence at Hekla Sund. As noted above, the basalt–rhyolite sequence is interlayered with sandstones correlated with the Independence Fjord Group, and forms part of the Caledonian thrust units. Zircons occur mainly as crystal fragments, up to 200 µm long, sometimes with euhedral terminations. Nine (out of 10) analyses on zircons from GGU 423424 and ten analyses on zircons from GGU 423425 yielded tight clusters on concordia at 1742 ± 10 and 1738 ± 11 Ma, respectively (Fig. 6, Tables 1, 2). Taken together the zircons from the two samples give a weighted mean age of 1740 ± 6 Ma (MSWD 0.52), which we interpret as dating the time of emplacement of the rhyolitic rocks and the associated basalts; this age has clear implications for the age of the sandstone sequence.

Discussion

Interpretation of the isotope data on the granitoid rocks

With one possible exception (GGU 418774) all investigated granitoid samples yielded Palaeoproterozoic zircon dates of 1730–2000 Ma, which normally would be interpreted as the age of igneous emplacement of the rocks. This does not agree with the impression gained during field work that some of the granitoid rocks could be of Caledonian age. However, granitoid rocks derived from crustal sources often contain zircons inherited from their parents (e.g. Pidgeon & Compston 1992), and the question has to be considered whether the analysed zircons could be inherited, and therefore give no information on the true age of the rocks. For several reasons we consider this as unlikely.

1. The granite for which a Caledonian age is most strongly supported by field observations (GGU 418774, which cuts through a Caledonian eclogite pod as well as its retrogressed rim), is also the only sample where zircon rims plot close to 400 Ma on a discordia line (Fig. 4G). Zircons from most other samples, cores as well as rims, plot on or close to concordia at 1750–2000 Ma (e.g. GGU 418777 and 418705; Fig. 4E, H). If these samples represent Caledonian granites, *all* analysed zircons would have to be inherited, whereas zircons formed during Caledonian granite formation are so rare that they were not detected. This is unlikely: Caledonian granites from Scotland, for example those studied by Pidgeon & Compston (1992), have both magmatic and inherited zircons present in significant proportions.

2. Inherited zircons in granitic rocks commonly yield widely variable ages (e.g. Pidgeon & Compston 1992). In the samples investigated here all zircons have more or less the same age (e.g. GGU 418705, Fig. 4H), which is less likely to be the case if they represent anatectic granites containing only inherited zircons.

3. Palaeoproterozoic zircons in several of the investigated samples are perfectly euhedral, with well preserved sharp pyramidal terminations (e.g. GGU 418705). Such features are unlikely to have survived Caledonian melting, since at least part of the zircon would probably go into solution (Watson & Harrison 1983).

4. Inherited zircons are common in anatectic granites, especially those formed at relatively low temperatures; they occur most frequently in S-type granites which are typically formed at temperatures of 700–750°C, compared to 800–900°C for I-type granitoids (Watson & Harrison 1983). The two samples within which inherited (Archaean) zircons have been found (GGU 418719 and 419802, see above) belong indeed to the group of low-temperature leucogranites shown in Fig. 3, but several of the other samples studied are more mafic I-type granodiorites or tonalitic rocks (for example GGU 418705 and 432871, Fig. 3), within which inherited zircons are much less common.

Together, we consider these features are very strong evidence that (with the possible exception of GGU 418774) the investigated granites were emplaced during Palaeoproterozoic, not Caledonian, orogenic events.

Interpretation of the isotope data on the sandstones

In view of the preponderance of Palaeoproterozoic gneisses and granitoid rocks in the region it is surprising that detrital 1750–2000 Ma zircons are relatively rare in the investigated sandstones from the Caledonian fold belt. Most zircons analysed are Archaean, but appear to have experienced severe Pb loss during high-grade Palaeoproterozoic metamorphism. Large areas in West Greenland and southern East Greenland are composed of Archaean rocks reworked during Palaeoproterozoic tectonothermal events around 1800–1850 Ma (see the Geological map of Greenland, 1:2 500 000, Escher &

Pulvertaft 1995). Such rocks also occur (at least locally) beneath the Inland Ice (Escher & Pulvertaft 1995; Weis *et al.* 1997). It is plausible that most zircons in the investigated metasandstones were derived by erosion of such a terrane.

Deposition of the sandstones probably took place after the end of the Palaeoproterozoic igneous and tectono-metamorphic events, in agreement with the undeformed and unmetamorphosed nature of the Independence Fjord Group sandstones in the Caledonian foreland. The presence of a few detrital zircons of Palaeoproterozoic age (1800–2050 Ma) in the sandstones of the Caledonian fold belt supports this suggestion. Since the 1740 Ma basalt sequence at Hekla Sund is interlayered with the metasandstones of Lambert Land and Kronprins Christian Land (Fig. 1), the age of the basalts provides a time point within the period of deposition of the sandstones. Deposition thus must have started already during the later Palaeoproterozoic, very soon after the end of the Palaeoproterozoic orogenic events in the region. Since any metamorphism of the sandstones must have taken place later than *c.* 1740 Ma, the strongly coloured, U-rich, 1775 Ma zircons in the sample from Lambert Land are probably detrital rather than *in situ* metamorphic in origin, which would constrain deposition of at least some of the sandstones on Lambert Land to the period 1775–1740 Ma. This is much earlier than anticipated: on the Geological map of Greenland (Escher & Pulvertaft 1995) the sandstones of Lambert Land and their assumed correlatives of the Independence Fjord Group in the Caledonian foreland are shown as Mesoproterozoic deposits.

Deposition of some of the sandstones around 1750 Ma ago would permit the possibility that they were intruded by the youngest of the dated granite sheets in the region. This may be the case in the Nørreland window where the quartzitic sandstones appear to be cut by granites. One of these (GGU 419966) has yielded an age of about 1730 Ma (Table 1), and may have been emplaced into very young sandstone. However, most of the granites (e.g. GGU 418705 in Lambert Land) are much older than the sandstones with which they are now spatially associated. Lambert Land is characterised by a complex history of Caledonian thrusting (Jones & Escher 1995); this thrusting has apparently brought rocks of different ages into close juxtaposition.

Why are there no Caledonian granites in the northern part of the Caledonian fold belt?

Formation of granitic magmas in collisional orogens is dependent on several factors, the most important being: (1) the temperatures reached during orogenic thickening and later extension, and (2) the presence of 'fertile' crustal lithologies (e.g. Vielzeuf *et al.* 1990; Brown 1994). The metamorphic temperatures estimated for the eclogites in the Caledonian fold belt are 700–800°C (Brueckner *et al.* 1998; K.A. Jones, unpublished data), which are less than required for the formation of I-type granitoid magmas (Watson & Harrison 1983, p. 303). In the area under consideration the Precambrian basement consists mainly of 'sterile' Palaeoproterozoic granitoid rocks, with relatively small amounts of biotite and hornblende (most commonly < 10%); these do not permit large proportions of granitic magma to be formed by dehydration melting at temperatures below *c.* 900°C, because only small amounts of water will be generated by dehydration (e.g. Clemens & Vielzeuf 1987). 'Fertile' lithologies, such as pelitic metasedimentary rocks are rare within the crystalline basement. Those metasedimentary units that are present comprise the quartz-rich sandstones of Lambert Land and Nørreland, which would not easily melt, and large units of Neoproterozoic to lower Palaeozoic semipelitic lithologies that are present in high-level Caledonian thrust units in Kronprins Christian Land (Fig. 1). Those, however, are at a very low metamorphic grade, and have never been very deeply buried.

In contrast to the northern part of the Caledonian fold belt investigated during the present study, Caledonian granites are common in the southern part of the Caledonian fold belt, south of Bessel Fjord (76°N). The Geological map of Greenland, 1:2 500 000 (Escher & Pulvertaft 1995) shows that large parts of that region are underlain by high-grade metasedimentary sequences. Furthermore, many of the Caledonian granites occur within units of metasedimentary rocks, and formation by anatexis of the metasediments is suggested by field observations and geochemical data (Kalsbeek *et al.* 1998). The rarity of corresponding metasedimentary units in the northernmost part of the Caledonian fold belt may be the main reason why Caledonian granites do not occur in this area.

Acknowledgements

We thank Professor W. Compston, Australian National University, for permission to use SHRIMP 1 for this study, Peter Venslev (Copenhagen) and Neil Gabbitas (Canberra) for assistance with the sample preparation, and Niels Henriksen, Stuart Watt and A.K. Higgins for critical reading of earlier versions of the manuscript.

References

Barker, F. 1979: Trondhjemite: definition, environment and hypotheses of origin. In: Barker, F. (ed.): Trondhjemites, dacites, and related rocks, 1–12. Amsterdam: Elsevier.

Brown, M. 1994: The generation, segregation, ascent and emplacement of granite magma: the migmatite-to-crustally-derived granite connection in thickened orogens. Earth-Science Reviews **36**, 83–130.

Brueckner, H.K., Gilotti, J.A. & Nutman, A.P. 1998: Caledonian eclogite-facies metamorphism of Early Proterozoic protoliths from the North-East Greenland eclogite province. Contributions to Mineralogy and Petrology **130**, 103–120.

Claoué-Long, J.C., Compston, W., Roberts, J. & Fanning, C.M. 1995: Two Carboniferous ages: A comparison of SHRIMP zircon dating with conventional zircon ages and $^{40}Ar/^{39}Ar$ analysis. In: Berggren, W.A. *et al.* (eds): Geochronology, time scales and global stratigraphic correlation. Society for Sedimentary Geology Special Publication **54**, 3–21.

Clemens, J.D. & Vielzeuf, D. 1987: Constraints on melting and magma production in the crust. Earth and Planetary Science Letters **86**, 287–306.

Collinson, J.D. 1980: Stratigraphy of the Independence Fjord Group (Proterozoic) of eastern North Greenland. Rapport Grønlands Geologiske Undersøgelse **99**, 7–23.

Collinson, J.D. 1983: Sedimentology of unconformities within a fluvio-lacustrine sequence; Middle Proterozoic of eastern North Greenland. Sedimentary Geology **34**, 145–166.

Compston, W., Williams, I.S. & Meyer, C.E. 1984: U-Pb geochronology of zircons from Lunar Breccia 73217 using a sensitive high mass-resolution ion microprobe. In: Boynton, W.V. & Schubert, G. (eds): Proceedings of the 14th lunar and planetary science conference. Part 2. Journal of Geophysical Research Supplement **89**, B525–B534.

Escher, J.C. & Pulvertaft, T.C.R. 1995: Geological map of Greenland, 1:2 500 000. Copenhagen: Geological Survey of Greenland.

Gilotti, J.A. 1993: Discovery of a medium temperature eclogite province in the Caledonides of North-East Greenland. Geology **21**, 523–526.

Haller, J. 1971: Geology of the East Greenland Caledonides, xxi + 413 pp. London: Interscience Publishers (J. Wiley and Sons).

Henriksen, N. 1985: The Caledonides of central East Greenland 70°–76°N. In: Gee, D.G. & Sturt, B.A. (eds): The Caledonide orogen – Scandinavia and related areas **2**, 1095–1113. Chichester, UK: John Wiley and Sons.

Henriksen, N. & Higgins, A.K. 1976: East Greenland Caledonian fold belt. In: Escher, A. & Watt, W.S. (eds): Geology of Greenland, 182–246. Copenhagen: Geological Survey of Greenland.

Higgins, A.K. 1995a: Caledonides of East Greenland. In: Williams, H. (ed.): Geology of the Appalachian-Caledonian orogen in Canada and Greenland. Geology of Canada **6**, 891–921. Ottawa: Geological Survey of Canada (also The geology of North America **F-1**, Geological Society of America).

Higgins, A.K. (ed.) 1995b: Express report: eastern North Greenland and North-East Greenland 1995, 171 pp. Unpublished report, Geological Survey of Greenland, Copenhagen.

Hull, J.M. & Friderichsen, J.D. 1995: Geology of basement rocks in northern North-East and eastern North Greenland. In: Higgins, A.K. (ed.): Express report: eastern North Greenland and North-East Greenland 1995, 11–21. Unpublished report, Geological Survey of Greenland, Copenhagen.

Hull, J.M., Friderichsen, J.D., Gilotti, J.A., Henriksen, N., Higgins, A.K. & Kalsbeek, F. 1994: Gneiss complex of the Skærfjorden region (76°–78°N), North-East Greenland. In: Higgins, A.K. (ed.): Geology of North-East Greenland. Rapport Grønlands Geologiske Undersøgelse **162**, 35–51.

Jones, K.A. & Escher, J.C. 1995: An E–W traverse across the Caledonian fold belt from Lambert Land to Norske Øer. In: Higgins, A.K. (ed.): Express report: eastern North Greenland and North-East Greenland 1995, 23–41. Unpublished report, Geological Survey of Greenland, Copenhagen.

Kalsbeek, F. & Jepsen, H.F. 1983: The Midsommersø Dolerites and associated intrusions in the Proterozoic platform of eastern North Greenland – a study of the interaction between intrusive basic magma and sialic crust. Journal of Petrology **24**, 605–634.

Kalsbeek, F. & Jepsen, H.F. 1984: The late Proterozoic Zig-Zag Dal Basalt Formation of eastern North Greenland. Journal of Petrology **25**, 644–664.

Kalsbeek, F., Nutman, A.P. & Taylor, P.N. 1993: Palaeoproterozoic basement province in the Caledonian fold belt of North-East Greenland. Precambrian Research **63**, 163–178.

Kalsbeek, F., Nutman, A.P. & Jepsen, H.F. 1998: Granites in the Caledonian fold belt, East Greenland. In: Frederiksen, K.S. & Thrane, K. (eds): Symposium on Caledonian geology in East Greenland. Abstract volume. Danmarks og Grønlands Geologiske Undersøgelse Rapport **1998/46**, 43–44.

Larsen, O. & Graff-Petersen, P. 1980: Sr-isotope studies and mineral composition of the Hagen Bræ Member in the Proterozoic clastic sediments at Hagen Bræ, eastern North Greenland. Rapport Grønlands Geologiske Undersøgelse **99**, 111–118.

Nutman, A.P. & Kalsbeek, F. 1994: Search for Archaean basement in the Caledonian fold belt of North-East Greenland. In: Higgins, A.K. (ed.): Geology of North-East Greenland. Rapport Grønlands Geologiske Undersøgelse **162**, 129–133.

O'Connor, J.T. 1965: A classification for quartz-rich igneous rocks based on feldspar ratios. U.S. Geological Survey Professional Paper **525B**, 79–84.

Peacock, J.D. 1956: The geology of Dronning Louise Land, N.E. Greenland. Meddelelser om Grønland **137**(7), 38 pp.

Peacock, J.D. 1958: Some investigations into the geology and petrography of Dronning Louise Land, N.E. Greenland. Meddelelser om Grønland **157**(4), 139 pp.

Pedersen, S.A.S., Craig, L.E. & Upton, B.G.J. 1995a: The Proterozoic basalt formation at Hekla Sund, Prinsesse Caroline Mathilde Alper, eastern North Greenland. In: Higgins, A.K. (ed.): Express report: eastern North Greenland and North-East Greenland 1995, 63–70. Unpublished report, Geological Survey of Greenland, Copenhagen.

Pedersen, S.A.S., Leslie, A.G. & Craig, L.E. 1995b: Proterozoic and Caledonian geology of the Prinsesse Caroline Mathilde Alper, eastern North Greenland. In: Higgins, A.K. (ed.): Express report: eastern North Greenland and North-East Greenland 1995, 71–85. Unpublished report, Geological Survey of Greenland, Copenhagen.

Pidgeon, R.T. & Compston, W. 1992: A SHRIMP ion microprobe study of inherited and magmatic zircons from four Scottish Caledonian granites. In: Brown, P.E. & Chappel, B.W. (eds): Proceedings of the second Hutton symposium on the origin of granites and related rocks. Geological Society of America Special Paper **272**, 473–483.

Sønderholm, M. & Jepsen, H.F. 1991: Proterozoic basins of North Greenland. In: Peel, J.S. & Sønderholm, M. (eds): Sedimentary basins of North Greenland. Bulletin Grønlands Geologiske Undersøgelse **160**, 49–69.

Strachan, R.A., Friderichsen, J.D., Holdsworth, R.E. & Jepsen, H.F. 1994: Regional geology and Caledonian structure, Dronning Louise Land, North-East Greenland. In: Higgins, A.K. (ed.): Geology of North-East Greenland. Rapport Grønlands Geologiske Undersøgelse **162**, 71–76.

Streckeisen, A.L. 1976: To each plutonic rock its proper name. Earth-Science Reviews **12**, 1–33.

Vielzeuf, D., Clemens, J.D., Pin, C. & Moinet, E. 1990: Granites, granulites and crustal differentiation. In: Vielzeuf, D. & Vidal, Ph. (eds): Granulites and crustal evolution, 59–85. Dordrecht: Kluwer.

Watson, E.B. & Harrison, T.M. 1983: Zircon saturation revisited: temperature and composition effects in a variety of crustal magma types. Earth and Planetary Science Letters **64**, 295–304.

Weis, D., Demaiffe, D., Souchez, R., Gow, A.J. & Meese, D.A. 1997: Ice sheet development in central Greenland: implications from the Nd, Sr and Pb isotopic compositions of basal material. Earth and Planetary Science Letters **150**, 161–169.

Williams, I.S. 1998: U-Th-Pb geochronology by Ion Microprobe. In: McKibben, M.A., Shanks III, W.C. & Ridley, W.I. (eds): Applications of microanalytical techniques to understanding mineralizing processes. Reviews in Economic Geology **7**, 1–35.

Williams, I.S. & Claesson, S. 1987: Isotopic evidence for the Precambrian provenance and Caledonian metamorphism of the high-grade paragneisses from the Seve Nappes, Scandinavian Caledonides, II. Ion microprobe zircon U-Th-Pb. Contributions to Mineralogy and Petrology **97**, 205–217.

York, D. 1969: Least squares fitting of a straight line with correlated errors. Earth and Planetary Science Letters **5**, 320–324.

Variability of XRF and AAS analyses from the Rock Geochemical Laboratory of the Geological Survey of Denmark and Greenland

Agnete Steenfelt

Chemical analyses by X-ray fluorescence spectrometry (XRF) and atomic absorption spectrometry (AAS) have been monitored since 1990 by five internal standards. Diagrams of the variability over nine years show that analytical data for major elements, Cr, Cu and V have been stable over the entire period, while data for Ni, Rb and Sr have been stable since 1993. Results for Ba, Zn and Zr have lower precision, but have maintained the same general level. Analysis of international reference material shows that nine of the trace element determinations are accurate or can be adjusted by simple arithmetic to match the recommended values for the reference material.

Geological Survey of Denmark and Greenland, Thoravej 8, DK-2400 Copenhagen NV, Denmark. E-mail: *ast@geus.dk*

Keywords: analysis, analytical methods, geochemical maps, quality control, X-ray fluorescence

The production of geochemical maps for large regions commonly involves the compilation of chemical data obtained over a period of time. In order to base such maps on a consistent data set, it is crucial to monitor chemical data and apply corrections to eliminate any analytical bias that may exist between data sets obtained at different times (Steenfelt 1999). Also in petrologic studies it is common to compare large amounts of chemical data from various sources, and if such data are not carefully controlled analytical biases may be misinterpreted as real differences between the analysed materials. This note presents the results of monitoring of analytical data from one laboratory using internal standards.

The Rock Geochemical Laboratory (RGL) of the Geological Survey of Denmark and Greenland (GEUS), formerly at the Geological Survey of Greenland (GGU), has delivered chemical analyses for geochemical mapping and exploration in Greenland since 1986. Samples of stream sediments and rocks have been analysed by simultaneous X-ray fluorescence spectrometry with a multichannel Philips PW1406 spectrometer on fused samples (using sodium tetraborate as flux) for major elements except sodium and for a short suite of trace elements. Determination of sodium (Na) and copper (Cu) are made by atomic absorption spectrometry (AAS). For details of the methods and instruments see Kystol & Larsen (1999, this volume). Major element analyses from RGL have been monitored by international reference material and have always been very reliable, whereas the quality of the trace element data, except for Cu, has been variable and until now not well documented. The main problem with the use of fused samples for trace element determination is the dilution of the samples by the flux which lowers the concentration of the trace elements and gives poorer counting statistics. The RGL is aware of the problem and stresses to customers that the trace element data are only of reconnaissance character.

Geochemical mapping of Greenland has been undertaken since 1981 and is based on stream sediment samples collected at a density of one sample per 20–50 km^2 (Steenfelt 1993, 1994, 1996). The less than 0.1 mm grain size fractions have been analysed over the years by several methods at a few laboratories besides RGL. In the course of this programme internal standards have been used since 1990 to monitor the quality of analyses from various sources and to detect if there is any bias between data determined by different methods, by the same method determined at different labo-

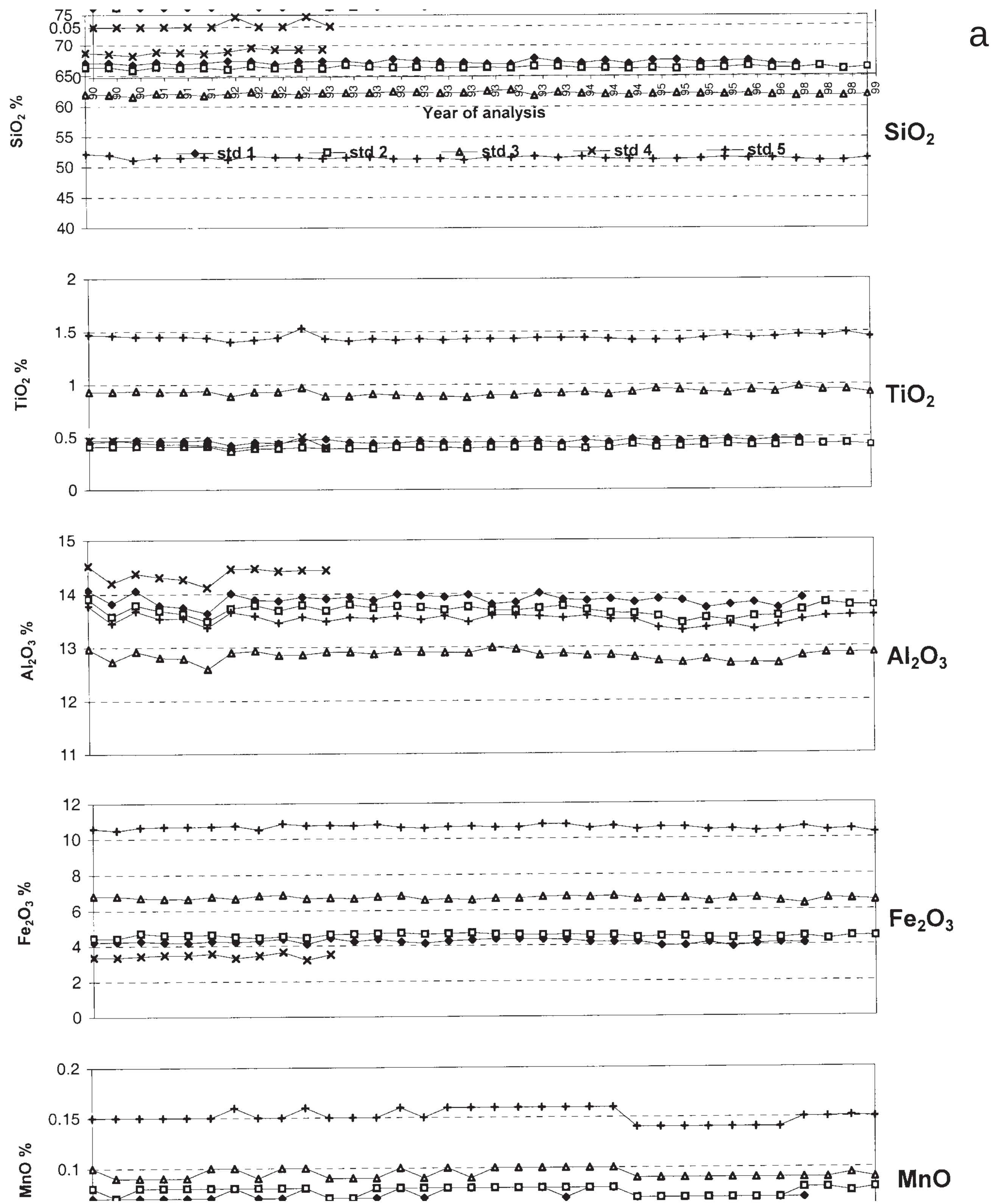

Fig. 1. **a**, **b**: Variability of major element results for five internal standards (std 1–5) in the period 1990 to 1999. The standards are analysed by simultaneous X-ray fluorescence spectrometry on glass discs and atomic absorption spectrometry (for Na) at the Rock Geochemical Laboratory, Geological Survey of Denmark and Greenland. Fe_2O_3 is total iron.

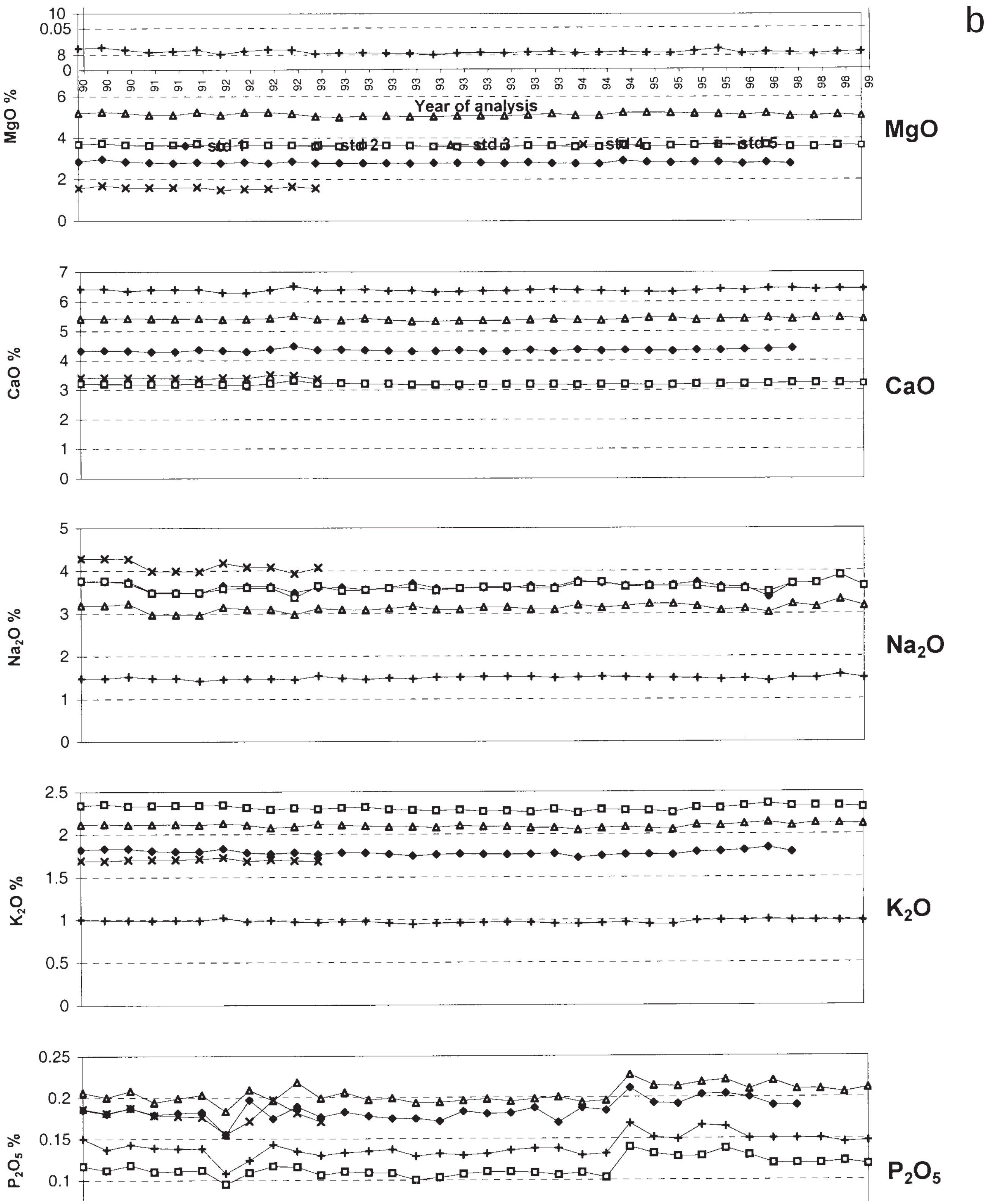

Fig. 1 *(continued)*

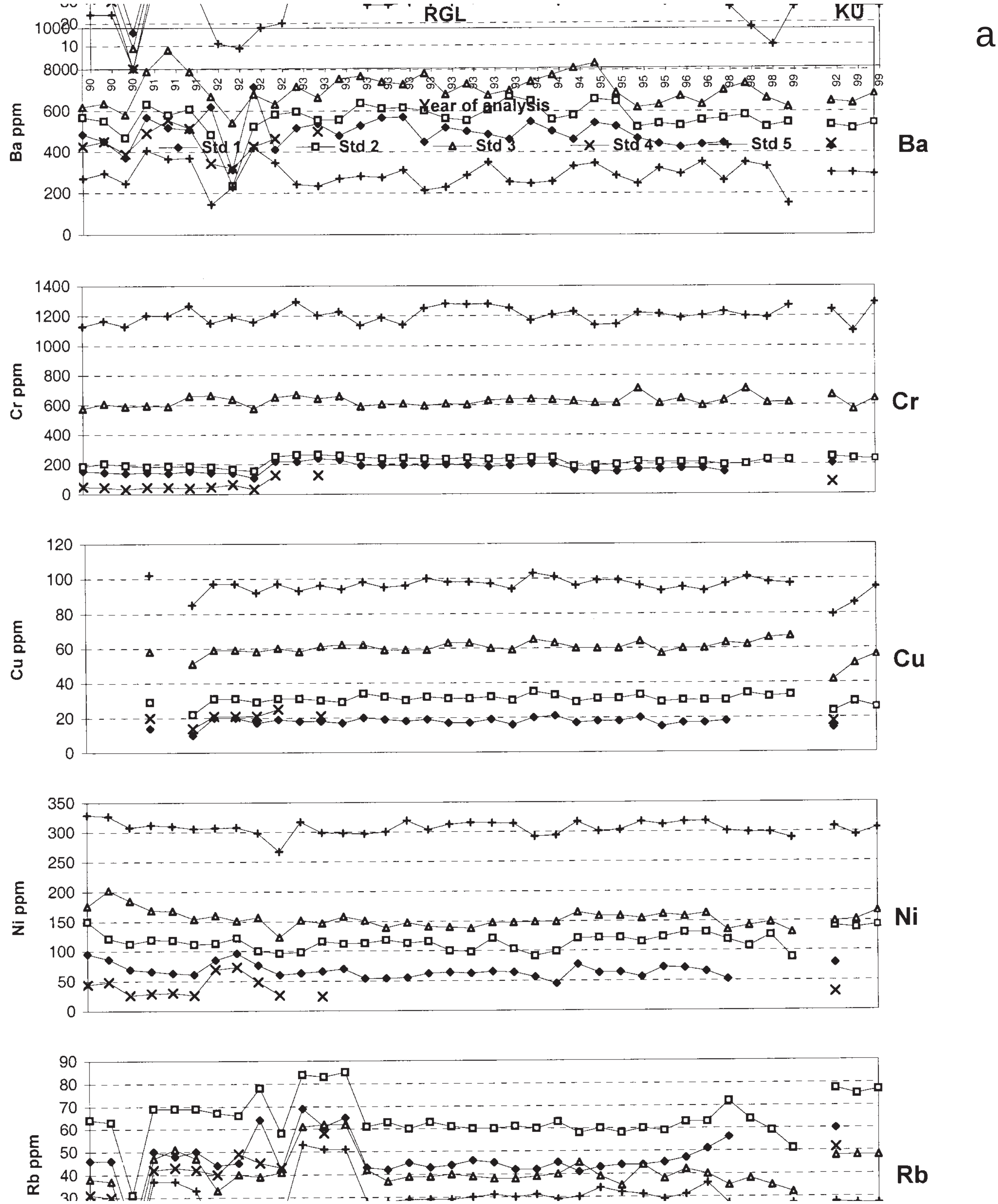

Fig. 2. **a**, **b**: Variability of trace element results for five internal standards (std 1–5) in the period 1990 to 1999. The standards are analysed by simultaneous X-ray fluorescence spectrometry (XRF) on glass discs, and atomic absorption spectrometry (for Cu) at the Rock Geochemical Laboratory (RGL), Geological Survey of Denmark and Greenland, and by sequential XRF on pressed powder pellets by J.C. Bailey, Geological Institute, University of Copenhagen (KU).

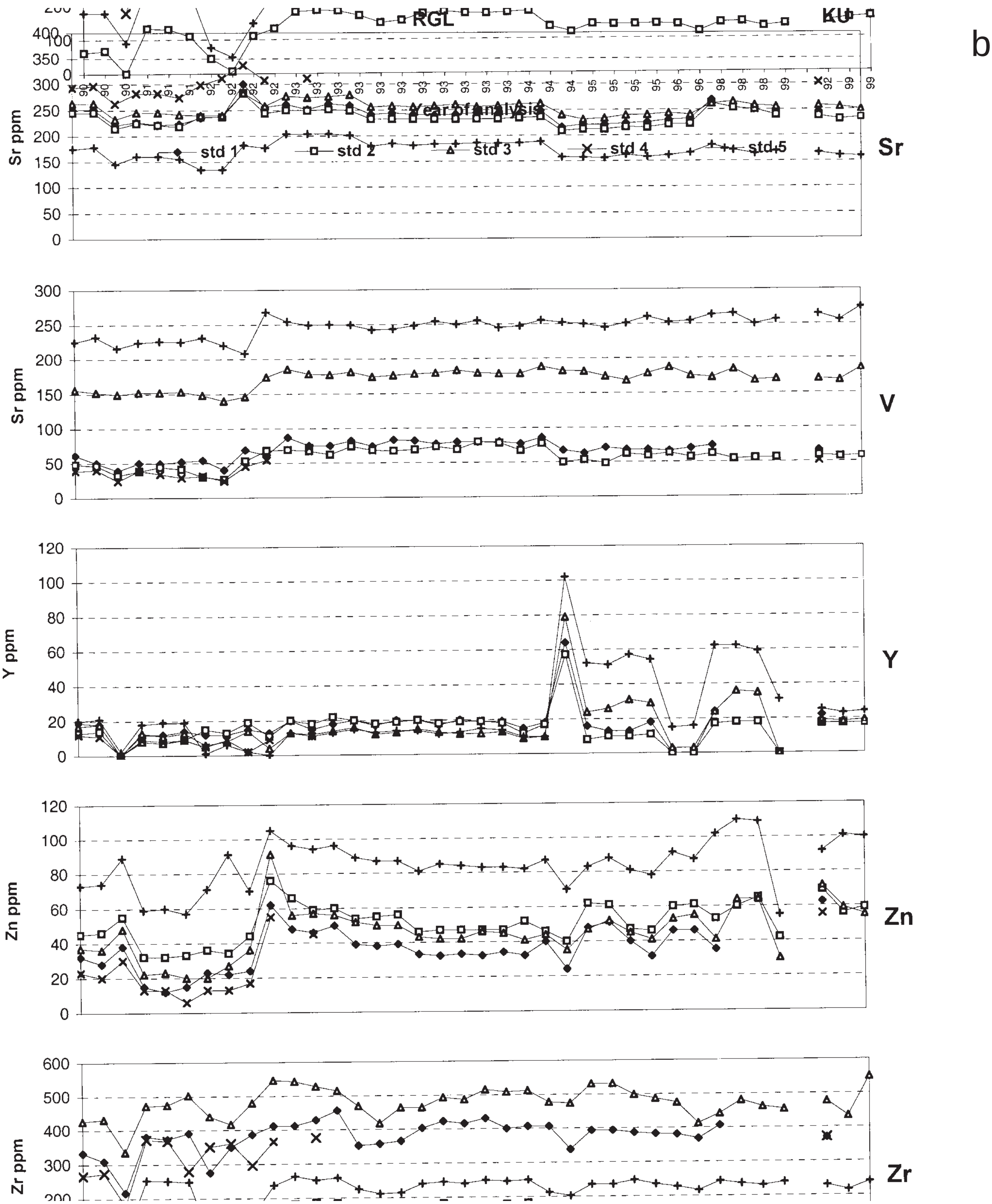

Fig. 2 *(continued)*

Table 1. Chemical analyses of international reference material. Data from RGL and recommended values

	SiO_2		TiO_2		Al_2O_3		Fe_2O_3		MnO		MgO	
	RGL	Rec.	RGL	Rec.	RGL	Rec.	RGL	Rec.	RGL	Rec.	RGL	Rec.
STSD-1	44.83	42.5	0.67	0.8	9.22	9.0	6.46	6.5	0.52	0.5	2.30	2.2
STSD-2	55.13	53.7	0.77	0.8	16.32	16.1	7.52	7.5	0.14	0.1	3.19	3.1
STSD-3	50.94	48.6	0.65	0.7	11.22	10.9	6.19	6.2	0.36	0.3	2.25	2.2
STSD-4	59.83	58.9	0.69	0.8	12.26	12.1	5.62	5.7	0.20	0.2	2.15	2.1
LKSD-1	41.24	40.1	0.50	0.5	7.95	7.8	4.01	4.1	0.09	0.1	1.80	1.7
LKSD-2	59.71	58.9	0.56	0.6	12.25	12.3	6.02	6.2	0.26	0.3	1.73	1.7
LKSD-3	59.86	58.5	0.50	0.5	12.42	12.5	5.81	5.7	0.19	0.2	2.01	2.0
LKSD-4	44.13	41.6	0.35	0.4	5.97	5.9	4.00	4.1	0.07	0.1	0.96	0.9

	CaO		Na_2O		K_2O		P_2O_5		l.o.i.		Sum	
	RGL	Rec.	RGL	Rec.	RGL	Rec.	RGL	Rec.	RGL	Rec.	RGL	Rec.
STSD-1	3.77	3.6	1.88	1.8	1.32	1.2	0.40	0.4	27.85	31.6	99.22	100.1
STSD-2	4.26	4.0	1.81	1.7	2.21	2.1	0.33	0.3	7.59	10.3	99.26	99.7
STSD-3	3.39	3.3	1.65	1.5	1.89	1.8	0.39	0.4	20.31	23.6	99.24	99.5
STSD-4	4.04	4.0	2.80	2.7	1.62	1.6	0.23	0.2	9.53	11.6	98.97	99.9
LKSD-1	10.87	10.8	2.13	2.0	1.16	1.1	0.16	0.2	26.70	29.9	96.61	99.9
LKSD-2	2.25	2.2	1.98	1.9	2.72	2.6	0.30	0.3	11.25	13.6	99.04	100.6
LKSD-3	2.38	2.3	2.41	2.3	2.30	2.2	0.25	0.2	11.23	13.4	99.36	99.8
LKSD-4	1.88	1.8	0.80	0.7	0.87	0.8	0.35	0.3	39.73	43.6	99.11	100.2

Analytical methods at RGL: X-ray fluorescence spectrometry and atomic absorption spectrometry for Na and Cu.
RGL: Rock Geochemical Laboratory of the Geological Survey of Denmark and Greenland.
Rec.: recommended values. l.o.i.: loss on ignition.

ratories or by the same method and laboratory at different times (Steenfelt 1999). The latter is relevant to the aim of this note which is a documentation of the variability of the analytical data delivered by RGL since 1990. The results are of interest to other users of analyses from RGL and to scientists working with analytical quality control.

Internal standards

The internal standards were made from five large samples of stream sediment collected in Greenland in 1989. Four of the streams drain areas of orthogneiss-dominated assemblages with various proportions of supracrustal rocks, whereas the fifth drains Tertiary basalts. Thus the material collected covers the concentration ranges found in most of the stream sediments in West and South Greenland. The samples were dried and sieved and the < 0.1 mm grain size fraction of each was homogenised and split into a large number of 7 g subsamples to serve as internal standards. A set of the five standards has since accompanied every batch of samples submitted for analysis within the geochemical mapping programme. However, standard no. 4 was exhausted during 1993 and no. 1 during 1998.

Variability diagrams

The diagrams in Figs 1, 2 for ten major element oxides and ten trace elements illustrate the temporal variation in the results delivered, i.e. the reproducibility over the nine year period. The analytical data are arranged from left to right in the chronological order they were obtained. The major element results have high reproducibility, whereas some of the trace element results have been fairly variable over time. In cases where the curves are conformable with each other the variation can be ascribed to changes in the analytical conditions, where they are non-conformable the most probable reason for the variation is analytical uncertainty or heterogeneity of the standards. Although RGL sets a recommended lower limit of detection at 50 ppm for the trace elements except Cu (5 ppm), Ba and Y (100 ppm) the customer also receives the values obtained

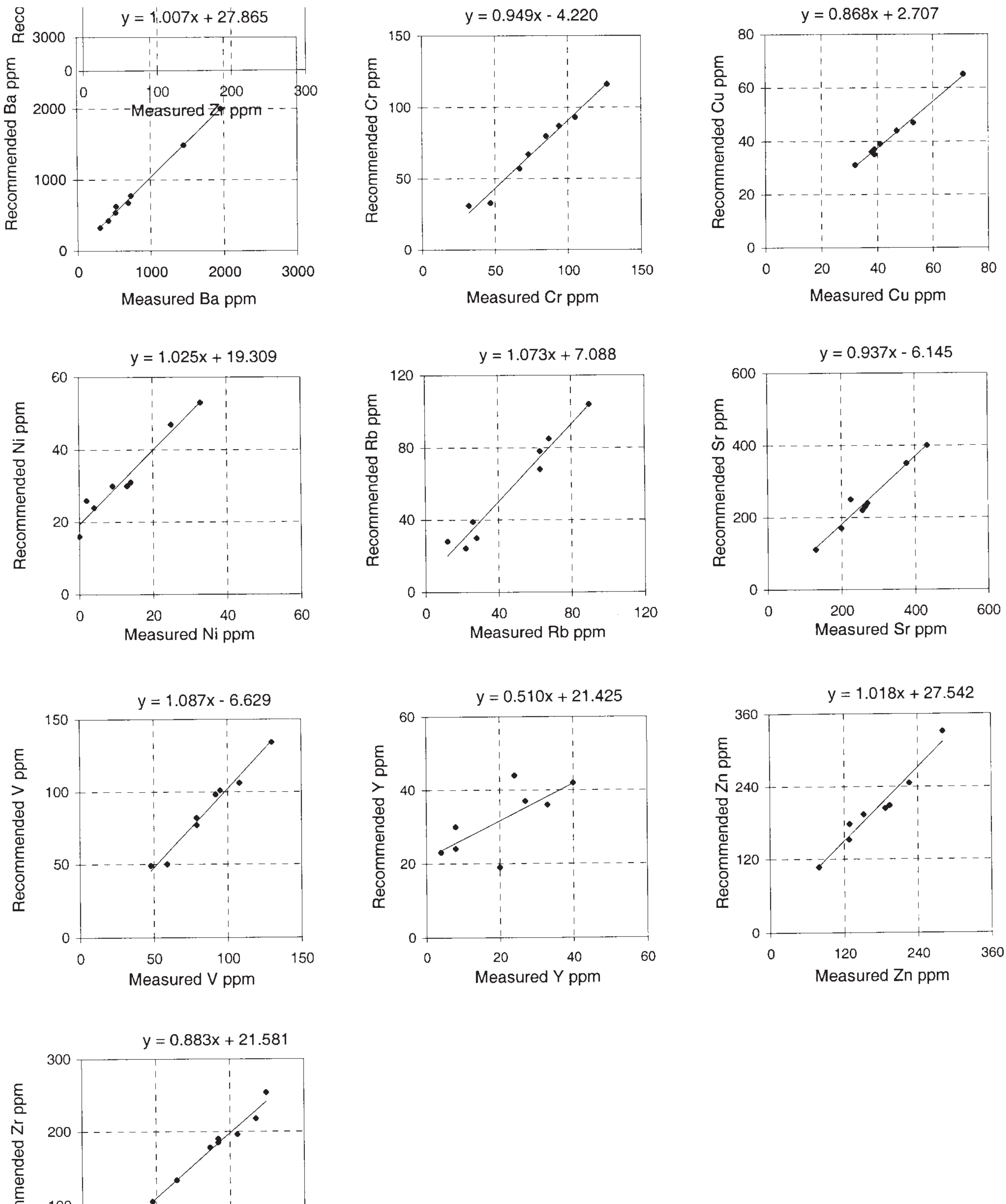

Fig. 3. Correlation of analytical data from the Rock Geochemical Laboratory, Geological Survey of Denmark and Greenland, with recommended values for eight certified international standards (CANMET, STSD 1–4, LKSD 1–4). Determinations of Cu by atomic absorption spectrometry, the others by X-ray fluorescence spectrometry.

below these limits. Therefore it is even possible to examine the quality of the low values.

Results of trace element analysis made on a sequential XRF instrument at the University of Copenhagen using pressed powder pellets and therefore giving more precise determinations are shown for comparison at the right hand side of the diagrams in Fig. 2.

Among the major element results only Al_2O_3 (Fig. 1a) and P_2O_5 (Fig. 1b) display a variability worth observing if results from different periods are to be compared. Trace element diagrams are shown for the elements considered by RGL to be of acceptable quality (Kystol & Larsen 1999, this volume). The remaining trace element data delivered (Nb, Mo, Sn, La and Ce) are totally unreliable at the levels found both in the internal standards and in common rocks. The most reproducible results are those for Cr, Cu and Ni (Fig. 2a), which have been stable throughout the monitored time period. The results for V (Fig. 2b) show a shift in level between 1992 and 1993 but the new level has been maintained since then. The diagram for Sr (Fig. 2b) shows variable results in the beginning of the period followed by more stable results since 1993. However, in the latter period there are three shifts in level, each changing the results 8–9%. There is a good deal of variability for Rb at the beginning and end of the monitored period and three years of good reproducibility in between, even though the concentration of Rb (Fig. 2a) for three of the standards is below the 50 ppm which the laboratory sets as the recommended lower limit of detection (LLD). The results for Ba (Fig. 2a), Zn and Zr (Fig. 2b) are more variable and the curves less conformable than is the case for the other trace elements. This probably reflects a higher degree of analytical uncertainty for these three elements. However, accepting this, the average levels of concentrations measured for each standard appear to have been constant since 1993. The concentrations of Y (Fig. 2b) in the standards are very low compared to the recommended LLD of 100 ppm, and the data delivered from the laboratory are not reliable, although the order of magnitude appears correct until late 1994 by comparison with the data provided by KU. However, as later Y data from RGL have shown erroneous values above 100 ppm, it cannot be recommended to use RGL's Y data.

Analyses of stream and lake sediment reference material

The accuracy of the RGL analyses has been examined by means of a set of eight internationally certified standards from the Canadian institution CANMET. The CANMET stream sediment standards STSD-1, STSD-2, STSD-3, STSD-4, and lake sediment standards LKSD-1, LKSD-2, LKSD-3, and LKSD-4 (Bowman 1994) were analysed together with the internal standards in 1999 (last data point for RLG analyses in Figs 1, 2). The results for the major elements show very close agreement between measured RGL values and recommended values for the CANMET standards (Table 1). The fact that RGL values for the element oxides are slightly higher than the recommended values is an expected consequence of the lower loss on ignition.

The results for the ten trace elements discussed here are illustrated by scatter diagrams in Fig. 3. All diagrams, except Y, show good correlation between measured and recommended values. The values for Ba, V and Zr are close to recommended values, whereas the other element determinations would need some adjustment to match the recommended level. Because of the linear correlation, such adjustment would only involve simple linear regression.

Concluding remarks

The result of monitoring analyses with internal standards has demonstrated that RGL has had problems keeping the trace element determinations by XRF at constant levels since 1990. For this reason the geochemical mapping programme has preferred to use other trace element analyses whenever possible. On the other hand, the results also show that the reproducibility has been good for certain elements within certain time periods, even at concentration levels close to the recommended lower limit of detection. Furthermore, the variability diagrams demonstrate that some changes are merely a shift in level affecting all standards in the same way, in which case a simple arithmetic calibration can be applied to make data from different periods comparable. In conclusion, monitoring with internal standards has identified element determinations which are generally unreliable, have low precision or are affected by periodic bias. In addition, it has provided a tool for improving the data quality through the possibility for correcting biased results. The correction parameters are found by linear regression of obtained values for the standards of a given set against reference values for each standard. The correction is then applied to the entire batch of samples analysed together with the given set of standards.

References

Bowman, W.S. 1994: Catalogue of certified reference materials. Canadian Certified Reference Material Project **94-1E**, 74 pp. Ottawa: CANMET, Natural Resources Canada.

Kystol, J. & Larsen, L.M. 1999: Analytical procedures in the Rock Geochemical Laboratory of the Geological Survey of Denmark and Greenland. Geology of Greenland Survey Bulletin **184**, 59–62 (this volume).

Steenfelt, A. 1993: Geochemical mapping – progress in Greenland. Journal of Geochemical Exploration **49**, 5–13.

Steenfelt, A. 1994: Large scale geochemical variation in the Precambrian of West and South Greenland. Rapport Grønlands Geologiske Undersøgelse **160**, 41–44.

Steenfelt, A. 1996: Distribution of gold, arsenic, and antimony in West and South Greenland: a guide to mineral exploration and environmental management. Bulletin Grønlands Geologiske Undersøgelse **172**, 55–61.

Steenfelt, A. 1999: Compilation of data sets for a geochemical atlas of West and South Greenland based on stream sediment surveys 1977 to 1997. Danmarks og Grønlands Geologiske Undersøgelse Rapport **1999/41**, 33 pp.

Analytical procedures in the Rock Geochemical Laboratory of the Geological Survey of Denmark and Greenland

Jørgen Kystol and *Lotte Melchior Larsen*

The analytical procedures for analysis of whole rocks for major and selected trace elements, mainly by X-ray fluorescence spectrometry (XRF), are described in detail. The quality of the results is evaluated and results for international standards are given.

Geological Survey of Denmark and Greenland, Thoravej 8, DK-2400 Copenhagen NV, Denmark. E-mail: *jk@geus.dk*

Keywords: analysis, analytical methods, X-ray fluorescence

The Rock Geochemical Laboratory of the Geological Survey of Denmark and Greenland (GEUS), formerly of the Geological Survey of Greenland (GGU), produces high-precision analyses for major elements together with reconnaissance data for selected trace elements, mostly on geological materials. The present analytical equipment is centred around a multichannel X-ray fluorescence spectrometer from 1985. A gradual development in the analytical and computational technique has taken place, but since 1993 the procedures have been essentially unchanged. In this period, the laboratory has analysed *c.* 14 000 samples for a variety of purposes, and the results are appearing in scientific papers, geochemical maps, technical reports, and students' theses. The aim of the present note is to provide an accessible and referable account of the analytical procedures in the laboratory.

Analytical procedures

Samples are routinely ground in a tungsten carbide ball mill. Alternatively, samples can be ground in a swing mill of tungsten carbide or agate.

Most elements are determined by X-ray fluorescence spectrometry (XRF) on fused glass discs. The rock powders are dried at 110°C for 2 hours and ignited in an electric furnace at 1000°C for 1 hour, with subsequent determination of the loss on ignition. The ignited samples are mixed with sodium tetraborate in the ratio 0.7500 g sample to 5.2500 g borate, and fused in Pt/Au crucibles over gas burners under continuous agitation for 1–1½ hours. After inspection for homogeneity the melts are poured into a Pt/Au mold, creating glass discs with 32 mm diameter. The X-ray fluorescence spectrometer is a Philips PW1606 multichannel instrument for simultaneous determination of a number of specific elements, equipped with a Rh-anode X-ray tube operated at 50 kV and 50 mA. Calibration and correction for background and line overlaps are calculated from measurements on synthetic mono-element glass discs, and corrections for matrix effects are calculated either from measurements on synthetic glass discs or from Heinrich's (1966) absorption coefficients (Sørensen 1975, 1976, 1981).

Na_2O and Cu are determined by atomic absorption spectrometry (AAS). Each dried sample (0.25–0.5 g) is treated with hydrofluoric acid in a PTFE beaker on a heating plate. After evaporation to dryness the residue is dissolved in a hydrochloric acid – potassium chloride solution, made up to 50 ml, and Na and Cu measured on a Perkin Elmer PE2280 AAS instrument.

For FeO determination each dried sample (0.1 g) is treated with ammonium vanadate – hydrofluoric acid overnight. Boric acid and a measured amount of iron(II) is added and surplus iron(II) is determined by automatic potentiometric titration using Cr(VII) as titrant. The method is a modification of that of Wilson (1955).

'Volatiles' is calculated as the loss on ignition corrected for the calculated gain of weight due to oxidation of iron(II) to iron(III) during ignition.

To give an indication of concentration levels in large

Table 1. Evaluation of analytical results from the Rock Geochemical Laboratory

Element	Line	Precision	LLD rec.	LLD theo.	Accuracy* std. error	Basalts* rel. error	Granites* rel. error	Quality
						% of amount	% of amount	
Major elements		wt%	wt%	wt%	wt%	present	present	
SiO_2	Kα	0.15	0.3	0.01	0.24	0.25	0.31	high
TiO_2	Kα	0.015	0.03	0.002	0.033	2.19	19.51	high
Al_2O_3	Kα	0.05	0.1	0.05	0.24	0.59	0.62	high
Fe_2O_3,T	Kα	0.1	0.2	0.0015	0.21	1.19	10.56	high
FeO	–	0.1	0.2	–	0.13	2.25	4.12	high
MnO	Kα	0.003	0.005	0.001	0.005	2.20	10.48	high
MgO	Kα	0.05	0.1	0.05	0.09	0.62	2.89[b]	high
CaO	Kα	0.03	0.05	0.0007	0.07	0.77	2.34	high
Na_2O	–	0.05	0.08	–	0.06	3.93	2.87	high
K_2O	Kα	0.005	0.01	0.003	0.038	1.26	0.28	high
P_2O_5	Kα	0.005	0.01	0.002	0.014	1.62	3.04[b]	good
Volat	–	0.10	–	–	–	–	–	good
						% of amount	% of amount	
Trace elements		ppm	ppm	ppm	ppm	present	present	
V	Kα	20	50	10	10.9	4.26	b.d.	good
Cr	Kα	40	50	10	12.0	2.02[a]	b.d.	good
Ni	Kα	15	50	5	12.0	14.3[a]	b.d.	good
Cu	–	2	5	3	5.3	10.1	21.0	good
Zn	Kα	10	50	3	14.0	10.6	8.76[a]	good
Rb	Kα	20	50	3	21.0	55[c]	12.9	moderate
Sr	Kα	20	50	2	38.8	6.35	1.32[b]	good
Y	Kα	20	100	2	32.8	b.d.	b.d.	poor
Zr	Kα	30	50	2	42.6	14.5	11.4	good
Nb	Kα	20	50	2	28.5	b.d.	39[c]	poor
Ba	Lα	60	100	80	47.7	11.2	16.2	moderate

Analyses by XRF except FeO (titration), volatiles (corrected loss on ignition), Na_2O and Cu (AAS).
Fe_2O_3,T: Total iron as Fe_2O_3.
Precision: One standard deviation based on experimental data (repeated analysis over time of a set of internal standards).
LLD rec.: Recommended lower limit of detection. These values (*c.* 1 standard deviation) are based on user experience with the analytical results and are not calculated figures. They include the facts that the matrix and background corrections are not always adequate for samples with strongly contrasting matrices and that there may be variations between different calibrations. For sets of samples with similar matrices run under the same calibration, the effective LLD will normally be somewhat lower.
LLD theo.: Theoretical lower limit of detection: 3 times counting statistical error.

**Results from analysis of 26 international standards*
Std. error: Standard error. Average distance of points from regression line.
Rel. error: The difference between measured and reference values as percentage of the reference value. See text for details.
Basalts: Average relative errors for the five basalt standards BCR-1, BHVO-1, BR, JB-1A and W-2.
Granites: Average relative errors for the four granite standards G-2, GA, GH and NIM-G.
[a-b-c] 1, 2, or 3 reference values are below the recommended lower limit of detection and have not been included in the average.
b.d.: all reference values are below the recommended lower limit of detection.
Quality is a subjective estimate of the reliability of results for concentrations significantly above the recommended LLD.

Table 2. Analytical results obtained for international standards, June 1999

Standard	AGV-1		BCR-1		BHVO-1		BIR-1		DNC-1		DT-N	
	measured	reference	measured	reference	measured	reference	measured	reference	measured	reference	measured	reference
SiO_2	59.91	59.43	54.70	54.55	49.79	49.97	47.83	47.80	47.03	47.20	37.14	36.51
TiO_2	1.08	1.06	2.26	2.26	2.78	2.71	0.96	0.96	0.51	0.48	1.34	1.40
Al_2O_3	17.40	17.32	13.68	13.75	13.76	13.82	15.70	15.36	18.69	18.36	58.97	59.29
Fe_2O_3,T	6.49	6.84	13.43	13.52	12.25	12.24	11.50	11.27	9.84	9.96	0.40	0.66
FeO	2.15	2.08	8.78	8.95	8.38	8.58	8.54	8.39	7.42	7.41	0.09	0.10
MnO	0.098	0.091	0.187	0.181	0.171	0.168	0.177	0.171	0.150	0.149	0.001	0.008
MgO	1.55	1.55	3.48	3.51	7.22	7.23	9.69	9.69	10.15	10.08	0.06	0.04
CaO	4.89	4.99	6.95	7.01	11.34	11.41	13.27	13.25	11.25	11.31	0.02	0.04
Na_2O	4.52	4.30	3.43	3.30	2.40	2.26	1.90	1.75	1.95	1.88	0.03	0.04
K_2O	2.960	2.950	1.750	1.700	0.528	0.520	0.022	0.027	0.230	0.230	0.125	0.120
P_2O_5	0.508	0.495	0.367	0.363	0.277	0.273	0.024	0.046	0.070	0.085	0.072	0.090
V	113	122	399	410	314	317	316	313	149	148	127	150
Cr	19	10	30	16	284	289	403	382	299	286	248	260
Ni	0	16	0	13	99	121	147	166	240	248	0	14
Cu	63	61	21	19	147	136	130	126	104	96	13	7
Zn	86	89	125	131	89	105	50	71	42	66	0	28
Rb	45	68	64	48	32	11	23	1	6	5	0	6
Sr	635	669	339	333	369	403	82	108	117	145	55	30
Y	0	20	66	38	65	27	50	16	28	18	0	7
Zr	199	229	220	192	203	179	69	16	60	41	320	371
Nb	0	15	40	14	55	19	21	1	22	3	0	34
Ba	1200	1238	743	687	108	139	0	7	14	114	97	130

Standard	G-2		MICA-FE		NIM-G		PCC-1		S-7		W-2	
	measured	reference	measured	reference	measured	reference	measured	reference	measured	reference	measured	reference
SiO_2	69.74	69.22	34.31	34.55	75.88	75.70	41.60	41.89	33.24	33.45	52.31	52.56
TiO_2	0.48	0.48	2.55	2.51	0.12	0.09	0.00	0.01	1.59	1.57	1.10	1.06
Al_2O_3	15.43	15.41	19.59	19.58	12.10	12.08	0.55	0.68	4.22	4.27	15.39	15.39
Fe_2O_3,T	2.46	2.66	25.44	25.76	1.70	2.03	8.12	8.29	9.40	9.31	10.70	10.76
FeO	1.43	1.46	18.63	18.99	1.26	1.30	5.32	5.08	4.45	n.a.	8.26	8.33
MnO	0.034	0.030	0.364	0.352	0.017	0.021	0.116	0.121	0.173	0.170	0.168	0.163
MgO	0.75	0.75	4.65	4.57	0.05	0.06	43.22	43.62	26.32	26.21	6.35	6.39
CaO	1.89	1.96	0.39	0.43	0.75	0.78	0.53	0.52	9.63	9.70	10.82	10.90
Na_2O	4.18	4.08	0.25	0.30	3.49	3.36	0.02	0.03	0.63	0.50	2.28	2.15
K_2O	4.500	4.490	9.010	8.790	4.990	4.990	0.003	0.007	1.040	1.040	0.635	0.628
P_2O_5	0.135	0.140	0.418	0.452	0.009	0.010	0.009	0.002	1.440	1.490	0.128	0.131
V	33	36	131	136	7	2	33	31	120	110	254	263
Cr	21	9	97	90	34	12	2749	2742	1301	1370	95	93
Ni	0	5	0	35	0	8	2395	2391	992	1032	57	70
Cu	13	11	31	5	12	12	13	10	68	55	113	103
Zn	82	86	1272	1306	43	50	35	42	54	66	62	77
Rb	143	170	2201	2209	280	320	0	0	68	54	28	20
Sr	487	479	104	5	33	10	28	0	1454	1700	171	194
Y	0	11	141	50	80	143	0	0	39	17	36	24
Zr	295	309	933	803	237	300	0	10	263	240	117	94
Nb	0	12	312	271	4	53	0	1	93	104	25	8
Ba	1953	1884	64	151	169	120	0	1	1627	1700	202	182

Major elements in wt%, trace elements in ppm, n.a.: not available.

Fe_2O_3,T: Total iron as Fe_2O_3.

Reference values for samples NIM-G and S-7 from Govindaraju (1989), others from Govindaraju (1994).

All reference values have been recalculated on dry basis (as dried but not ignited powders).

regional sample sets and samples of economic interest, a number of trace elements are measured simultaneously with the major elements. Calibration and correction for background, line overlaps and matrix effects are carried out as described above for the major elements. The use of glass discs for trace element analysis, in contrast to the normally used pressed powder pellets, poses some problems. Firstly, the weaker signal due to the flux dilution gives higher theoretical lower limits of detection (LLD). Secondly, the calculated corrections for backgrounds and spectral overlaps are not always adequate. The method works satisfactorily for the elements V, Cr, Ni, Zn, Sr and Zr, and less so for Rb, Y, Nb and Ba. Other elements measured are Mo, Sn, La and Ce, but these give poor results and are not used. Because of the high LLDs, concentrations of Nb and Y in most geological materials, and Rb in some, are beyond the limitation of the method.

Quality of results

The major element analyses from the laboratory, obtained by XRF analysis on a routine basis since 1977, have a long-standing record of being highly reproducible. On the other hand, the trace element results have been more variable. The determination of trace element concentrations commenced in 1986, and in the beginning there were problems with reproducibility for a number of the elements. In particular, significant absolute variations between different calibrations were observed. The variability of the results has been monitored with internal standards since 1990, as presented by Steenfelt (1999a, b, this volume). This work confirms the high and uniform quality over time of the major element analyses, with some variations in P_2O_5 at levels below 0.1%. It also illustrates the variations in the early trace element analyses, and, in particular, that the trace element results have been fairly stable since 1993. Table 1 presents estimates of the precision and LLD for both major and trace element determinations, applicable for analyses from 1993 and later.

Analytical results for a set of 26 international standards have been used to evaluate the accuracy of the data. For this exercise, Table 1 includes for each element the *standard error*, which is the average distance of the data points from the regression line for reference values versus measured values. The *relative error* for an element in a sample is the difference between the measured and the reference values, expressed as percentage of the reference value. The relative errors are much larger at low concentrations than at high. Table 1 includes average relative errors for groups of international standards of comparable composition, viz. basaltic and granitic. For some elements in low concentrations, e.g. TiO_2, MnO and Cu in granites, the relative errors in Table 1 may be at least as dependent on the quality of the reference values as on the quality of the measured values. Table 2 shows the analytical results compared to the reference values for 12 of the international standards, selected to illustrate the large compositional range covered by the method.

Conclusions

The Rock Geochemical Laboratory produces major element analyses of high quality and long-term consistency. The reconnaissance trace element analyses obtained on the glass discs have high detection limits, but above these limits the data are of good quality for V, Cr, Ni, Cu, Zn, Sr and Zr, of moderate quality for Rb and Ba, and of poor quality for Y and Nb.

References

Govindaraju, K. 1989: Compilation of working values and sample description for 272 geostandards. Geostandards Newsletter **13**, special issue July 1989, 1–113.

Govindaraju, K. 1994: Compilation of working values and sample description for 383 geostandards. Geostandards Newsletter **18**, special issue July 1994, 1–158.

Heinrich, K.F.J. 1966: X-ray absorption uncertainty. In: McKinley, T.D., Heinrich, K.F.J. & Wittry, D.B. (eds): The electron microprobe, 296–377. New York: John Wiley & Sons.

Sørensen, I. 1975: X-ray fluorescence spectrometry at GGU. Rapport Grønlands Geologiske Undersøgelse **75**, 16–18.

Sørensen, I. 1976: Progress in calibrating an X-ray spectrometer. Rapport Grønlands Geologiske Undersøgelse **80**, 149–150.

Sørensen, I. 1981: A calculated background correction method for XRF. Spectrochimica Acta **36B**, 243–249.

Steenfelt, A. 1999a: Compilation of data sets for a geochemical atlas of West and South Greenland based on stream sediment surveys 1977 to 1997. Danmarks og Grønlands Geologiske Undersøgelse Rapport **1999/41**, 33 pp.

Steenfelt, A. 1999b: Variability of XRF and AAS analyses from the Rock Geochemical Laboratory of the Geological Survey of Denmark and Greenland. Geology of Greenland Survey Bulletin **184**, 49–57 (this volume).

Wilson, A.D. 1955: A new method for the determination of ferrous iron in rocks and minerals. Bulletin Geological Survey of Great Britain **9**, 56–58.

Danmarks og Grønlands Geologiske Undersøgelse (GEUS)
Geological Survey of Denmark and Greenland
Thoravej 8, DK-2400 Copenhagen NV
Denmark

Bulletin Grønlands Geologiske Undersøgelse

150 Stratigraphy and structure of the Fiskenæsset Complex, southern West Greenland. 1985. 72 pp.
By J.S. Myers. 200.00

151 The geology of the Qôrqut granite complex north of Qôrqut, Godthåbsfjord, southern West Greenland. 1985. 43 pp.
By C.R.L. Friend, M. Brown, W.T. Perkins & A.D.M. Burwell. 155.00

152 Reaction between picrite magma and continental crust: early Tertiary silicic basalts and magnesian andesites from Disko, West Greenland. 1985. 126 pp.
By A.K. Pedersen. 275.00

153 The Kimmeridgian ammonite faunas of Milne Land, central East Greeenland. 1985. 56 pp.
By T. Birkelund & J.H. Callomon. 185.00

154 The early Archaean to Proterozoic history of the Isukasia area, southern West Greenland. 1986. 80 pp.
By A.P. Nutman. 235.00

155 Topographical and geological maps of Hall Land, North Greenland. Description of a computer-supported photogrammetrical research programme for production of new maps, and the Lower Palaeozoic and surficial geology. 1987. 88 pp.
By P.R. Dawes. 425.00

156 Stratabound scheelite and stratiform tourmalinites in the Archaean Malene supracrustal rocks, southern West Greenland. 1987. 26 pp.
By P.W.U. Appel & A.A. Garde. 130.00

157 Geology and petrology of the Lower Tertiary plateau basalts of the Scoresby Sund region, East Greenland. 1989. 164 pp.
By L.M. Larsen, W.S. Watt & M. Watt. 275.00

158 Petroleum geology of North Greenland. 1989. 92 pp. (9 articles)
Edited by F.G. Christiansen. 200.00

159 Conodonts from the Upper Ordovician - Lower Silurian carbonate platform of North Greenland. 1990. 151 pp.
By H.A. Armstrong. 295.00

160 Sedimentary basins of North Greenland. 1991. 164 pp. (6 articles)
Edited by J.S. Peel & M. Sønderholm. 295.00

161 Functional morphology, evolution and systematics of Early Palaeozoic univalved molluscs. 1991. 116 pp. (2 articles)
By J.S. Peel. 210.00

162 Upper Cretaceous - Lower Tertiary decapod crustaceans from West Greenland. 1992. 46 pp.
By J.S.H. Collins & H. Wienberg Rasmussen. 85.00

163 Upper Llandovery and Wenlock *Cyrtograptus* from the Silurian Peary Land Group, North Greenland. 1992. 31 pp.
By M. Bjerreskov. 65.00

164 Acritarchs from the Lower Cambrian Buen Formation in North Greenland. 1993. 35 pp.
By G. Vidal & J.S. Peel. 75.00

165 Lithostratigraphy of the continental Devonian sediments in North-East Greenland. 1993. 108 pp.
By H. Olsen & P.-H. Larsen. 170.00

166 Dinoflagellate cyst stratigraphy of the Barremian to Albian, Lower Cretaceous, North-East Greenland. 1993. 171 pp.
By H. Nøhr-Hansen. 300.00

167 Lithostratigraphic framework of the Upper Proterozoic Eleonore Bay Supergroup of East and North-East Greenland. 1993. 38 pp.
By M. Sønderholm & H. Tirsgaard. 75.00

168 Sedimentary basin analysis of the continental Devonian basin in North-East Greenland. 1993. 80 pp.
By H. Olsen. 145.00

169 Palaeontology, stratigraphy and environmental setting of Middle Cambrian outer shelf deposits, North Greenland. 1994. 155 pp. (5 articles)
Edited by J.S. Peel. 290.00
170 Upper Cretaceous dinoflagellate cyst stratigraphy, onshore West Greenland. 1996. 104 pp.
By H. Nøhr-Hansen. 235.00
171 Research Papers. Collection of scientific articles. 1996. 90 pp. (4 articles) 110.00
172 Report of Activities, 1995. 1996. 119 pp. (20 articles) 180.00

Geology of Greenland Survey Bulletin

173 Cambrian shelf stratigraphy of North Greenland. 1997. 120 pp.
By J.R. Ineson & J.S. Peel. 250.00
174 The Proterozoic Thule Supergroup, Greenland and Canada: history, lithostratigraphy and development. 1997. 150 pp.
By P.R. Dawes. 300.00
175 Stratigraphy of the Neill Klinter Group; a Lower – lower Middle Jurassic tidal embayment succession, Jameson Land, East Greenland. 1998. 80 pp.
By G. Dam & F. Surlyk.
176 Review of Greenland Activities 1996. 1997. 112 pp. (18 articles)
Edited by A.K. Higgins & J.R. Ineson. 200.00
177 Accretion and evolution of an Archaean high-grade grey gneiss – amphibolite complex: the Fiskefjord area, southern West Greenland. 1997. 115 pp.
By A.A. Garde. 200.00
178 Lithostratigraphy, sedimentary evolution and sequence stratigraphy of the Upper Proterozoic Lyell Land Group (Eleonore Bay Supergroup) of East and North-East Greenland. 1997. 60 pp.
By H. Tirsgaard & M. Sønderholm.
179 The Citronen Fjord massive sulphide deposit, Peary Land, North Greenland: discovery, stratigraphy, mineralization and structural setting. 1998. 40 pp.
By F.W. van der Stijl & G.Z. Mosher. 200.00
180 Review of Greenland activities 1997. 1998. 176 pp. (26 articles)
Edited by A.K. Higgins & W.S. Watt. 200.00
181 Precambrian geology of the Disko Bugt region, West Greenland. 1999. 179 pp. (15 articles)
Edited by F. Kalsbeek. 240.00
182 Vertebrate remains from Upper Silurian – Lower Devonian beds of Hall Land, North Greenland. 1999. 80 pp.
By H. Blom. In press
183 Review of Greenland activities 1998. 1999. 80 pp. (10 articles)
Edited by A.K. Higgins & W.S. Watt. In press
184 Collected research papers: palaeontology, geochronology, geochemistry. 1999. 62 pp. (6 articles)
185 Greenland from Archaean to Quaternary. Descriptive text to the Geological map of Greenland, 1:2 500 000. 88 pp. + map.
By N. Henriksen, A.K. Higgins, F. Kalsbeek & T.C.R. Pulvertaft. In press

Prices are in Danish kroner exclusive of local taxes, postage and handling

The series *Geology of Greenland Survey Bulletin* is a continuation of *Bulletin Grønlands Geologiske Undersøgelse* and incorporates *Rapport Grønlands Geologiske Undersøgelse*. These two series were issued by the former Grønlands Geologiske Undersøgelse (GGU) which was merged in 1995 with the former Danmarks Geologiske Undersøgelse (DGU) to form a new national geological survey: Danmarks og Grønlands Geologiske Undersøgelse (The Geological Survey of Denmark and Greenland) with the pet-name GEUS. Two other scientific series are issued by GEUS: *Geology of Denmark Survey Bulletin* and *Geology of Denmark and Greenland Map Series.*